UNIVERSIDADE DE SÃO PAULO
INSTITUTO DE FÍSICA DE SÃO CARLOS

Cleverson Francisco Cherubim

Out-of-equilibrium thermodynamics and non-thermal heat engines

São Carlos

2020

Cleverson Francisco Cherubim

Out-of-equilibrium thermodynamics and non-thermal heat engines

Thesis presented to the Graduate Program in Physics at the Instituto de Física de São Carlos, Universidade de São Paulo, to obtain the degree of Doctor in Science.

Concentration area: Basic Physics

Advisor: Prof. Dr. Frederico Borges de Brito

Corrected version

São Carlos

2020

Cherubim, Cleverson Francisco
Out-of-equilibrium thermodynamics and non-thermal heat engines / Cleverson Francisco Cherubim; advisor Frederico Borges de Brito - corrected version -- São Carlos 2020.
97 p.

Thesis (Doctorate - Graduate Program in Basic Physics) -- Instituto de Física de São Carlos, Universidade de São Paulo - Brasil , 2020.

1. Out-of-equilibrium thermodynamics. 2. Steady-state thermodynamics. 3. Quantum thermodynamics. 4. Quantum heat engine. I. de Brito, Frederico Borges, advisor. II. Title.

Este trabalho é dedicado aos alunos da USP, como uma contribuição das Bibliotecas do Campus USP de São Carlos para o desenvolvimento e disseminação da pesquisa científica da Universidade.

ACKNOWLEDGEMENTS

First and foremost I'd like to thank my family for all the support they gave me throughout all those years of grad school.

The most important thank goes to my PhD advisor Frederico Brito, since the very beginning he's being very supportive and helpful, guiding me throughout all this journey, not only with technical related stuff but also through his personal perspectives on the possible choices to take on my career. He did that without cutting most of my freedom of how to proceed and which steps to take, which is an essential part of every grad student.

I also would like to greatly thank Sebastian Deffner for advising me during part of my PhD, he was very welcoming since the very beginning and was very helpful along the time that we had together. Also a big thanks for the members (and alumni) of his group, Josey Stevens, Mujibur Bhuniyan, Gregory Huxtable, Christopher Dottellis and Matthew Holland. I am also grateful for the UMBC's hospitality when I was working there.

A special thanks to Diogo Soares Pinto for fruitful conversations and for collaborating with new ideas on this project.

Big thanks to Victor Teizen and Pedro Soares, great of mine in grad school, for all the amazing conversations on physics and funny moments. I'd also like to thank André Hernandes, a PhD student of our group, for all the fruitful conversations about quantum and stochastic thermodynamics and physics in general.

A huge thanks to IFSC for all the amazing time that I've spent there, not only due to its very enriching environment for someone looking for knowledge, but specially to the friendship of amazing people that had crossed my path along the years that I've been there.

And finally, I would like to acknowledge the financial support given by the Coordenação de Aperfeiçoamento de Pessoal de Nível Superior—Brasil (CAPES)—Finance Code 001. During my stay at UMBC, I was supported by the CAPES scholarship PDSE/process No. 88881.132982/2016-01.

"Entropy is the price of structure."
Ilya Prigogine

ABSTRACT

CHERUBIM, C. F. **Out-of-equilibrium thermodynamics and non-thermal heat engines**. 2020. 97p. Thesis (Doctor in Science) - Instituto de Física de São Carlos, Universidade de São Paulo, São Carlos, 2020.

Quantum thermodynamics (QT) is an emerging field of research that aims to investigate how the laws of thermodynamics and quantum mechanics merge together in small quantum systems. With advances at the necessary technology to control and measure those small physical systems this field has acquired even more importance, not only in the sense that it can be tested, which is a good thing for basic research, but that new applications could be implemented at these scales, so a better comprehension of the limitations imposed by quantum thermodynamics turns out to be of crucial importance for these goals, which forces theoreticians to produce experimentally relevant versions of these new concepts. Another important aspect present at those systems is that part of them work in a regime where its constituents are described by non-thermal states, and in particular non-thermal steady states, which brings to light a different thermodynamic description, usually called *steady-state thermodynamics*, therefore one of the goals that we are willing to achieve with this thesis is to give an introduction to QT of systems out-of-equilibrium. One of the related subtopics that physicists deal with in QT and the one that we will be focusing on this work are the use of non-thermal stationary states to build heat engines in the quantum domain, and the analyses of the features that this new regime could possibly allow, like the use of quantum resources as a way to overcome classical limitations imposed on its performance, like to attain efficiencies higher than Carnot's or operate in certain regimes unattainable using only classical resources. Therefore, in order to clarify the underlying physics of those systems in a non-thermal regime, any experimentally well suited content is more than welcome. So keeping that in mind we devised an experimentally relevant thermodynamic cycle for a transmon qubit WS interacting with a non-thermal environment composed by two subsystems, an externally excited cavity and a classical heat bath with temperature T. The WS undergoes a non-conventional cycle (different from Otto, Carnot, etc.) through a succession of non-thermal stationary states obtained by slowly varying its bare frequency and the amplitude of the field applied on the cavity. The efficiency of this engine obtains a maximum value up to 47% in the regime of operation used. We also wanted to look for the role played by the different types of coherences, present at the WS, on the behavior of the engine and its efficiency. By different types of coherence we mean the so called modes of coherence, whose definition is based on how they respond to symmetry transformations. We did that for the trivial case of the qubit, that only contains the modes 1 and -1, and that has shown to be extremely important for the efficiency of the machine. The same procedure was repeated for a 3-level system WS. The modes 1 and -1 was again very important, not only to the absolute value of the engine's efficiency but to the regime of

operation of the machine. The additional modes, 2 and -2, had a negative impact on the efficiency, reducing its absolute value. This result appears to show some evidences that quantumness won't necessarily bring improvements to the operation of those machines.

Keywords: Out-of-equilibrium thermodynamics. Steady-state thermodynamics. Quantum thermodynamics. Quantum heat engine.

RESUMO

CHERUBIM, C. F. **Termodinâmica fora do equilíbrio e máquinas não-térmicas**. 2020. 97p. Tese (Doutor em Ciência) - Instituto de Física de São Carlos, Universidade de São Paulo, São Carlos, 2020.

Termodinâmica quântica (TQ) é um campo de pesquisa recente que visa investigar como as leis da termodinâmica e da mecânica quântica funcionam em conjunto em pequenos sistemas quânticos. Com avanços na tecnologia necessária para controlar e medir esses pequenos sistemas, esta área de pesquisa tem adquirido cada vez mais importância, não somente no sentido de que agora eles podem começar a serem testadas, o que é algo de extrema importância para pesquisa, mas também que novas aplicações podem ser implementadas nessas escalas, portanto, uma boa compreensão das limitações impostas pela termodinâmica quântica torna-se de suma importância na busca desses objetivos, o que força físicos teóricos a produzir conteúdos experimentalmente relevantes desses novos conceitos. Outro aspecto importante associado a estes sistemas é que parte deles pode operar fora do equilíbrio termodinâmico, sendo descritos por estados não térmicos, e em particular estados não térmicos estacionários, devendo portanto serem descritos termodinamicamente de maneira distinta, o que geralmente recebe o nome de *termodinâmica de estados estacionários*, portanto um dos principais objetivos desta tese será o de fornecer uma introdução a TQ de sistemas fora do equilíbrio. Um dos mais importantes subtópicos estudados em TQ e o que daremos bastante ênfase nesta tese será o uso de estados estacionários não térmicos na construção de máquinas operando no regime quântico, e a análise das novas características que este regime podem propiciar, como o uso de recursos quânticos com o intuito de superar limitações clássicas em sua performance, como a obtenção de eficiências superiores a eficiência de Carnot ou operar em certos regimes não permitidos usando somente ingredientes clássicos. Portanto, vemos que é de suma importância tornar mais clara a compreensão de sistemas operando fora do regime térmico e que qualquer conteúdo produzido que esteja bem adequado a verificações experimentais é muito mais que bem-vindo. Elaboramos um ciclo termodinâmico relevante sob o ponto de vista experimental usando um transmon no regime de qubit como ST em contato com um ambiente não térmico composto por dois subsistemas, uma cavidade excitada por um campo externo e banho clássico com temperatura T. A ST passa por um ciclo não convencional (diferente dos ciclos de Otto, Carnot, etc.) através de uma sucessão de estados estcionários não térmicos obtidos através da variação muito lenta de sua frequência e da amplitude do campo externo aplicado à cavidade. A eficiência dessa máquina adquire um valor máximo da ordem de 47% no regime de operação usado. Também queríamos olhar para o papel dos diferentes tipos de coerência, presentes na ST, sobre o comportamento da máquina e sua eficiência. Por diferentes tipos de coerência nós nos referimos aos tão conhecidos modos de

coerência, cuja definição se baseia em como elas respondem a transformações de simetria. Fizemos essa análise para o caso trivial do qubit, que contém somente os modos 1 e -1, e que se demonstraram ser de extrema importante para a eficiência da máquina. O mesmo procedimento foi repetido para um sistema de 3 níveis usado como ST. Os modos 1 e -1 se demonstraram novamente bastante importantes, não somente para o valor absoluto da máquina mas também para o regime de funcionamento desta. Os modos adicionais, 2 e -2, tiveram um impacto negativo na eficiência, reduzindo seu valor absoluto. Este resultado parece nos fornecer evidências de que “quantumness" não necessariamente trará ganhos à operação dessas máquinas.

Palavras-chave: Termodinâmica fora do equilíbrio. Termodinâmica de estados estacionários. Termodinâmica quântica. Máquina térmica quântica.

LIST OF FIGURES

LIST OF TABLES

CONTENTS

1 CLASSICAL EQUILIBRIUM THERMODYNAMICS

1.1 Classical equilibrium thermodynamics

Classical thermodynamics[1–5] is a phenomenological theory that describes the average behavior of classical systems composed of a large number of particles. It is essentially an equilibrium theory, which means that it is only capable of describing equilibrium states and equilibrium processes regardless of their microscopic structure. A classical system is said to be in equilibrium if their macroscopic properties don't change in time. The thermodynamic equilibrium could be, e.g., of a mechanical type, which means that a closed system's volume does not change in time, possibly due to the lack of any gradient of pressure. It could also be a thermal equilibrium, when the temperature is fixed in time. By equilibrium process, we mean a succession of "frozen pictures" of equilibrium states, achieved theoretically in an infinite amount of time, so the theory is not truly dynamic considering that it doesn't have an explicit time-dependent evolution in their phenomenological quantities. But the interesting thing is that when we execute those processes in a sufficiently slow pace, what it is called *quasi-static process*, it turns out that we can achieve with good approximation a theoretical equilibrium process. In this chapter we are going to give a review of the core ideas of the classical thermodynamics[6] to contrast with a more modern approach given by non-equilibrium thermodynamics and in particular the steady state thermodynamics which is analogous to the equilibrium thermodynamics in the sense that its macroscopic properties do not change in time but the system is still out-of-equilibrium.

1.1.1 Internal energy and the first law of thermodynamics

A thermodynamic system can be characterized by a quantity called **internal energy** which quantifies the total energy of the system and is uniquely determined by the current state of it, therefore, the internal energy is called a state function. In order to build this quantity we first pick two arbitrary points A and C in a p-V diagram (See Fig. 1), that characterizes the state of a system in equilibrium, and associate to them the internal energies U_A and U_C respectively. The next step is to connect these two energies by means of a adiabatic curve $A \to B$ where only work $W_{A\to B}$ is extracted from the system and an isochoric $B \to C$ where only heat $Q_{B\to C}$ is exchanged with an external bath. By following the process described above we relate the internal energies U_A and U_C by means of

$$U_C = U_A + W_{A\to B} + Q_{B\to C}. \tag{1.1}$$

Considering that we can connect any pair of points in the p-V diagram by means of an adiabatic and an isochoric, once we have fixed the value of the internal energy of an

arbitrary point A, we are able to calculate the internal energy of any other point C.

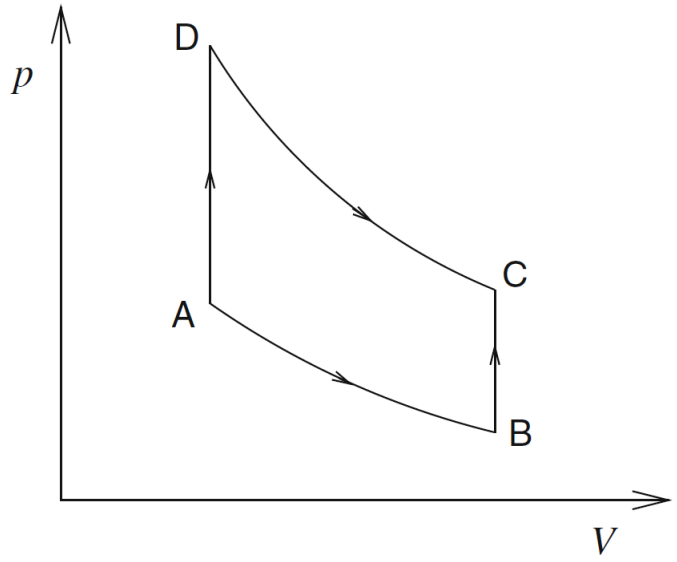

Figure 1 – p-V diagram used to define the internal energy.

Source: By the author.

We could interconnect the points A and C through a different path A $\rightarrow$ D $\rightarrow$ C which results in

$$U_C = U_A + Q_{A\rightarrow D} + W_{D\rightarrow C}. \tag{1.2}$$

Notice that along this new process the heat and work produced are different than the first presented path, which needs to be the case considering that these two quantities are path-dependent. But the variation in internal energy $\Delta U = U_C - U_A$ is exactly the same, and this is what is called the first law of thermodynamics or *principle of conservation of energy*, turning the internal energy a state variable or path-independent variable. In conclusion, for a small variation of the system we can write the first law in a differential form

$$dU = đW + đQ, \tag{1.3}$$

with đW being the work and the type of energy variation that can be controlled and used in a useful manner and đQ, called heat, is the wasted part, that we don't have direct control. It is important to point out that these two types of energy can be converted between each other, feature used by the heat engines to use energy from a heat source and generate work for a certain application.

1.1.2 Carnot cycle and the second law of thermodynamics

The most famous thermodynamic cycle is the Carnot one, which is very justifiable considering that it is the cycle that has the highest attainable efficiency for an engine operating among two thermal reservoirs and is used as statement, in a more application-oriented fashion, of the second law of thermodynamics. The cycle is composed of four

strokes, with two isothermals and two adiabatics. In order to describe this cycle imagine a gas, which will be the working substance (WS) of the engine, inside a container with a volume that can be varied at will allowing for the application or extraction of work. The gas also can exchange heat with an external bath. The gas starts at thermal equilibrium with temperature $\mathrm{T_A} = \mathrm{T_h}$ (See Fig. 2) equal to a hot bath's temperature. The WS undergoes an isothermal equilibrium process ($\mathrm{A} \rightarrow \mathrm{B}$) in contact with this bath receiving amount of heat $Q_{\mathrm{A}\rightarrow\mathrm{B}} = Q_h$ and applying work $W_{\mathrm{A}\rightarrow\mathrm{B}}$ in an external system. The next stroke is a quasi-static adiabatic expansion ($\mathrm{B} \rightarrow \mathrm{C}$), therefore $Q_{\mathrm{B}\rightarrow\mathrm{C}} = 0$, and the work is given by $W_{\mathrm{B}\rightarrow\mathrm{C}}$. Along this process the temperature is slowly varying and the system is always described by a thermal state. The final temperature at this stroke $\mathrm{T_C}$ must be equal to the temperature of the cold bath T_c to be used in the next stroke in order to keep the system in equilibrium. The WS is now isothermally compressed ($\mathrm{C} \rightarrow \mathrm{D}$) with a temperature T_c, delivering heat to the cold bath equal to $Q_{\mathrm{C}\rightarrow\mathrm{D}} = Q_c$ and with work $W_{\mathrm{C}\rightarrow\mathrm{D}}$ applied on WS. To finish this cycle off, the WS goes through a final adiabatic compression ($\mathrm{D} \rightarrow \mathrm{A}$) with $Q_{\mathrm{D}\rightarrow\mathrm{A}} = 0$ and $W_{\mathrm{D}\rightarrow\mathrm{A}}$. The temperature changes along this stroke finishing the cycle with the same initial temperature T_h. The interesting thing to be noticed here is that the WS is always in equilibrium, which makes this cycle reversible.

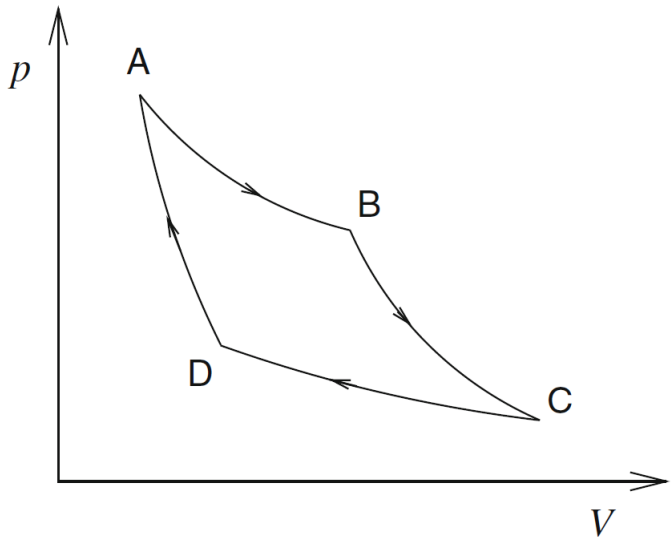

Figure 2 – p-V plot of a Carnot cycle. This cycle is composed of 4 strokes, being $\mathrm{A} \rightarrow \mathrm{B}$ an isothermal expansion, $\mathrm{B} \rightarrow \mathrm{C}$ an adiabatic expansion, $\mathrm{C} \rightarrow \mathrm{D}$ an isothermal compression and $\mathrm{D} \rightarrow \mathrm{A}$ an adiabatic compression.

Source: By the author.

The efficiency of the cycle is defined as the amount of absorbed heat Q_h that is converted into work $W = W_{\mathrm{A}\rightarrow\mathrm{B}} + W_{\mathrm{B}\rightarrow\mathrm{C}} + W_{\mathrm{C}\rightarrow\mathrm{D}} + W_{\mathrm{D}\rightarrow\mathrm{A}}$, given by $\eta = W/Q_h$. Using the conservation of energy of the first law we have that $W = Q_h - |Q_c|$, therefore the efficiency acquires the form $\eta = 1 - |Q_c|/Q_h$. And here comes the formulation of Carnot principles, that states that **(a)** all heat engines operating between two thermal reservoirs are less

efficient than their associated Carnot cycle operating between those same reservoirs, and **(b)** the efficiency associated to any Carnot cycle depends only on the temperatures of the baths used in it. Which makes us to conclude that the term $|Q_c|/Q_h$ has some functional dependence with T_h and T_c, like in $|Q_c|/Q_h = f(\mathrm{T}_h, \mathrm{T}_c)$. Now we will be using this information to obtain f. Imagine the Carnot cycle with either absorbed and damped heat equal to Q_1 and Q_2 respectively which forms the following relation

$$\frac{|Q_2|}{Q_1} = f(\mathrm{T}_1, \mathrm{T}_2). \tag{1.4}$$

The heat damped by this engine is used as input heat in a second Carnot cycle

$$\frac{|Q_3|}{|Q_2|} = f(\mathrm{T}_2, \mathrm{T}_3). \tag{1.5}$$

Multiplying Eq. 1.5 by Eq. 1.4 gives us the equation $|Q_3|/Q_1 = f(\mathrm{T}_1, \mathrm{T}_2)f(\mathrm{T}_2, \mathrm{T}_3)$, but $|Q_3|/Q_1$ is also equal to $f(\mathrm{T}_1, \mathrm{T}_3)$ producing the following equation

$$f(\mathrm{T}_2, \mathrm{T}_3) = \frac{f(\mathrm{T}_1, \mathrm{T}_3)}{f(\mathrm{T}_1, \mathrm{T}_2)}. \tag{1.6}$$

Considering that the left side of the Eq. 1.6 is independent of T_1 we conclude that $f(\mathrm{A}, \mathrm{B}) = g(\mathrm{A})q(\mathrm{B})$, generating the expression

$$f(\mathrm{T}_2, \mathrm{T}_3) = \frac{g(\mathrm{T}_1)q(\mathrm{T}_3)}{g(\mathrm{T}_1)q(\mathrm{T}_2)} = \frac{q(\mathrm{T}_3)}{q(\mathrm{T}_2)}. \tag{1.7}$$

Therefore, the ratio of heats $|Q_3|/|Q_2| = q(\mathrm{T}_3)/q(\mathrm{T}_2)$. Monotonicity is the only property assumed on the function $q(\mathrm{T})$, for simplicity and to match with the linear dependence of the internal energy of an ideal gas, we choose $q(\mathrm{T}) = \mathrm{T}$. We conclude that the absorbed and damped heats determine the ratio of temperatures, therefore, in order to obtain a scale of temperature we have to use a reference temperature, like the triple point of water. Using the damped heat $|Q_3| = |Q_c|$ and the absorbed one $|Q_2| = Q_h$ we obtain the well known Carnot's efficiency

$$\eta = 1 - \frac{\mathrm{T}_c}{\mathrm{T}_h} = \eta_{\mathrm{C}}. \tag{1.8}$$

As we've mentioned before, this efficiency is used to express the second law of thermodynamics, which can be stated at the following form:

> *All heat engines operating between thermal reservoirs are less efficient than their associated Carnot cycle operating between those same reservoirs.*

1.1.3 Definition of entropy and the second law of thermodynamics in terms of entropy production

We will reformulate the previous definition of the second law through the introduction of a quantity called **entropy** defined for equilibrium processes and being a state

function. This quantity will be defined in a way that it does not change itself when the system undergoes a process along an adiabatic curve. The entropy of the system of interest will be represented by the letter S. A p-V diagram (see Fig. 3-(a)) is basically composed of a set of curves that has a constant temperature, called isotherms, and a set of adiabatics, where there is no heat being exchanged with the environment, and these curves sweep all the possible ordinate sets (p,V). In Fig. 3-(a) we have two curves formed by A $\rightarrow$ B and C $\rightarrow$ D that are isotherms with temperatures T_1 and T_2 respectively and two curves formed by A $\rightarrow$ C and B $\rightarrow$ D that form two adiabatics that will have an entropy equal to S_A and S_B respectively. The relation between S_B and S_A is defined as

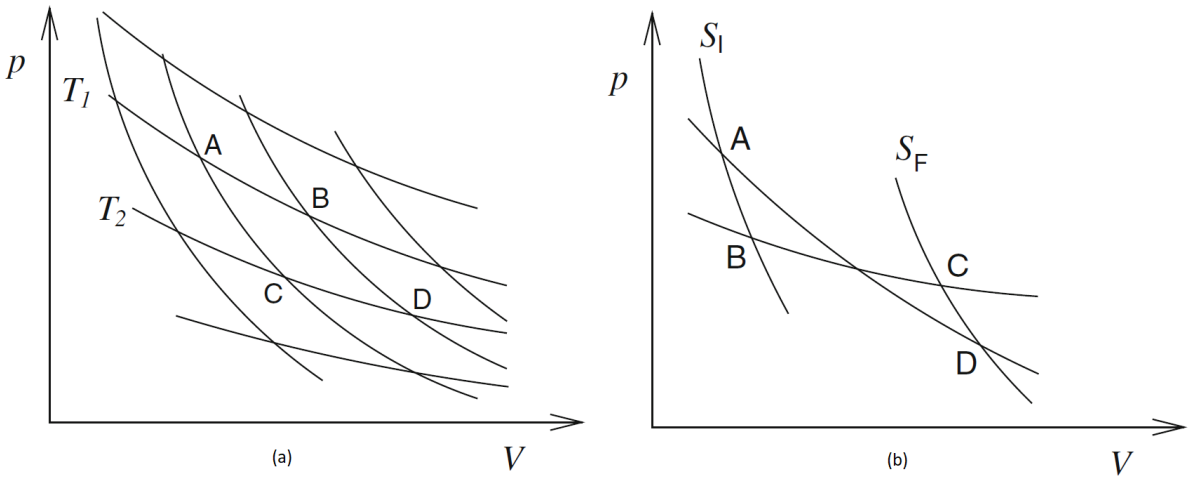

Figure 3 – (a) Adiabatics and isotherms in a p-V diagram. The curves formed by A $\rightarrow$ B and C $\rightarrow$ D form two isotherms with temperatures T_1 and T_2 respectively. The curves formed by A $\rightarrow$ C and B $\rightarrow$ D form two adiabatics with entropies S_A and S_B respectively. (b) p-V diagram used to obtain the Clausius equality.

Source: By the author.

$$S_B = S_A + \frac{Q_1}{T_1}, \tag{1.9}$$

where Q_1 is the amount of heat absorbed by the system from the bath of temperature T_1 when going from point A to B in Fig 3-(a). The other relation between S_B and S_A is obtained by going from C to D,

$$S_B = S_A + \frac{Q_2}{T_2}, \tag{1.10}$$

with Q_2 being the amount of heat absorbed by the system from the bath of temperature T_2. For the two equations 1.9 and 1.10 to be equal, the relation $Q_1/T_1 = Q_2/T_2$ must be true, which is actually in accordance with the Carnot's statement, so once we've defined the value of the entropy on a certain adiabatic, all the others will be defined. Actually we can generalize the above expressions through the Clausius equality which is valid for any equilibrium path. For any two points I and F in the phase-space the variation in entropy

is given by

$$S_{\mathrm{F}} - S_{\mathrm{I}} = \int \frac{đQ}{\mathrm{T}}, \tag{1.11}$$

where the integral is calculated over an arbitrary path. To prove this equality we first have to calculate the variation in entropy along an arbitrary path by means of an additional isotherm and adiabatics. To make things easier to understand we are going to focus on a monotonic decreasing curve as our arbitrary curve, but the analysis can be expanded to a more complex case. Therefore imagine that we have an arbitrary monotonic decreasing curve A $\rightarrow$ D as depicted in Fig. 3-(b) and we include two adiabatics represented by the paths A $\rightarrow$ B and C $\rightarrow$ D that have entropies equal to S_{I} and S_{F} respectively. Considering that those curves have the points A and D belonging to them, the entropies associated to these points will be given by S_{I} and S_{F} too. The points B and C were actually chosen in order to form an isotherm which work $\mathrm{W}_{\mathrm{A}\rightarrow\mathrm{B}\rightarrow\mathrm{C}\rightarrow\mathrm{D}}$ generated along the path A $\rightarrow$ B $\rightarrow$ C $\rightarrow$ D is equal to the work $\mathrm{W}_{\mathrm{A}\rightarrow\mathrm{D}}$ produced along the original arbitrary path A $\rightarrow$ D. Using the fact that $\mathrm{W}_{\mathrm{A}\rightarrow\mathrm{B}\rightarrow\mathrm{C}\rightarrow\mathrm{D}} = \mathrm{W}_{\mathrm{A}\rightarrow\mathrm{D}}$, the first law of thermodynamics and that the variation in internal energy is path-independent we conclude that $\mathrm{Q}_{\mathrm{A}\rightarrow\mathrm{B}\rightarrow\mathrm{C}\rightarrow\mathrm{D}} = \mathrm{Q}_{\mathrm{A}\rightarrow\mathrm{D}}$, with these being the heat absorbed by the system along those same paths. But considering that A $\rightarrow$ B and C $\rightarrow$ D are adiabatics we can further state that $\mathrm{Q}_{\mathrm{A}\rightarrow\mathrm{B}\rightarrow\mathrm{C}\rightarrow\mathrm{D}} = \mathrm{Q}_{\mathrm{B}\rightarrow\mathrm{C}}$ producing the equality $\mathrm{Q}_{\mathrm{A}\rightarrow\mathrm{D}} = \mathrm{Q}_{\mathrm{B}\rightarrow\mathrm{C}}$. By using this final equality and the definition of entropy we have that

$$S_{\mathrm{F}} - S_{\mathrm{I}} = \frac{Q_{\mathrm{B}\rightarrow\mathrm{C}}}{\mathrm{T}_{\mathrm{B}}} = \frac{Q_{\mathrm{A}\rightarrow\mathrm{D}}}{\mathrm{T}_{\mathrm{B}}}. \tag{1.12}$$

The problem with this last expression is that we still don't have the temperature T_{A} of the initial point but this can be solved by taking this arbitrary path small enough to the point where $\mathrm{T}_{\mathrm{B}} \rightarrow \mathrm{T}_{\mathrm{A}}$:

$$S_{\mathrm{F}} - S_{\mathrm{I}} = \frac{Q_{\mathrm{A}\rightarrow\mathrm{D}}}{\mathrm{T}_{\mathrm{B}}} \rightarrow \frac{Q_{\mathrm{A}\rightarrow\mathrm{D}}}{\mathrm{T}_{\mathrm{A}}}. \tag{1.13}$$

That means that we can pickup any arbitrary path and divide it into those small paths where Eq. 1.13 is valid and calculate the net variation in entropy as

$$\sum_i \frac{Q_i}{\mathrm{T}_i}, \tag{1.14}$$

and obtaining Eq. 1.11 in limit of infinitesimal small paths. Therefore, given an equilibrium state of reference with entropy S_0, we can calculate the entropy S of any equilibrium state of the system by means of an equilibrium process interconnecting them and using the Clausius equality $S = S_0 + \int đQ/\mathrm{T}$ or in its differential form $\mathrm{d}S = đQ/\mathrm{T}$ for infinitesimal steps. But that still lacks an ingredient towards the statement of the second law, which is what happens with the Clausius equality if the process interconnecting states are non-equilibrium process, it turns that this equality becomes the inequality

$$\mathrm{N} = S - S_0 - \int \frac{đQ}{\mathrm{T}} \geq 0. \tag{1.15}$$

This inequality means that the variation of entropy $\Delta S = S - S_0$ in the system along this process is not only due to exchange of heat with the bath, given by $\int \text{đ}Q/\text{T}$, but also due to some sort of created entropy N inside the system associated to the irreversible nature of the process. The equality holds for the reversible process where all the entropy variation inside the system is due to the flux of heat to the bath. Let's take a look in these statements in its differential form[7–9] and elaborate them even further. The variation of entropy $\text{d}S$ for the system of interest can be divided into two terms

$$\text{d}S = \text{d}S_e + \text{d}S_i, \tag{1.16}$$

with $\text{d}S_e$ being the entropy exchanged with the environment due to the flux of particles and(or) heat and $\text{d}S_i$ is the entropy produced inside the system. There is no constraint to $\text{d}S_e$, so the system can either receive or give entropy to the environment, but this freedom doesn't apply to the second term which must abide to the inequality

$$\text{d}S_i \geq 0 \tag{1.17}$$

which means that for any thermodynamic process no destruction of entropy is allowed, with the equality holding for equilibrium process. Using this last inequality we have that $\text{d}S \geq \text{d}S_e$. This is a formulation of the second law of thermodynamics and it can be analyzed in different contexts, for an **isolated system**, there is no heat or matter being exchanged with the environment and therefore no entropy flux, with $\text{d}S_e = 0$ making the variation in entropy of the system be completely generated by entropy production, $\text{d}S = \text{d}S_i$. Using Eqs. 1.16 and 1.17 the second law then reads

$$\text{d}S \geq 0, \tag{1.18}$$

which means that for an isolated system its total entropy cannot be decreased, i.e, a isolated system cannot become more organized. For a **closed system** heat is allowed to be exchanged with the environment but not matter, so there is a non-vanishing variation in the system's entropy $\text{d}S_e = \text{đ}Q/\text{T}$ due to flux of heat $\text{đ}Q$ to the external bath of temperature T. Using again the Eqs. 1.16 and 1.17 the second law is given by

$$\text{d}S \geq \frac{\text{đ}Q}{T}. \tag{1.19}$$

Notice that in this case the entropy S of the system can actually be decreased, which can be achieved by dumping more entropy into the bath, through heat ΔQ, than the amount created into the system. The important point here is that the amount created inside the system ($\text{d}S_i$) cannot be negative, implying that the total entropy, system plus bath, will increase. And for an **open system** both energy and matter are allowed to be exchanged. This adds a term of entropy flux $\text{d}S_{\text{mat}}$ due to the flux of matter and the reasoning to obtain the second law is the same used above.

1.1.4 Otto cycle

And to finish this chapter off the last but not least important topic is the one of the most famous and used cycle, which is the one used in internal combustion engines present in automobiles, it's the so-called Otto cycle. We are presenting this along with the Carnot's not only because of their importance in thermodynamics but in order to compare them with their quantum versions later on in this thesis. It is composed of four strokes as well, with two adiabatics and two isochorics as you can see in the p-V diagram 4.

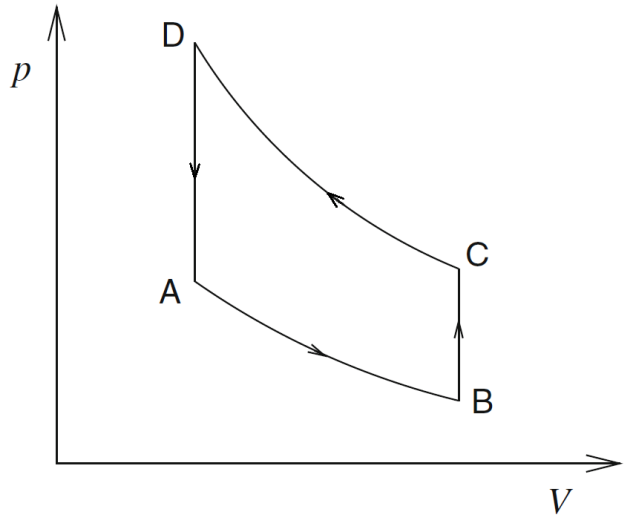

Figure 4 – p-V diagram of an Otto cycle. The cycle is composed of two adiabatics strokes, an expansion A → B and a compression C → D, and two isochoric strokes B → C and D → A

Source: By the author.

Two of the strokes are given by the adiabatics A → B and C → D generating only work as consequence:

$$\begin{aligned} W_{A\to B} &= U_B - U_A, \\ W_{C\to D} &= U_D - U_C. \end{aligned} \tag{1.20}$$

To complete the cycle two isochorics are added exchanging heat with the environment

$$\begin{aligned} Q_{B\to C} &= U_C - U_B, \\ Q_{D\to A} &= U_A - U_D. \end{aligned} \tag{1.21}$$

The efficiency of this cycle is given by

$$\eta_{\text{Otto}} = -\frac{W_{A\to B} + W_{C\to D}}{Q_{B\to C}} = 1 - \frac{U_D - U_A}{U_C - U_B}. \tag{1.22}$$

A special case for this cycle is obtained when we use an ideal gas as working substance that has an internal energy given by $U = cpV/R = NcT$, with c being a non-universal constant, which means that its value depends on the gas used, and R a universal constant,

called universal gas constant, and N the number of moles contained in the gas. In addition to that we know that an ideal gas has the following expressions for an adiabatic curve

$$\begin{aligned} \mathrm{pV}^{\gamma} &= \text{const}, \\ \mathrm{TV}^{\gamma-1} &= \text{const} \end{aligned} \tag{1.23}$$

with $\gamma = (c + R)/c$, which is a constant given by the gas used. Using those informations and the fact that $\mathrm{p_A} = \mathrm{p_D}$ and $\mathrm{p_B} = \mathrm{p_C}$ we obtain the following expression for the efficiency of a ideal gas along an Otto cycle:

$$\eta_{\mathrm{Otto}} = 1 - \left(\frac{\mathrm{V_A}}{\mathrm{V_B}}\right)^{\gamma-1} = 1 - \frac{\mathrm{T_B}}{\mathrm{T_A}} = 1 - \frac{\mathrm{T_C}}{\mathrm{T_D}}. \tag{1.24}$$

2 INTRODUCTION TO STOCHASTIC THERMODYNAMICS

2.1 What about small systems and small time scales?

As we stated before, the thermodynamics and their laws were designed to give a phenomenological description of systems with a large number of particles and for long-timing processes, but what happens when one scales all the way down to just a few particles and small time-scales, what is going to happen with those laws? Do they need to be reformulated? The answer turns out to be yes. At those scales the energy regime is of the order of thermal energy per degree of freedom and the fluctuations start to play a dominant rule producing non-negligible fluctuating heat and work, which means that they can be described by stochastic variables with a distribution function, implying for example that in a given process we don't know which value of work we will end up extracting. At those scales one could expect that heat could be converted to work, destroying entropy, apparently contradicting the second law as stated before for systems in the thermodynamic limit. And when we look at the equations of motion in time-reversible systems, both trajectories are allowed, the forward ones that creates entropy and their reversible counterparts that destroys entropy by the same amount. So how to reconcile the irreversible macroscopic phenomena that only creates entropy with those small systems that apparently violate this pattern? Trying to answer this question, Evans *et al.*[10] obtained an analytic expression for the probability that dissipative flux flows in a reversed direction, violating the second law in small systems and over short interval of times. But the interesting feature found was that the distribution of probabilities of those events happening, the ones that satisfy the second law and those that violate it as well, satisfy a strict constraint under the form of an equality called **fluctuation theorem**[11] and written as follows:

$$\frac{\mathrm{P}(\Sigma_t = a)}{\mathrm{P}(\Sigma_t = -a)} = e^a. \tag{2.1}$$

In this equation we have the probability $\mathrm{P}(\Sigma_t = a)$ of observing a trajectory of duration t that produces an amount of entropy $\Sigma_t = a$ with $a > 0$. This same trajectory can be executed in a reversed order and the probability of that happening is given by $\mathrm{P}(\Sigma_t = -a)$, destroying the same amount o entropy a, produced in the regular trajectory. The first feature that pops out of equation 2.1 when looking at its right side, is that the probability of $\mathrm{P}(\Sigma_t = a)$ of observing an entropy-producing trajectory is exponentially bigger than observing its entropy-decreasing counterpart $\mathrm{P}(\Sigma_t = -a)$, so in this sort of reformulated second law, decreasing entropy is not necessarily forbidden, it is just exponentially suppressed. The other thing that we can observe in this equation is that the exponential suppression increases with the entropy production Σ_t, and considering that entropy production is an extensive quantity that scales up with system's size and

time, therefore we immediately answer the question of why we don't observe those entropy-decreasing process in our everyday life.

Using equation 2.1 and Jensen's inequality $f\left(\langle \mathrm{X} \rangle\right) \geq \langle f(\mathrm{X}) \rangle$, with $\langle \cdot \rangle$ being the mean value in the possible outcomes of the stochastic variable X, $\{x \in \mathrm{X}, \mathrm{P}(x)\}$, given by

$$\langle f(\mathrm{X}) \rangle = \int_{x \in \mathrm{X}} f(x)\mathrm{P}(x)\mathrm{d}x, \tag{2.2}$$

we obtain an inequality analogous to the Clausius expression

$$\langle \Sigma \rangle \geq 0, \tag{2.3}$$

recovering the usual formulation by averaging over the set of possible outcomes $\mathrm{X} = \Sigma_t = a$. Actually this is only one of many other fluctuation theorems[11,12] that are at the heart of what is called **stochastic thermodynamics**[13,14] that takes the old thermodynamics to a whole new level, describing small systems and small time-scale process, where the fluctuations take their toll.

2.1.1 Relating fluctuations of work with equilibrium Helmholtz free energy

Here we present one of the most important classical fluctuation theorems that deals with the statistics on work and relates them with the good and old equilibrium Helmholtz free energy. The first derivation of this relation was presented by C. Jarzynski[15] as an equality relating the averaged exponential of work over an ensemble of executions with the exponential of Helmholtz free energy difference between equilibrium states associated with the ending points related to this process, this equality is called Jarzynski's equality and it is given by

$$\langle e^{-\beta \mathrm{W}} \rangle = e^{-\Delta \mathrm{F}}. \tag{2.4}$$

Rather than presenting a derivation of the equality itself, we will do it to its associated fluctuation theorem, which was actually derived by G. Crooks[16,17] after Jarzynski's work, and from there we recover Eq. 2.4.

Consider a finite classical system described by the Hamiltonian $\mathrm{H}(\Gamma_t, \lambda_t)$ with Γ_t being its microstate at time t, given by its internal degrees of freedom, like position and momentum, and λ_t the externally controlled work-parameter, like volume. This system is in contact with a heat bath of temperature $\mathrm{T} = \beta^{-1}(k_\mathrm{B} = 1)$. This system will evolve in time, from $t = 0$ up to $t = t_{\max}$, where the work parameter follows a predetermined protocol $\vec{\lambda}$ and the microstates as well with trajectory given by $\vec{\Gamma}$. The time-evolution is discretized in n intervals $t_{\max}/n$, with current time given by $t_i = it_{\max}/n$. Using this discretization the protocol and phase-space trajectory are evaluated in $\vec{t} = (t_1, ..., t_n)$ with $\vec{\lambda} = (\lambda_1, ..., \lambda_n)$ and $\vec{\Gamma} = (\Gamma_1, ..., \Gamma_n)$ respectively. We also assume that the system is **Markovian**[18] which means that the transition probability from Γ_i to Γ_{i+1} for a given parameter λ_{i+1}, given by $\mathrm{P}(\Gamma_i \to \Gamma_{i+1}|\lambda_{i+1})$, is independent of its past. This can be summarized in the following

equation where the probability of following the path $\Gamma_0 \xrightarrow{\lambda_1} \Gamma_1 \xrightarrow{\lambda_2} \Gamma_2 \cdots \Gamma_{n-1} \xrightarrow{\lambda_n} \Gamma_n$ in phase space can be decomposed as

$$\Pr\left(\Gamma_0 \xrightarrow{\lambda_1} \Gamma_1 \xrightarrow{\lambda_2} \Gamma_2 \cdots \Gamma_{n-1} \xrightarrow{\lambda_n} \Gamma_n\right) = \mathrm{P}(\Gamma_0 \to \Gamma_1|\lambda_1)\mathrm{P}(\Gamma_1 \to \Gamma_2|\lambda_2)\cdots\mathrm{P}(\Gamma_{n-1} \to \Gamma_n|\lambda_n). \tag{2.5}$$

In addition to markovianity we assume that the system satisfies **detailed balance**

$$\mathrm{P}(\Gamma_i \to \Gamma_j|\lambda)e^{-\beta \mathrm{H}(\Gamma_i,\lambda)} = \mathrm{P}(\Gamma_i \leftarrow \Gamma_j|\lambda)e^{-\beta \mathrm{H}(\Gamma_j,\lambda)}, \tag{2.6}$$

with $\mathrm{P}(\Gamma_i \to \Gamma_j|\lambda)$ being the probability of transition from the microstate Γ_i to Γ_j with a work-parameter fixed in λ. Notice that the exponential $e^{-\beta \mathrm{H}(\Gamma_{i(j)},\lambda)}$ comes from the Gibbs distribution.

In order to start the process, we first prepare the system in a Gibbs state $\mathrm{p}_{eq}(\Gamma_0, \lambda_0) \propto e^{-\beta \mathrm{H}(\Gamma_0,\lambda_0)}$ by letting it thermalize with the bath. Once thermalization is achieved, it is time to initiate the forward process, the one that creates entropy, but first we define a forward step through the sequence $(\Gamma_i, \lambda_i) \to (\Gamma_i, \lambda_{i+1}) \to (\Gamma_{i+1}, \lambda_{i+1})$, where we update the working parameter and then the system undergoes a random jump to the next microstate. The system then undergoes the complete forward path $\vec{\Gamma}$ and associated with that we have the variation in internal energy

$$\Delta \mathrm{U} = \mathrm{H}(\Gamma_n, \lambda_n) - \mathrm{H}(\Gamma_0, \lambda_0) = \mathrm{W} + \mathrm{Q}, \tag{2.7}$$

which is a state function and consequently path-independent, and the two path-dependent quantities, work and heat

$$\begin{aligned} \mathrm{W} &= \sum_{i=0}^{n-1} \mathrm{H}(\Gamma_i, \lambda_{i+1}) - \mathrm{H}(\Gamma_i, \lambda_i), \\ \mathrm{Q} &= \sum_{i=0}^{n-1} \mathrm{H}(\Gamma_{i+1}, \lambda_{i+1}) - \mathrm{H}(\Gamma_i, \lambda_{i+1}). \end{aligned} \tag{2.8}$$

Once the last change on the working-parameter is complete we let the system relax again in a thermal state $\mathrm{p}_{eq}(\Gamma_n, \lambda_n) \propto e^{-\beta \mathrm{H}(\Gamma_n,\lambda_n)}$. The probability of undergoing this trajectory is given by

$$\mathrm{P}_{\mathrm{F}}(\vec{\Gamma}) = \mathrm{p}_{eq}(\Gamma_0, \lambda_0)\Pr\left(\Gamma_0 \xrightarrow{\lambda_1} \Gamma_1 \xrightarrow{\lambda_2} \Gamma_2 \cdots \Gamma_{n-1} \xrightarrow{\lambda_n} \Gamma_n\right) = \mathrm{p}_{eq}(\Gamma_0, \lambda_0) \prod_{i=0}^{n-1} \mathrm{P}(\Gamma_i \to \Gamma_{i+1}|\lambda_{i+1}). \tag{2.9}$$

The backwards or conjugated trajectory $\vec{\Gamma}^{\dagger} = (\Gamma_n, ..., \Gamma_0)$ is obtained by following the same steps as the original one but in reversed order. The backward step is $(\Gamma_{i+1}, \lambda_{i+1}) \leftarrow (\Gamma_{i+1}, \lambda_i) \leftarrow (\Gamma_i, \lambda_i)$ and the probability of executing this backward trajectory is given by

$$\mathrm{P}_{\mathrm{B}}(\vec{\Gamma}^{\dagger}) = \mathrm{p}_{eq}(\Gamma_n, \lambda_n)\Pr\left(\Gamma_0 \xleftarrow{\lambda_1} \Gamma_1 \xleftarrow{\lambda_2} \Gamma_2 \cdots \Gamma_{n-1} \xleftarrow{\lambda_n} \Gamma_n\right) = \mathrm{p}_{eq}(\Gamma_n, \lambda_n) \prod_{i=0}^{n-1} \mathrm{P}(\Gamma_i \leftarrow \Gamma_{i+1}|\lambda_{i+1}). \tag{2.10}$$

In the backward trajectory the work W_B is equal to $-W$. Dividing the Eq. 2.9 by the Eq. 2.10 and using the property of detailed balance we obtain a fluctuation theorem for a specific trajectory $\vec{\Gamma}$ and their respective conjugate $\vec{\Gamma}^{\dagger}$[16]:

$$\frac{P_F(\vec{\Gamma})}{P_B(\vec{\Gamma}^{\dagger})} = e^{\beta(W_F(\vec{\Gamma})-\Delta F)} \tag{2.11}$$

with $\Delta F = F(\lambda_n) - F(\lambda_0)$ being the variation in Helmholtz free energy $F(\lambda_\alpha) = -\beta^{-1}\sum_{\Gamma_i} e^{-\beta E(\Gamma_i,\lambda_\alpha)}$ associated to the equilibrium states of the initial (Γ_0, λ_0) and final (Γ_n, λ_n) coordinated pairs defining the state of the system. But we want to go one step further and derive a fluctuation theorem for the work produced along the trajectories, so we integrate over all possible paths, obtaining the probability distribution of producing a amount of work $W(-W)$

$$\begin{aligned} \Pr(W) &= \int d\vec{\Gamma} P_F(\vec{\Gamma})\delta(W - W_F(\vec{\Gamma})), \\ \Pr(-W) &= \int d\vec{\Gamma}^{\dagger} P_B(\vec{\Gamma}^{\dagger})\delta(W - W_B(\vec{\Gamma}^{\dagger})). \end{aligned} \tag{2.12}$$

Doing the same thing on equation 2.11 we finish it off with the Crooks fluctuation theorem[17]

$$\frac{\Pr(W)}{\Pr(-W)} = e^{\beta(W-\Delta F)} \tag{2.13}$$

relating the distribution work produced in the forward and backward trajectories with the variation in Helmholtz free energy. Integrating Eq. 2.13 over the ensemble of possible amounts of work W we recover the so-called Jarzynski's equality $\langle e^{-\beta W}\rangle = e^{-\beta\Delta F}$.

2.1.2 Quantum fluctuation theorems

Now that we have some insights about how thermodynamics work at out-of-equilibrium small systems it's time to spice it up a bit and see what happens when those systems reach a quantum regime. In quantum mechanics the physical quantities are described by Hermitian operators, called **observables**, that act on the state of the system at a given time and extract the possible values for those specific physical quantities, e.g. the operator position $\hat{X}$ extracts the possible positions x for a given system, so it's fair to say that the physical quantities described by observables are state functions because they only depend on the state of the system at the time that they being measured. But as we all know, work is a path-dependent quantity, so it can't be represented by an observable, actually P. Talkner et. al.[19] demonstrated that the characteristic function of the work probability distribution is given by a time-ordered correlation function of the exponential of the system's Hamiltonian rather than expectation values on an operator associated to work and that is the first issue that must be addressed in order to obtain the quantum version of the fluctuation theorem for work.[20–25]

Analogous to the classical case we have a quantum system described the Hamiltonian operator $\hat{H}(\lambda_t)$, with a classical work-parameter λ_t. This system is put in equilibrium with

a bath of temperature $\mathrm{T} = \beta^{-1}$ and with the work-parameter fixed in λ_0 and consequently described by the Gibbs state $\hat{\rho}_{\mathrm{th}}(\lambda_0) = e^{-\beta\hat{\mathrm{H}}(\lambda_0)}/Z(\lambda_0)$ with $Z(\lambda_0) = \mathrm{tr}\left(\mathrm{e}^{-\beta\hat{\mathrm{H}}(\lambda_0)}\right)$. There is nothing different from the classical version so far, but here is where the applied work comes into play, as we've mentioned before, we can't associate to it an observable $\hat{\mathrm{W}}$, and in order to overcome this issue J. Kurchan[20] used the two measurement approach. In this approach we first apply a measurement on the initial state $\hat{\rho}_{\mathrm{th}}(\lambda_0)$ using the system's energy eigenbasis $\{\mathrm{E}_n(\lambda_0), |\mathrm{E}_n(\lambda_0)\rangle\}$ associated with the initial Hamiltonian $\hat{\mathrm{H}}(\lambda_0)$, collapsing the system in one of its eigenstates

$$\hat{\rho_n} = \frac{\Pi_n(\lambda_0)\hat{\rho}_{\mathrm{th}}(\lambda_0)\Pi_n^\dagger(\lambda_0)}{\mathrm{p}_n(\lambda_0)}, \tag{2.14}$$

with $\Pi_n(\lambda_0) = |\mathrm{E}_n(\lambda_0)\rangle\langle\mathrm{E}_n(\lambda_0)|$ and $\mathrm{p}_n(\lambda_0) = e^{-\beta\mathrm{E}_n(\lambda_0)}/Z(\lambda_0)$. After that, a unitary evolution U is applied on it, evolving the system isolated from the environment and varying the working parameter up to λ_1. At the end of it we measure the system one more time using the system's energy eigenbasis $\{\mathrm{E}_m(\lambda_1), |\mathrm{E}_m(\lambda_1)\rangle\}$ associated with the final Hamiltonian $\hat{\mathrm{H}}(\lambda_1)$ with the state of system becoming

$$\hat{\rho}_{m,n} = \frac{\Pi_m(\lambda_1)\mathrm{U}\hat{\rho_n}\mathrm{U}^\dagger\Pi_m^\dagger(\lambda_1)}{\mathrm{p}_{m|n}(\lambda_1)} = \frac{\Pi_m(\lambda_1)\mathrm{U}\Pi_n(\lambda_0)\hat{\rho}_{\mathrm{th}}(\lambda_0)\Pi_n^\dagger(\lambda_0)\mathrm{U}^\dagger\Pi_m^\dagger(\lambda_1)}{\mathrm{p}_{m|n}(\lambda_1)\mathrm{p}_n(\lambda_0)}, \tag{2.15}$$

with $\Pi_m(\lambda_1) = |\mathrm{E}_m(\lambda_1)\rangle\langle\mathrm{E}_m(\lambda_1)|$ and $\mathrm{p}_{m|n}(\lambda_1) = \mathrm{tr}\left(\Pi_m(\lambda_1)\mathrm{U}\hat{\rho_n}\mathrm{U}^\dagger\right) = |\langle\mathrm{E}_m(\lambda_1)|\mathrm{U}|\mathrm{E}_n(\lambda_0)\rangle|^2$. Once this process is completed we define the work along this trajectory $\mathrm{w}_{m,n}$ as the variation in energy from the first measurement when the system has an energy equal to $\mathrm{E}_n(\lambda_0)$, to second measurement, after the unitary evolution, when the energy is equal to $\mathrm{E}_m(\lambda_1)$:

$$\mathrm{w}_{m,n} = \mathrm{E}_m(\lambda_1) - \mathrm{E}_n(\lambda_0). \tag{2.16}$$

The probability of obtaining the work $\mathrm{w}_{m,n}$ is given by $\mathrm{p}_{m,n} = \mathrm{p}_{m|n}(\lambda_1)\mathrm{p}_n(\lambda_0)$ and we can use it to obtain the probability distribution of the work w given by

$$\mathrm{p}(\mathrm{w}) = \sum_{m,n} \delta\left[\mathrm{w} - (\mathrm{E}_m(\lambda_1) - \mathrm{E}_n(\lambda_0))\right] \mathrm{p}_{m,n}, \tag{2.17}$$

with $\delta[\cdot]$ being the Dirac delta function. The characteristic function $G(\mathrm{u})$ associated to

this distribution is given by

$$
\begin{aligned}
G(\mathrm{u}) &= \int d\mathrm{w} e^{i\mathrm{u}\mathrm{w}} \mathrm{p}(\mathrm{w}), \\
&= \sum_{m,n} \int d\mathrm{w} e^{i\mathrm{u}\mathrm{w}} \delta\left[\mathrm{w} - (\mathrm{E}_m(\lambda_1) - \mathrm{E}_n(\lambda_0))\right] \mathrm{p}_{m,n}, \\
&= \sum_{m,n} e^{i\mathrm{u}[\mathrm{E}_m(\lambda_1) - \mathrm{E}_n(\lambda_0)]} \langle \mathrm{E}_m(\lambda_1)|\mathrm{U}|\mathrm{E}_n(\lambda_0)\rangle\langle \mathrm{E}_n(\lambda_0)|\mathrm{U}^\dagger|\mathrm{E}_m(\lambda_1)\rangle \frac{e^{-\beta \mathrm{E}_n(\lambda_0)}}{Z(\lambda_0)}, \\
&= \sum_{m,n} \langle \mathrm{E}_m(\lambda_1)|\mathrm{U} e^{-i\mathrm{u}\hat{\mathrm{H}}(\lambda_0)} \frac{e^{-\beta \hat{\mathrm{H}}(\lambda_0)}}{Z(\lambda_0)} |\mathrm{E}_n(\lambda_0)\rangle\langle \mathrm{E}_n(\lambda_0)|\mathrm{U}^\dagger e^{i\mathrm{u}\hat{\mathrm{H}}(\lambda_1)}|\mathrm{E}_m(\lambda_1)\rangle, \\
&= \sum_{m} \langle \mathrm{E}_m(\lambda_1)|\mathrm{U} e^{-i\mathrm{u}\hat{\mathrm{H}}(\lambda_0)} \hat{\rho}_{\mathrm{th}}(\lambda_0) \left\{ \sum_n |\mathrm{E}_n(\lambda_0)\rangle\langle \mathrm{E}_n(\lambda_0)| \right\} \mathrm{U}^\dagger e^{i\mathrm{u}\hat{\mathrm{H}}(\lambda_1)}|\mathrm{E}_m(\lambda_1)\rangle, \\
&= \mathrm{tr}\left\{ \mathrm{U} e^{-i\mathrm{u}\hat{\mathrm{H}}(\lambda_0)} \hat{\rho}_{\mathrm{th}}(\lambda_0) \mathrm{U}^\dagger e^{i\mathrm{u}\hat{\mathrm{H}}(\lambda_1)} \right\}, \\
&= \mathrm{tr}\left\{ \mathrm{U}^\dagger e^{i\mathrm{u}\hat{\mathrm{H}}(\lambda_1)} \mathrm{U} e^{-i\mathrm{u}\hat{\mathrm{H}}(\lambda_0)} \hat{\rho}_{\mathrm{th}}(\lambda_0) \right\}, \\
&= \mathrm{tr}\left\{ e^{i\mathrm{u}\hat{\mathrm{H}}_{\mathrm{H}}(\lambda_1)} e^{-i\mathrm{u}\hat{\mathrm{H}}(\lambda_0)} \hat{\rho}_{\mathrm{th}}(\lambda_0) \right\} = \langle e^{i\mathrm{u}\hat{\mathrm{H}}_{\mathrm{H}}(\lambda_1)} e^{-i\mathrm{u}\hat{\mathrm{H}}(\lambda_0)} \rangle.
\end{aligned}
\tag{2.18}
$$

with $\hat{\mathrm{H}}_{\mathrm{H}}(\lambda_1) = \mathrm{U}^\dagger \hat{\mathrm{H}}(\lambda_1)\mathrm{U}$ being the Heisenberg representation of the Hamiltonian. As we can see from the previous equations, the characteristic function $G(\mathrm{u})$ is given by the time-ordered correlation function $\langle e^{i\mathrm{u}\hat{\mathrm{H}}_{\mathrm{H}}(\lambda_1)} e^{-i\mathrm{u}\hat{\mathrm{H}}(\lambda_0)} \rangle$ evaluated on the initial ensemble described by $\hat{\rho}_{\mathrm{th}}(\lambda_0)$. To show in a more explicit form that this last sentence is time-ordered, we need to write the exponentials using the time-ordering operator, $e^{i\mathrm{u}\hat{\mathrm{H}}_{\mathrm{H}}(\lambda_1)} e^{-i\mathrm{u}\hat{\mathrm{H}}(\lambda_0)} = \mathrm{T}_{\leftarrow}\left[e^{i\mathrm{u}\left[\hat{\mathrm{H}}_{\mathrm{H}}(\lambda_1) - \hat{\mathrm{H}}(\lambda_0)\right]} \right]$. Notice that both operators were put together in the same exponential, and that holds due to the time-ordering operator. By manipulating the probability $\mathrm{p}(\mathrm{w})$ a little bit further we can derive the fluctuation theorem[20,21,26]:

$$
\begin{aligned}
e^{-\beta \mathrm{w}} \mathrm{p}(\mathrm{w}) &= e^{-\beta \mathrm{w}} \sum_{m,n} \delta\left[\mathrm{w} - (\mathrm{E}_m(\lambda_1) - \mathrm{E}_n(\lambda_0))\right] \left|\langle \mathrm{E}_m(\lambda_1)|\mathrm{U}|\mathrm{E}_n(\lambda_0)\rangle\right|^2 \frac{e^{-\beta \mathrm{E}_n(\lambda_0)}}{Z(\lambda_0)}, \\
&= \sum_{m,n} \delta\left[-\mathrm{w} - (\mathrm{E}_n(\lambda_0)) - \mathrm{E}_m(\lambda_1)\right] \left|\langle \mathrm{E}_n(\lambda_0)|\mathrm{U}^\dagger|\mathrm{E}_m(\lambda_1)\rangle\right|^2 \frac{e^{-\beta \mathrm{E}_n(\lambda_0)}}{Z(\lambda_0)} e^{-\beta[\mathrm{E}_m(\lambda_1) - \mathrm{E}_n(\lambda_0)]}, \\
&= \sum_{m,n} \delta\left[-\mathrm{w} - (\mathrm{E}_n(\lambda_0)) - \mathrm{E}_m(\lambda_1)\right] \left|\langle \mathrm{E}_n(\lambda_0)|\mathrm{U}^\dagger|\mathrm{E}_m(\lambda_1)\rangle\right|^2 \frac{e^{-\beta \mathrm{E}_m(\lambda_1)}}{Z(\lambda_1)} \frac{Z(\lambda_1)}{Z(\lambda_0)}, \\
&= \frac{Z(\lambda_1)}{Z(\lambda_0)} \sum_{m,n} \delta\left[-\mathrm{w} - (\mathrm{E}_n(\lambda_0)) - \mathrm{E}_m(\lambda_1)\right] \left|\langle \mathrm{E}_n(\lambda_0)|\mathrm{U}^\dagger|\mathrm{E}_m(\lambda_1)\rangle\right|^2 \frac{e^{-\beta \mathrm{E}_m(\lambda_1)}}{Z(\lambda_1)}, \\
&= \frac{Z(\lambda_1)}{Z(\lambda_0)} \mathrm{p}(-\mathrm{w}) = e^{-\beta \Delta \mathrm{F}} \mathrm{p}(-\mathrm{w}),
\end{aligned}
\tag{2.19}
$$

where $Z(\lambda_1)/Z(\lambda_0) = e^{-\beta \Delta \mathrm{F}} = e^{-\beta[\mathrm{F}(\lambda_1) - \mathrm{F}(\lambda_0)]}$ and $\mathrm{p}(-\mathrm{w})$ is given by

$$
\mathrm{p}(-\mathrm{w}) = \sum_{m,n} \delta\left[-\mathrm{w} - (\mathrm{E}_n(\lambda_0)) - \mathrm{E}_m(\lambda_1)\right] \left|\langle \mathrm{E}_n(\lambda_0)|\mathrm{U}^\dagger|\mathrm{E}_m(\lambda_1)\rangle\right|^2 \frac{e^{-\beta \mathrm{E}_m(\lambda_1)}}{Z(\lambda_1)}, \tag{2.20}
$$

and analogous to the classical version, represents the probability of producing negative work $-\mathrm{w}$ along the conjugated paths obtained by reversing the unitary evolution U. And

we end up with the Tasaki-Crooks quantum fluctuation theorem

$$\frac{\mathrm{p(w)}}{\mathrm{p(-w)}} = e^{\beta(\mathrm{w}-\Delta\mathrm{F})}. \tag{2.21}$$

The interesting thing here is that in this case we have two types of fluctuations, the first one of classical origin, due to the contact with the bath forcing the system to equilibrate with it, and the second one of quantum origin, due to the uncertainty of the measurement.

2.2 Steady state thermodynamics

As we could see, out-of-equilibrium systems present a very rich behavior, having fluctuation theorems as one of their most astonishing features, creating constraints that limit the behavior of their fluctuating quantities. In general those systems have an explicit time-dependent behavior, but that is not a must when it comes to achieving out-of-equilibrium regimes, actually there is a special subset of states and process that don't have time-dependence and are still out-of-equilibrium states, i.e. there is a trade-off between production and flux of entropy in order to keep themselves in this steady configuration or to connect to other set of time-independent out-of-equilibrium states. These states are a common place in non-equilibrium thermodynamics and are known as **non-equilibrium steady states** or **non-equilibrium stationary states (NESS)**.[7] Considering this class of states and inspired by equilibrium thermodynamics, a new field of research started to be investigated, called **steady state thermodynamics (SST)**,[27–38] having the purpose of devising a phenomenological theory analogous to equilibrium thermodynamics, but this time working with NESS and the quasi-static process interconnecting them, dubbed **quasi-steady process**.

As we've seen before, when dealing with an equilibrium process for a closed system, the amount of heat đQ exchanged with a bath of temperature $\mathrm{T} = \beta^{-1}$ along an infinitesimal path in the parameter space, makes an infinitesimal amount of entropy $\mathrm{d}S = \beta$đQ flows from (to) the system of interest to (from) the bath. It's worth reaffirming here that this flux of heat truly changes the state of the system, by changing its probability distribution in the phase space or its density matrix in the quantum version. One of the first questions asked when formulating this new theory was concerned with the Clausius equality, what would be the version of it in this new context? Therefore, some reasoning concerning out-of-equilibrium states and process comes in handy to answer this question. Imagine that same system described by a Hamiltonian H_α, with α being a set parameters, and it being in contact with that same heat bath of temperature T, but this time we add an external source of energy, like an electric field or an additional bath which prevents this system of relaxing to an equilibrium state, so for a fixed set of working parameters the system ends up in a non-equilibrium steady-state. In a **first case** imagine that the system is already in that stationary state for that fixed α, and as times goes by, considering that

we are in an out-of-equilibrium evolution, entropy is being created inside the system and in order to keep it in that stationary state, all that entropy must be dumped into the bath. Therefore there is this type of energy flux responsible for keeping the system in that same initial stationary state for that same fixed set of parameters α, this energy was called **housekeeping heat** Q_{hk}.[27,28] Notice here that this energy does not actually change the entropy of the system and consequently its state, it's actually necessary to keep it the way that it is. Imagine now as **second case** that rather than keeping the set of parameters α fixed, we change them along a certain path. In this case, considering that we are in a non-equilibrium system, all the process will create entropy. Therefore, in analogy to the quasi-equilibrium process, we use a slow process that dissipates the least, called **quasi-steady process**.[28] Along this process the state of the system is going to change, and consequently its entropy, therefore in addition to the housekeeping heat, there must exist another energy term responsible for that, this term was called **excess heat** Q_{ex}. This analysis leads to the conclusion that during a quasi-steady process the total heat $Q_{tot} = Q_{hk} + Q_{ex}$ exchanged with the bath is composed of two terms, with only one of them being responsible for entropy variation in the system, leading to the modified Clausius equality defined as

$$\mathrm{d}S = \beta đQ_{ex}. \tag{2.22}$$

Steady state thermodynamics has received classical[27,28,39,40] and quantum[32,41–43] contributions. In an isolated quantum system[40] described by the Hamiltonian $\hat{\mathrm{H}}$ and in contact with a heat bath of temperature $\mathrm{T} = \beta^{-1}$, pumped in a way that produces a steady state $\hat{\rho}_{ss}$. Assuming that the entropy is given by the von Neumann entropy $\mathcal{S}(\hat{\rho}) = -\mathrm{tr}\left(\hat{\rho}\ln\hat{\rho}\right)$, for a steady state $\hat{\rho}_{ss}$ it is given by

$$\begin{aligned}\mathcal{S}(\hat{\rho}_{ss}) &= -\mathrm{tr}\left[\hat{\rho}_{ss}\ln\left(\hat{\rho}_{ss}\right)\right], \\ &= -\mathrm{tr}\left[\hat{\rho}_{ss}\ln\left(\hat{\rho}_{ss}\right)\right] + \left\{\mathrm{tr}\left[\hat{\rho}_{ss}\ln\left(\hat{\rho}_{th}\right)\right] - \mathrm{tr}\left[\hat{\rho}_{ss}\ln\left(\hat{\rho}_{th}\right)\right]\right\}.\end{aligned} \tag{2.23}$$

with $\hat{\rho}_{th} = e^{-\beta\mathrm{H}}/Z$. The last expression can be simplified using the relative entropy between states $\mathrm{S}(\hat{\rho}_{ss}||\hat{\rho}_{th}) = \mathrm{tr}\left[\hat{\rho}_{ss}\left(\ln\hat{\rho}_{ss} - \ln\hat{\rho}_{th}\right)\right]$, the internal $\mathcal{E} = \mathrm{U}(\hat{\rho}_{ss}) = \mathrm{tr}(\hat{\rho}_{ss}\hat{\mathrm{H}})$ energy associated with $\hat{\rho}_{ss}$ and the equilibrium Helmholtz free energy $\mathrm{F} = -\ln Z/\beta$:

$$\mathcal{S} = \beta\left\{\mathcal{E} - \left[\mathrm{F} + \mathrm{TS}(\hat{\rho}_{ss}||\hat{\rho}_{th})\right]\right\}. \tag{2.24}$$

An additional definition can be made by taking $\mathcal{F} = \mathrm{F} + \mathrm{TS}(\hat{\rho}_{ss}||\hat{\rho}_{th})$ which represents the generalized Helmholtz free energy[44–46]:

$$\mathcal{S} = \beta\left(\mathcal{E} - \mathcal{F}\right). \tag{2.25}$$

Along an infinitesimal isothermal quasi-steady process

$$\begin{aligned}\mathrm{d}\mathcal{S} &= \beta\left\{\mathrm{tr}(\mathrm{d}\hat{\rho}_{ss}\hat{\mathrm{H}}) + \left[\mathrm{tr}(\hat{\rho}_{ss}\mathrm{d}\hat{\mathrm{H}}) - \mathrm{d}\mathcal{F}\right]\right\}, \\ &= \beta\left\{đQ_{tot} - đQ_{hk}\right\} = \beta đQ_{ex},\end{aligned} \tag{2.26}$$

with $đQ_{tot} = \mathrm{tr}(d\rho_{ss}\mathrm{H})$ and $đQ_{hk} = \mathcal{F} - \mathrm{tr}(\rho_{ss}d\mathrm{H})$ are the total heat and the housekeeping heat respectively with the Clausius equality $\mathrm{d}\mathcal{S} = \beta đQ_{ex}$ being recovered for the excess heat $đQ_{ex} = đQ_{tot} - đQ_{hk}$.

2.3 Ergotropy and passive energy

A different way of looking at this problem, for systems that are not necessarily in a steady state is through the introduction of two types of energy, the *ergotropy* and the *passive energy*. To understand their meaning let's look back at he first law of thermodynamics again. The variation of internal energy is given by $\Delta E(t) = W(t) + Q(t)$, states that a variation of the internal energy along a thermodynamic process can be divided into two different parts, work $W(t)$ and heat $Q(t)$, where for Lindblad dynamics we have,[43,47]

$$\begin{aligned} W(t) &= \int_0^t \mathrm{tr}\left\{\rho(t')\dot{H}(t')dt'\right\}, \\ Q(t) &= \int_0^t \mathrm{tr}\left\{\dot{\rho}(t')H(t')dt'\right\}. \end{aligned} \tag{2.27}$$

Typically, work is understood as a controllable energy exchange, which can be used for something useful, while heat cannot be controlled, emerging from the unavoidable interaction of the engine with its environment. As stated before, there are certain situations in which it can be shown that part of $Q(t)$ does not cause any entropic variation.[48] This has led to proposals for the differentiation of two distinct forms of energy contributions to Q: the *passive energy* $\mathcal{Q}(t)$, which is responsible for the variation in entropy, and the variation in *ergotropy* $\Delta\mathcal{W}(t)$ which is a "work-like energy" that can be extracted by means of a cyclic unitary transformation not causing any entropic change. Both terms are defined as

$$\begin{aligned} \mathcal{Q}(t) &= \int_0^t \mathrm{tr}\left\{\dot{\pi}(t')H(t')dt'\right\}, \\ \Delta\mathcal{W}(t) &= \int_0^t \mathrm{tr}\left\{[\dot{\rho}(t') - \dot{\pi}(t')]H(t')dt'\right\}, \end{aligned} \tag{2.28}$$

with $\pi(t)$ being the passive state[49,50] associated with the state $\rho(t)$ at time t. A state $\hat{\pi}$ is said to be a *passive state* with respect to a Hamiltonian $\hat{H}$ if it satisfies the following two conditions:

1. If $\hat{\pi}$ commutes with $\hat{H}$ and consequently is diagonal with respect to the energy eigenbasis $\{|n\rangle\}$,

$$\begin{aligned} \hat{\pi} &= \sum_n r_n |n\rangle\langle n|, \\ \hat{H}|n\rangle &= E_n|n\rangle \end{aligned} \tag{2.29}$$

2. If π is not population inverted,

$$\begin{aligned} r_n &\geq r_{n+1}, \forall n \\ E_n &\leq E_{n+1}, \forall n \end{aligned} \tag{2.30}$$

Every state that does not satisfies these two conditions is called *non-passive state* with respect to this Hamiltonian.

An arbitrary state $\hat{\rho}$ can have a passive state associated to it and it can be obtained as follows. Given an arbitrary system $\hat{\rho}$ and a Hamiltonian $\hat{H}$, with $[\hat{\rho}, \hat{H}] \neq 0$, which makes the state $\hat{\rho}$ being non-passive. We can always find a passive state $\hat{\pi}$ associated to $\hat{\rho}$ via a unitary transformation V, through $\hat{\pi} = V\hat{\rho}V^{\dagger}$. First we have to decompose $\hat{\rho}$ in this its eigenbasis $\{|n\rangle, r_n\}$ ordering its eigenvalues in a decreasing way:

$$\hat{\rho} = \sum_n r_n |n\rangle\langle n|, \ r_n \geq r_{n+1}, \forall n. \tag{2.31}$$

After that we write a passive state using the eigenvalues $\{r_n\}$ keeping its ordering and the eigenbasis of $\hat{H}$, $\{|E_n\rangle\}$ in an increasing order:

$$\begin{aligned} \hat{\pi} &= \sum_n r_n |E_n\rangle\langle E_n|, \ r_n \geq r_{n+1}, \forall n, \\ \hat{H}|E_n\rangle &= E_n|E_n\rangle, \ E_n \leq E_{n+1}, \forall n. \end{aligned} \tag{2.32}$$

And the last step is to connect these two states $\hat{\pi}$, $\hat{\rho}$ via the unitary transformation $V = \sum_m |E_m\rangle\langle m|$, $\hat{\pi} = V\hat{\rho}V^{\dagger}$.

Therefore, in order to calculate the upper bound on the efficiency for systems that exhibit these different "flavors" of energy one should replace Q by $\mathcal{Q}$ in statements of the second law, since the *ergotropy* is essentially a mechanical type of energy, and consequently not limited by the second law, resulting in a different upper bound (see also Ref.[48]), so distinguishing these types of energy exchanged with the environment is crucial when one is interested in determining the fundamental upper bounds on the efficiency.

3 SUPERCONDUCTING QUBITS AND ITS INTERACTION WITH THE CAVITY

3.1 Josephson junction

In quantum mechanics the basic unity for storing and processing of quantum information is the qubit, which analogous to classical systems is just a two level system but with some quantum "ingredients" that makes them work in a very unique way. Usually most of the quantum systems have more than two levels which forces us to be a little bit inventive to restrict their dynamics in only two of those levels, generally the ones with lower energy. So in order to implement this qubit, the first thing that we should care about is the energy scales involved in the system, like temperature for example, which should not be too high or it will cause the levels of higher energy to be populated ruining our qubit. The other important thing that must be addressed is the connection (or transitions) between the two levels, so the energy gap that separates them must be unique, in this way if we apply an external stimulus with a frequency that matches the frequency of this gap, only transitions between these two levels are going to be stimulated, so a degree of anharmonicity is desired.

A system that can match these two criteria are the composition of two superconducting electrodes separated by a thin non-conducting material, forming the well known Josephson junction.[51] First let's take a quick look at the energy spectrum[52] of only one of this superconducting device. Supposing that the system has an even number of electrons, their ground state are going to be given by a single state $|N\rangle$ with N being the number of Cooper pairs formed by all the electrons composing this electrode. The first excited state is obtained by breaking one of these Cooper pairs and their energy gap is given by 2Δ and it is around several kelvin (See Fig. 5). In order to keep our system into the ground state $|N\rangle$ we must restrict our energy scales to low temperatures and frequencies in comparison to the gap 2Δ. Once those restrictions are satisfied we have only one state available, but that is not enough to build a qubit, that is why we add an additional superconducting electrode separated by a thin non-conducting material (See Fig. 5) and supposing once again an even number of electrons, and assuming the formation of $2N$ Cooper pairs equally divided between the electrodes and given by the state $|N, N\rangle$. But in this case we have an additional quantum feature, given by the coherent tunneling of those Cooper pairs between the electrodes through the thin barrier. This system is called Josephson junction.[51]

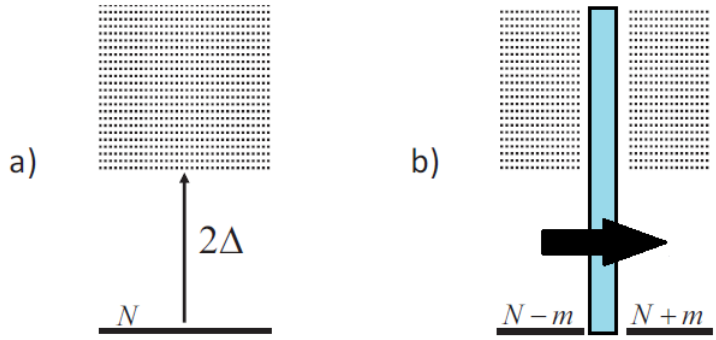

Figure 5 – (a) Spectrum of a superconducting electrode. (b) Josephson junction

Source: Adapted from GIRVIN, S. M.[53]

The number of Cooper pairs that tunnel through the junction are going to be given by the number m and this tunneling process gives rise to a set of degenerate states $\{|N-m, N+m\rangle\}$ (without Coulomb interaction) and it forms the so wanted qubit as far as it satisfies the aforementioned conditions. This system is described by the phenomenological Hamiltonian

$$\hat{\mathrm{H}} = -\frac{1}{2}\mathrm{E_J} \sum_{m=-\infty}^{\infty} (|m\rangle\langle m+1| + |m+1\rangle\langle m|) \tag{3.1}$$

with $\mathrm{E_J}$ being the Josephson coupling energy that quantifies the intensity of the tunneling process of Cooper pairs from one side to the other. The basis $\{|m\rangle\}$ with $m = -\infty ... + \infty$ represents the number of Cooper pairs that tunneled into the island, and the negative values represent the opposite process, when Cooper pairs tunnel out of it.

3.2 Cooper pair box (CPB)

Once we've understood the functioning of a Josephson junction it's time to use it in a circuit to build a qubit. The superconducting electrode on the right, depicted above in Fig. 5-b, at which we were counting the number of Cooper pairs that had tunneled to it, in the context of the circuit is going to be called the "island". And as before, the number of Cooper pairs that tunnel to it will still be counted and used to represent the state of the system. But in that case we haven't taken into account the Coulomb interaction between the charges that jumped into the island. In addition to those Cooper pairs that tunneled to the island we might have as well some other charges due to an applied voltage V_g used to induce the tunneling of Cooper pairs to the Island. There is also some unavoided capacitive couplings to other parts of the circuit which induces some additional charges in the island as well but we are not going to detail them here. The essential part of the circuit describing the qubit is given by the following image:

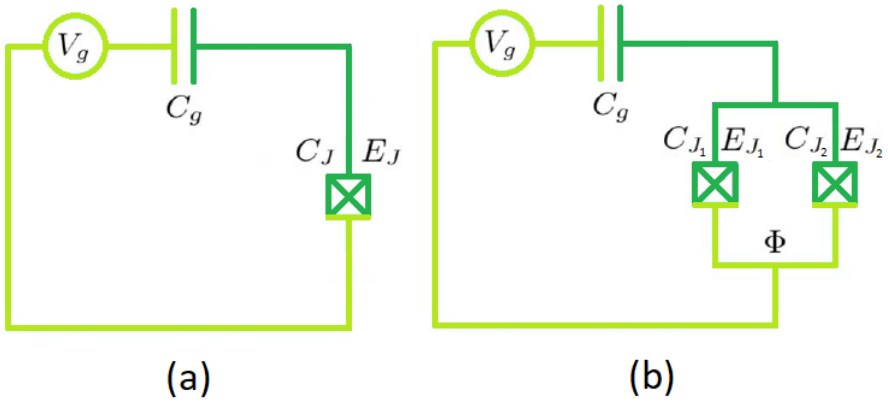

Figure 6 – (a) Simple sketch of the Cooper pair box circuit. The island is given by the greener part. (b) Also a Cooper pair box circuit but this time using two Josephson junctions in parallel forming a SQUID used to change the effective tunneling energy $\tilde{\mathrm{E}}_J$ through an external magnetic flux Φ.

Source: By the author.

Notice that this circuit is divided essentially in two different parts, the one tinted in light green is one of the superconducting electrodes used as a reservoir of Copper pairs and the greener part is the island itself. This system gives rise to the so called Cooper pair box (CPB).[54] By adding the Coulomb interaction term $4\mathrm{E_C}\left(\hat{n}-n_g\right)^2$ to Eq. 3.1 we end up with the CPB Hamiltonian

$$\hat{\mathrm{H}} = 4\mathrm{E_C}\left(\hat{n}-n_g\right)^2 - \frac{1}{2}\mathrm{E_J}\sum_{m=-\infty}^{\infty}\left(|m\rangle\langle m+1| + |m+1\rangle\langle m|\right), \tag{3.2}$$

with $\mathrm{E_C} = e^2/2\mathrm{C}_\Sigma$ being the charging energy. The total capacitance of the CPB is given by $\mathrm{C}_\Sigma = \mathrm{C_J} + \mathrm{C}_g$ and e being the fundamental charge of the electron. The additional voltage V_g added to the circuit is responsible for the additional charge n_g given by

$$n_g = \frac{\mathrm{C}_g V_g}{2e}. \tag{3.3}$$

The diagonalization of this Hamiltonian in the basis $\{|m\rangle\}$ is made numerically in a specific truncated subspace and the energy spectrum of its 3 lowest energy eigenstates as a function of the induced charge n_g, for $\mathrm{E}_J = \mathrm{E}_C$, is given as follows:

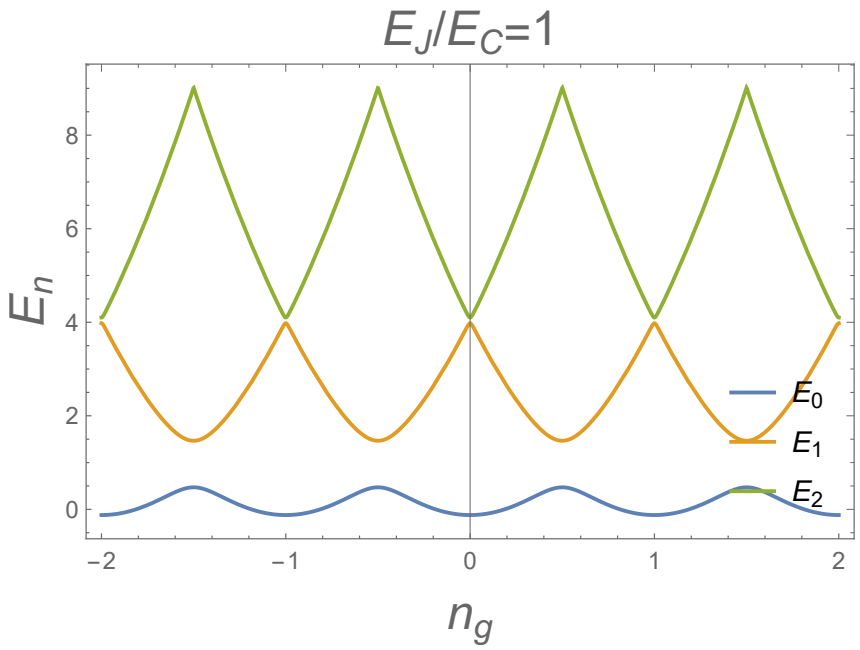

Figure 7 – First 3 energy levels of the CPB as a function of the induced charge n_g in the regime $\mathrm{E}_J/\mathrm{E}_C = 1$. The eigenvalues were obtained numerically using 10 energy levels, $m = \{-4, -3, ..., 4, 5\}$,

Source: By the author.

The energy spectrum has the desired anharmonicity to build a qubit. We've numerically obtained its eigenenergies. However, through a suitable change of basis, namely, the phase basis $\{|\varphi\rangle\}$, new insights can be obtained about the structure of this qubit. This basis will be useful later on when we discuss the behavior of the qubit energy levels through the application of an external magnetic flux. The vectors $|\varphi\rangle$ are defined in terms of the basis $\{|m\rangle\}$ as

$$|\varphi\rangle = \sum_{m=-\infty}^{\infty} e^{im\varphi}|m\rangle, \tag{3.4}$$

which straightforwardly leads to

$$|m\rangle = \int_0^{2\pi} d\varphi e^{-im\varphi}|\varphi\rangle, \tag{3.5}$$

the value φ represents the eigenvalues of the operator $\hat{\varphi}$ with eigenvector $|\varphi\rangle$, which is the quantum-mechanical phase difference across the Josephson junction, or phase difference between the wave functions describing the system in each one of the superconducting electrodes separated by the weak-link. Using Eq. 3.4 we can rewrite the Hamiltonian 3.1 in the following form:

$$\hat{\mathrm{H}} = -\mathrm{E_J}\cos(\hat{\varphi}), \tag{3.6}$$

with $\cos(\hat{\varphi})$ being given by

$$\cos(\hat{\varphi}) = \frac{1}{2}\sum_{m=-\infty}^{\infty}(|m\rangle\langle m+1| + |m+1\rangle\langle m|). \tag{3.7}$$

The quantum-mechanical phase operator $\hat{\varphi}$ represents the conjugated variable to the number operator $\hat{n}$, i.e. $[\hat{\varphi}, \hat{n}] = i$, with

$$\hat{n} = \sum_{m=-\infty}^{\infty} m|m\rangle\langle m| = i\frac{\partial}{\partial\varphi}. \tag{3.8}$$

By means of the above expressions we can rewrite the CPB Hamiltonian in the phase representation[55]:

$$\hat{\mathrm{H}} = 4\mathrm{E_C}\left(i\frac{\partial}{\partial\varphi} - n_g\right)^2 - \mathrm{E_J}\cos(\hat{\varphi}). \tag{3.9}$$

3.2.1 Flux quantization and the use of a SQUID to control the energy levels of a CPB

In the last section we've presented the CPB, but it's desirable to have a Josephson junction with properties that can be changed on demand. In order to implement that lets take a look at an important property of superconducting materials, the flux quantization. Through the Schrodinger's equation of a quantum system subjected to a magnetic field of vector potential A the current density is given by

$$\mathrm{J} = \frac{e\hbar}{2mi}\left(\psi^*\nabla\psi^* - \psi\nabla\psi^*\right) - \frac{e^2\mathrm{A}}{mc}\psi^*\psi. \tag{3.10}$$

The superconducting state can be described by the macroscopic wave function $\psi(\mathbf{r}) = \sqrt{n(\mathbf{r})}e^{\theta(\mathbf{r})}$[56,57] that describes the system as a whole, with $n(\mathbf{r})$ and $\theta(\mathbf{r})$ being respectively the Cooper pairs number density and its phase at position $\mathbf{r}$. Replacing this wave function at current density J we end up with the following expression:

$$\hbar\nabla\theta = e\Lambda\mathrm{J} + e\mathrm{A}/c, \tag{3.11}$$

with $\Lambda = 4\pi\lambda_\mathrm{L}^2/c^2$, where λ_L is the penetration depth of a magnetic field inside a superconductor, which is exponentially suppressed due to Meissner effect. Integrating this expression along a path connecting two points 1 and 2 leads to

$$\int_1^2\left(e\Lambda\mathrm{J} + \frac{e\mathrm{A}}{c}\right)\cdot\mathrm{d}\mathbf{r} = \hbar\int_1^2\nabla\theta\cdot\mathrm{d}\mathbf{r} = \hbar(\theta_2 - \theta_1). \tag{3.12}$$

Taking a closed path $(1 = 2)$ and using the fact that the wave function $\psi(\mathbf{r})$ must be single valued, the phase difference must be quantized, with $(\theta_2 - \theta_1) = 2\pi n$, $n \in \mathbb{Z}$ leading to a quantized integral

$$\lim_{1\to2}\int_1^2(c\Lambda\mathrm{J} + \mathrm{A})\cdot\mathrm{d}\mathbf{r} = \oint(c\Lambda\mathrm{J} + \mathrm{A})\cdot\mathrm{d}\mathbf{r} = \frac{\hbar c}{e}\oint\nabla\theta\cdot\mathrm{d}\mathbf{r} = \frac{2\pi n\hbar c}{e} = n\phi_0. \tag{3.13}$$

The interesting thing is that the integer values n have a dependence on the topology[58] of the piece of superconducting material (represented by gray squares in Fig. 8). Take for example a simply connected topology as depicted in Fig. 8-a, where there is no holes passing through the piece of superconducting material, which means that any loop Γ_1

built inside this piece of superconductor can be continuously deformed into smaller loops ($\Gamma_1 \to \Gamma_2 \to \Gamma_3 \cdots$) to the limit where it becomes a point Γ_∞ and in this case there is no variation in phase θ,

$$\oint_{\Gamma_\infty} \nabla\theta \cdot \mathrm{d}\mathbf{r} = 0, \tag{3.14}$$

which means that $\theta_1 = \theta_2$ and consequently the only possible value for the integer is $n = 0$. If we infinitesimally increase the size of the loop Γ_∞ the variation of phase still is going to be zero which means that if we keep doing that bit by bit up to an arbitrary loop, like Γ_1 for example, and still observing no variation of phase, we will conclude that the only possible value for the integer n, in any trajectory, is zero.

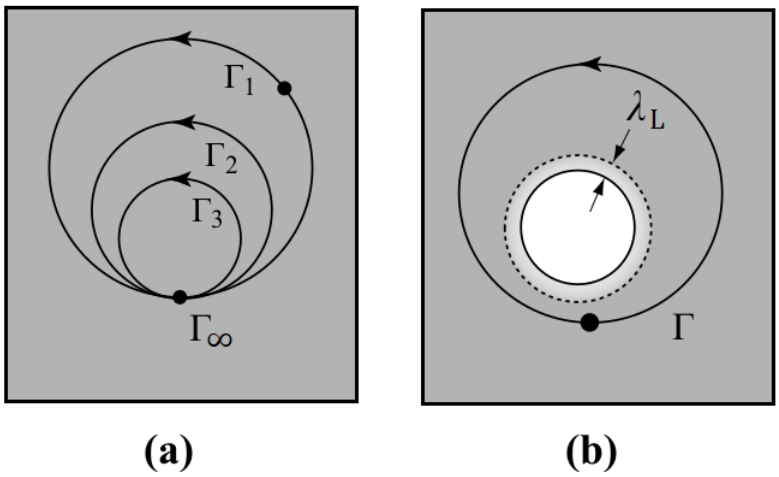

Figure 8 – (a) Simply connected topology (without holes) and (b) multiply connected topology (with at least one hole). In this case a ring-shaped piece, which contains only on hole.

Source: By the author.

The other topology that we'd like to address here is the multiply connected one, which has at least one hole in it, in Fig. 8-b we can see a ring-shaped topology, which contains only one hole. In this topology the path that contains the hole cannot be reduced up to a point, therefore there is no reason for the variation in phase to be zero in general, which means that the integer n is non-vanishing too. If the piece of superconducting material is thick enough, compared to the penetration depth λ_L, we can choose a path of integration far away from the border, with the supercurrent $\mathrm{J} = 0$ due to Meissner effect resulting in the following integration

$$\oint \mathrm{A} \cdot \mathrm{d}\mathbf{r} = \int \mathrm{B} \cdot \mathrm{d}\mathbf{s} = n\phi_0, \tag{3.15}$$

and as we can see the magnetic flux inside the ring is a quantized quantity and this feature is used to build a CPB structure with Josephson junctions with properties that can be adjusted by the use of an external magnetic field, therefore the CPB is built with two Josephson junctions that are put together in parallel as presented in Fig. 6-b, this structure

is known as **superconducting quantum interference device (SQUID)**[59] and it has a ring-shaped geometry and as we will see later, the resultant Josephson energy associated to it can be changed by the application of an external magnetic flux Φ through the loop formed by the two junctions. The Hamiltonian of tunneling of Cooper pairs associated to this new system is given by

$$\hat{\mathrm{H}}_J = -\mathrm{E}_{J_1}\cos\hat{\varphi}_1 - \mathrm{E}_{J_2}\cos\hat{\varphi}_2, \tag{3.16}$$

with E_{J_i} and φ_i being respectively the Josephson energy and phase difference across the i_{th} junction with $i = 1, 2$. The next step here is to write an expression relating these two phase differences φ_1 and φ_2 and in order to do that we are going to be using the quantization of the flux Φ applied on the SQUID producing the expression[51,56,57,60]

$$\varphi_1 - \varphi_2 = 2\pi n + 2\pi\frac{\Phi}{\Phi_0} \tag{3.17}$$

with $n \in \mathbb{Z}$ and $\Phi_0 = h/2e$ the flux quantum. Defining the quantities $\varphi = (\varphi_1 + \varphi_2)/2$, $\mathrm{E}_\Sigma = \mathrm{E}_{J_1} + \mathrm{E}_{J_2}$ and $\mathrm{d} = (\mathrm{E}_{J_1} - \mathrm{E}_{J_2})/(\mathrm{E}_{J_1} + \mathrm{E}_{J_2})$ and using the previous relation we can rewrite the Hamiltonian as follows:

$$\begin{aligned}\hat{\mathrm{H}}_J &= -\mathrm{E}_\Sigma\left[\cos\left(\pi\frac{\Phi}{\Phi_0}\right)\cos\hat{\varphi} + \mathrm{d}\sin\left(\pi\frac{\Phi}{\Phi_0}\right)\sin\hat{\varphi}\right], \\ &= \mathrm{E}_\Sigma\cos\left(\pi\frac{\Phi}{\Phi_0}\right)\sqrt{1+\mathrm{d}^2\tan^2\left(\pi\frac{\Phi}{\Phi_0}\right)}\cos\left(\hat{\varphi}-\varphi_0\right),\end{aligned} \tag{3.18}$$

with $\tan\varphi_0 = \mathrm{d}\tan(\pi\Phi/\Phi_0)$. This new expression works as a generalization of the previous case with only one Joseph junction where we have replaced the Josephson energy E_J by an effective Josephson energy $\mathrm{E}_\Sigma\cos(\pi\Phi/\Phi_0)\sqrt{1+\mathrm{d}^2\tan^2(\pi\Phi/\Phi_0)}$ controlled by an external magnetic field. In the limit of small asymmetry $\mathrm{d} \approx 0.1$ this effective Josephson energy becomes $\mathrm{E}(\Phi) \approx \mathrm{E}_J^{\max}\cos(\pi\Phi/\Phi_0)$.

3.2.2 Charge dispersion, anharmonicity and the transmon regime

As we've seen in the Fig. 7 the energy levels in the CPB change quite significantly with the variation of the induced charge n_g due to the gate voltage V_g (Actually the energy spectrum changes with the offset induced by the environment as well). The problem is that this charge can be hard to control and subjected to noise, which makes it vary randomly and consequently changing the energy spectrum in a random fashion as well. The interesting thing is that by changing the ratio $\mathrm{E}_J/\mathrm{E}_C$ we observe a change in the "landscape" of the energy spectrum that makes that oscillating pattern turns into an almost flat spectrum, independent of the induced charge n_g making it less susceptible to the variations of charge due to noise. This flattening can be seeing in the Fig. 10. But besides this desirable flattening of the energy spectrum we observe a reduction in its anharmonicity, i.e. the spacing between energy levels start to be constant, which raises

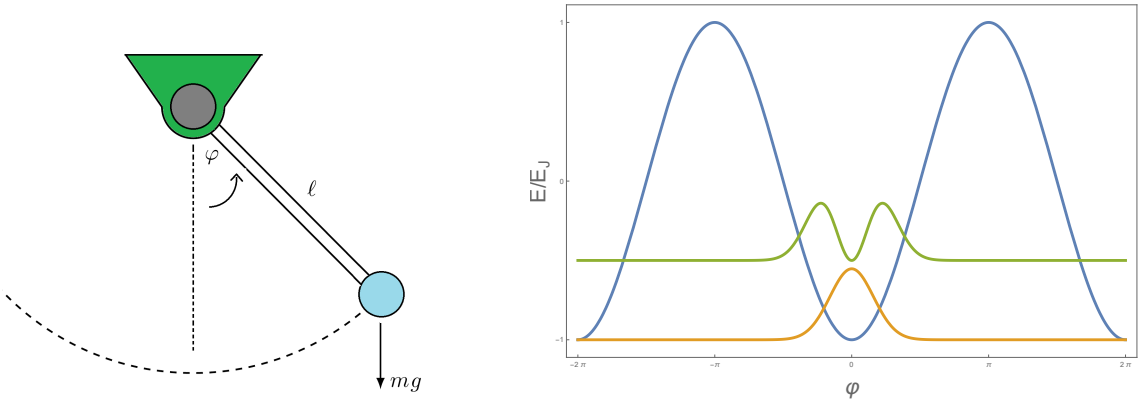

(a) (b)

Figure 9 – (a) Classical rotor of length l and described by the degree of freedom φ. (b) The rotor's potential energy as a function of the angle φ and its first two eigenstates.

Source: By the author.

the question if this system can be used as a qubit. And it turns out through the work of J. Koch et. al[61] that these two quantities, the **charge dispersion** and the **anharmonicity**, reduce in a different pace with the ratio $\mathrm{E}_J/\mathrm{E}_C$, luckily in a way that permits this new regime of increasing $\mathrm{E}_J/\mathrm{E}_C$ be used to build a qubit. Let's take a look at the charge dispersion behavior first, the CPB system can be described by a tight-biding model and the m_{th} energy state with energy $\mathrm{E}_m(n_g)$ can be approximated by the relation

$$\mathrm{E}_m(n_g) \approx \mathrm{E}_m(n_g = 1/4) + \frac{\epsilon_m}{2}\cos(2\pi n_g), \tag{3.19}$$

with charge dispersion given by $\epsilon_m = \mathrm{E}_m(n_g = 1/2) - \mathrm{E}_m(n_g = 0)$, which is essentially the difference between the smallest and the highest possible energy for the m_{th} energy level, therefore the smallest ϵ_m the more flat and independent of n_g the energy levels become. In the asymptotic regime $\mathrm{E}_J/\mathrm{E}_C >> 1$ the charge dispersion exponentially decreases with $\sqrt{8\mathrm{E}_J\mathrm{E}_C}$ as we can see in the following expression

$$\epsilon_m \approx (-1)^m \mathrm{E}_C \frac{2^{4m+5}}{m!}\sqrt{\frac{2}{\pi}}\left(\frac{\mathrm{E}_J}{2\mathrm{E}_C}\right)^{\frac{m}{2}+\frac{3}{4}} e^{-\sqrt{8\mathrm{E}_J\mathrm{E}_C}}. \tag{3.20}$$

But as we've seen, accompanied by this decrease in the sensitivity to the charge n_g there is a decrease in anharmonicity, which could compromise the use of this system as a qubit. In order to analyze this problem the authors at[61] mapped this system to a quantum charged rotor (See Fig. 9a) and used the approximation of small oscillations expanding the Hamiltonian as a Duffing oscillator around $\varphi = 0$. Therefore imagine a mass m attached to a rigid massless rod of length l fixed to a pivot without friction, used as the origin of the reference frame. The description of this system is given by cylindrical coordinates $(r = l, \varphi, z = 0)$. The mass is subjected to a gravitational field $\vec{g} = g\hat{x}$. Its potential energy is given by $\mathrm{U} = -mgl\cos\varphi$ and kinetic energy $\mathrm{E}_{\text{kin}} = \mathrm{L}_z^2/2ml^2$, where $\mathrm{L}_z = \left|\vec{\mathrm{L}}_z\right|$ with

$\vec{\mathrm{L}}_z = (\vec{r} \times \vec{p}) \cdot \hat{z}$ being the z-component of the angular momentum associated to the mass m. The quantized Hamiltonian of this system is given by

$$\hat{\mathrm{H}}_{\mathrm{rot}} = \frac{\hat{\mathrm{L}}_z^2}{2ml^2} - mgl\cos\hat{\varphi}, \tag{3.21}$$

with the angular momentum operator $\hat{\mathrm{L}}_z = -i\hbar\frac{\partial}{\partial\varphi}$. Notice that this Hamiltonian has almost the same functional dependence than the CPB Hamiltonian without the induced charge bias ($n_g = 0$), when we replace $\hat{n} \to \hat{\mathrm{L}}_z/\hbar$, $\mathrm{E}_J \to mgl$ and $\mathrm{E}_C \to \hbar/8ml^2$. In order to include a non-vanishing offset n_g we suppose that the particle in the problem is charged with a charge q and we apply a constant magnetic field $\vec{\mathrm{B}} = \mathrm{B}_0\hat{z}$ with vector potential $\vec{\mathrm{A}} = -y\mathrm{B}_0/2\hat{x} + x\mathrm{B}_0/2\hat{y} + 0\hat{z}$. In this new environment the momentum of the particle is transformed like $\vec{p} \to \vec{p} - q\vec{\mathrm{A}}$ which makes its angular momentum $\mathrm{L}_z \to \mathrm{L}_z + q\mathrm{B}_0 l^2/2$. Right now the mapping is complete with $n_g \to q\mathrm{B}_0 l^2/2\hbar$ and it's interesting to notice that in the original system (CPB), the operator $\hat{n}$ had discrete numbers and this quantization were obtained due to the fact that their states were single-valued, $\psi(\varphi + 2\pi) = \psi(\varphi)$, and this property is similarly reproduced in the rotor angular momentum $\hat{\mathrm{L}}_z$ due to the fact that after a complete rotation (2π) the rotor ends up subjected to the same potential $\mathrm{V}(\varphi + 2\pi) = \mathrm{V}(\varphi)$.

Considering that we are interested in the limit $\mathrm{E}_J/\mathrm{E}_C \gg 1$ (at least for the qubit case) which in the context of the rotor means that it is subjected to a strong gravitational field which makes it have a tendency to be in a small oscillations regime. Therefore looking at this behavior of small oscillations around the equilibrium position $\varphi = 0$ we expand the Hamiltonian up to fourth order

$$\hat{\mathrm{H}} = 4\mathrm{E}_C(\hat{n} - n_g)^2 - \mathrm{E}_J + \frac{\mathrm{E}_J}{2}\hat{\varphi}^2 - \frac{\mathrm{E}_J}{24}\hat{\varphi}^4. \tag{3.22}$$

An additional detail that is worth mentioning here is that for small energies the tunneling process across the potential barrier for the CPB, or a complete cycle for the rotor ($\Delta\varphi = 2\pi$), becomes less probable which allows us not to worry about the periodicity of the potential, which in fact was already lost when expanding $\cos\hat{\varphi}$ in a finite power law. And in the context of the rotor, the induced charge n_g is given by the external vector potential $\vec{\mathrm{A}}$ and it only manifests itself in complete cycles due to Aharonov-Bohm effect,[62] and considering that those cycles are unlikely to happen in this case, we can ignore the induced charge n_g in the Hamiltonian 3.22:

$$\hat{\mathrm{H}} = 4\mathrm{E}_C\hat{n}^2 - \mathrm{E}_J + \frac{\mathrm{E}_J}{2}\hat{\varphi}^2 - \frac{\mathrm{E}_J}{24}\hat{\varphi}^4. \tag{3.23}$$

This Hamiltonian can be seen as a harmonic oscillator with a 4_{th} order anharmonicity. By defining the creation (annihilation) operators $b(b^\dagger)$ associated to this harmonic oscillator (without the perturbation) with eigenstates $|m\rangle$ we end up with the following Hamiltonian:

$$\hat{\mathrm{H}} = -\mathrm{E}_J + \sqrt{8\mathrm{E}_C\mathrm{E}_J}\left(\hat{b}^\dagger\hat{b} + \frac{1}{2}\right) + \frac{\mathrm{E}_C}{12}(\hat{b} + \hat{b}^\dagger)^4. \tag{3.24}$$

The first correction of the m_{th} eigenenergy is given by $\mathrm{E}_m^1 = -\mathrm{E}_C\langle m|(b+b^\dagger)^4|m\rangle/12 = -\mathrm{E}_C(6m^2+6m+3)/12$, therefore the m_{th} eigenenergy is

$$\mathrm{E}_m = -\mathrm{E}_J + \sqrt{8\mathrm{E}_C\mathrm{E}_J}\left(m+\frac{1}{2}\right) - \frac{\mathrm{E}_C}{12}(6m^2+6m+3)^4. \tag{3.25}$$

The transition energy from n_{th} to the m_{th} level is defined as $\mathrm{E}_{n\to m} = \mathrm{E}_m - \mathrm{E}_n$ and the variation of the transition energy between the levels $m-1$ and m, $\mathrm{E}_{m-1\to m}$, and the transition energy between the levels m and $m+1$, $\mathrm{E}_{m\to m+1}$, is given by the absolute anharmonicity $\alpha_m = \mathrm{E}_{m\to m+1} - \mathrm{E}_{m-1\to m}$ which in the regime $\mathrm{E}_J/\mathrm{E}_C \gg 1$ is given by $\alpha_m \approx -\mathrm{E}_C$. The relative anharmonicity $\alpha_m^r = \alpha_m/\mathrm{E}_{0\to 1}$ in this same limit is given by

$$\alpha_m^r \approx -\left(\frac{8\mathrm{E}_J}{\mathrm{E}_C}\right)^{-1/2}, \tag{3.26}$$

decreasing algebraically with $\mathrm{E}_J/\mathrm{E}_C$, which is good news, so we use the regime of $\mathrm{E}_J/\mathrm{E}_C \gg 1$ in order to obtain a high decrease of sensitivity to charge noise, through an exponential decrease in the charge dispersion ϵ_m, and a loss of anharmonicity α_m^r with a weaker power law, allowing for the selection of two specific energy levels in order to build a qubit. This proposed system was called **transmon qubit** or a CPB operating in the **transmon regime**[61] and it is going to be used in part of this thesis.

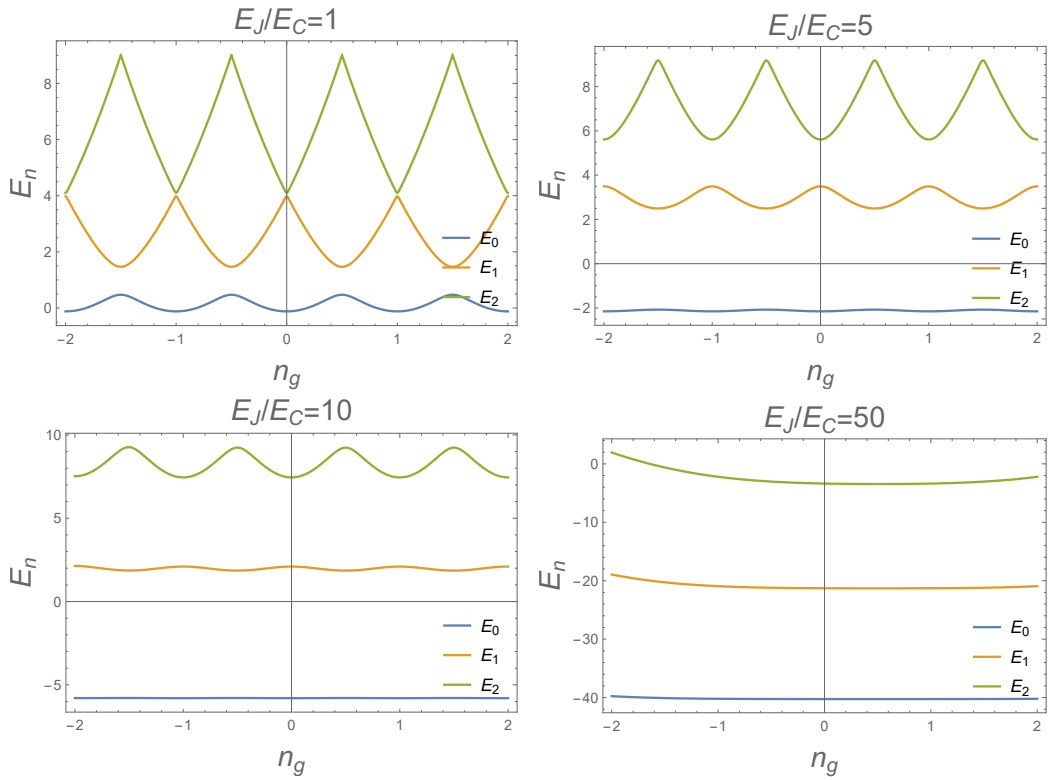

Figure 10 – First 3 energy levels of the CPB as a function of the induced charge n_g in different regimes of E_J/E_C. The first plot shows the charge regime where $E_J/E_C = 1$ with highly oscillating energy levels. And as the ratio E_J/E_C progressively increases, the oscillatory behavior starts to vanish, with E_n being almost independent of n_g. The eigenvalues were obtained numerically using 10 energy levels, $m = \{-4, -3, ..., 4, 5\}$.

Source: By the author.

3.3 Circuit quantum electrodynamics and the qubit-light interaction inside a cavity

Once we've delineated the superconducting qubit to be subsequentially used, it's time to describe the place where it will be put in order to be controlled through an external agent. This external source will be some additional field besides the magnetic flux used to control its energy-level spacing. Therefore, the qubit is put inside superconducting transmission line resonator, which works like a cavity where we can apply some light source in order to control and read the qubit state. The study of interaction of matter with light using superconducting circuits is termed circuit quantum electrodynamics or circuit QED.[63,64] To describe a superconducting cavity we look up first to the circuit representation of a harmonic oscillator,[65] which is given by a simple LC-circuit with Hamiltonian

$$\mathrm{H_{LC}} = \frac{q^2}{2\mathrm{C}} + \frac{\phi^2}{2\mathrm{L}}, \tag{3.27}$$

with q and ϕ being the charge stored in the capacitor and the flux through the inductor respectively. This Hamiltonian can be quantized[53,66] through the usual replacement of

$q \to \hat{q}$ and $\phi \to \hat{\phi}$ with $\hat{q}$ and $\hat{\phi}$ being conjugated operators. We can introduce the creation (annihilation) operator $\hat{a}(\hat{a}^\dagger)$, satisfying $[\hat{a}, \hat{a}^\dagger] = 1$, and rewrite $\hat{q}$ and $\hat{\phi}$ as

$$\begin{aligned} \hat{q} &= -i\sqrt{\frac{\hbar}{2Z}}\left(\hat{a} - \hat{a}^\dagger\right), \\ \hat{\phi} &= \sqrt{\frac{\hbar Z}{2}}\left(\hat{a} + \hat{a}^\dagger\right), \end{aligned} \tag{3.28}$$

with impedance $Z = \sqrt{\mathrm{L/C}}$. This leads to the well known harmonic oscillator Hamiltonian $\hat{\mathrm{H}} = \hbar\omega\left(\hat{a}^\dagger\hat{a} + 1/2\right)$ with frequency $\omega = \sqrt{1/\mathrm{LC}}$. The cavity can be seen as a continuum chain of LC-circuits producing a infinite set of modes ω_n,

$$\hat{\mathrm{H}} = \sum_n \hbar\omega_n\left(\hat{a}_n^\dagger\hat{a}_n + \frac{1}{2}\right), \tag{3.29}$$

but we are interested in only one mode, which is the one that resonates with the applied eletric field. The superconducting cavity is composed of a full wave section of a coplanar wave guide (CPW), which is composed of a central superconducting strip and two grounded superconductors parallel to it and separated by a distance d. These strips have a length L (full-wave section) equal to a wave-length λ of the applied field. The transmon is fabricated in between these strips in its central part as depicted in Fig. 11, right in point where the anti-node of the mode $m = 2$ of voltage between the superconducting strips lies.

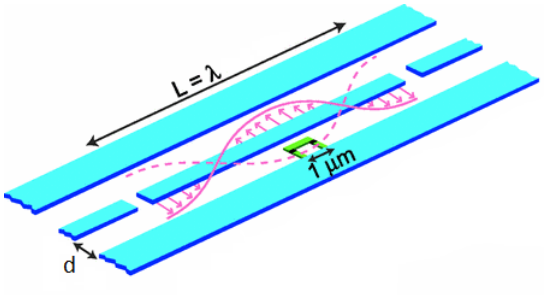

Figure 11 – Full wave section of a coplanar wave guide (CPW) of length $L = \lambda$ and inter-spacing d between strips. The transmon is placed in between the strips in a central position in a way that the mode $m = 2$ of the voltage, between the center and external superconducting strips, has its central anti-node located.

Source: Adapted from BLAIS, A. *et al.*[63]

In addition to the DC voltage V_g there is a quantum voltage between the center superconducting strip and the external one, due to the presence of photons, and the transmon feels the voltage

$$\hat{\mathrm{V}} = \mathrm{V}^0_{\mathrm{rms}}\left(\hat{a} + \hat{a}^\dagger\right), \tag{3.30}$$

with $\mathrm{V}^0_{\mathrm{rms}} = \sqrt{\hbar\omega_c/2C_c}$ being the root mean square voltage in the middle position where the transmon is located. The operators $\hat{a}(\hat{a}^\dagger)$ represent the annihilation (creation) of photons inside the cavity, ω_c and C_c represent the frequency and capacitance of this section

of length L of the CPW. As we've told before the frequency of the cavity ω_c is equal to the frequency of the applied field, which in this case it is ω_2, the frequency of its second mode. The complete Hamiltonian for this system is given by

$$\hat{\mathrm{H}} = 4\mathrm{E_C}\left(\hat{n} - n_g\right)^2 - \frac{1}{2}\mathrm{E_J}\cos\left(\hat{\varphi}\right) + \hbar\omega_c\hat{a}^\dagger\hat{a} + 2\frac{C_g}{C_\Sigma}e\mathrm{V}^0_{\mathrm{rms}}\hat{n}\left(\hat{a} + \hat{a}^\dagger\right). \tag{3.31}$$

Rewriting this Hamiltonian in the transmon basis $\{|j\rangle\}$ we obtain the expression

$$\hat{\mathrm{H}} = \hbar\sum_m \omega_m|m\rangle\langle m| + \hbar\omega_c\hat{a}^\dagger\hat{a} + \hbar\sum_{i,j} g_{ij}|i\rangle\langle j|\left(\hat{a} + \hat{a}^\dagger\right), \tag{3.32}$$

with $\hbar g_{ij} = 2C_g e\mathrm{V}^0_{\mathrm{rms}}\langle i|\hat{n}|j\rangle/C_\Sigma = \hbar g^*_{ji}$ being the coupling strength connecting the states $|i\rangle$ and $|j\rangle$. In the asymptotic limit $\mathrm{E}_J/\mathrm{E}_C \to \infty$, the number operator is given by

$$\hat{n} = -i\left(\frac{\mathrm{E}_J}{8\mathrm{E}_C}\right)^{1/4}\frac{(\hat{b} - \hat{b}^\dagger)}{\sqrt{2}}, \tag{3.33}$$

therefore the matrix elements of $\hat{n}$ are given by

$$|\langle j+1|\hat{n}|j\rangle| \approx \sqrt{\frac{j+1}{2}}\left(\frac{\mathrm{E}_J}{8\mathrm{E}_C}\right)^{1/4}, \tag{3.34}$$

$$\lim_{\mathrm{E}_J/\mathrm{E}_C\to\infty}|\langle j+k|\hat{n}|j\rangle| = 0, \forall k \text{ with } |k| > 1. \tag{3.35}$$

Notice here that only near neighbor states are connected, this property is going to be used in part of this work, but latter on we will loosen this property up.

4 NON-THERMAL HEAT ENGINES

4.1 Heat engines in the quantum regime

Here we present the quantum versions of the Carnot and Otto cycles paying special attention to the differences between the classical and quantum adiabatic segments and what conditions must be attained in order to build reversible cycles.

4.1.1 Classical and quantum adiabatic processes

Classical adiabaticity[67,68] is defined as the property of any process that does not exchange heat with the environment. These processes can be achieved through either slow or fast variation of a working parameter. Notice that in the case of fast variation, the populations can possibly change due to internal excitations, so the process is not necessarily isentropic. On the other hand quantum adiabaticity does not have the same meaning as its classical counterpart,[67,68] and it must be divided in two different definitions, one involving closed evolutions (unitary) and one more general, with open quantum systems (non-unitary). In the case of closed systems,[62] quantum adiabaticity is defined as the property of systems with a Hilbert space that can be decomposed into energy eigenspaces that evolve independently in time, meaning that if you prepare a system in some eigenenergy $|\psi(0)\rangle = |n(0)\rangle$ associated to its initial Hamiltonian $\mathrm{H}(0)$, it stays there along the evolution, evolving to $|\psi(t)\rangle \propto |n(t)\rangle$ (appearing an additional phase), with $|n(t)\rangle = \mathrm{U}(t,0)|n(0)\rangle$ being the evolved eigenstate associated to the Hamiltonian $\mathrm{H}(t)$. In general, in order to achieve this adiabatic condition, the Hamiltonian evolution must be accomplished in a slow pace, making the time interval of the evolution small compared to the characteristic time given by the smallest energy gap of $\mathrm{H}(t)$. The eigenvalues of $\mathrm{H}(t)$ also must not present any crossing (degeneracy) along the evolution. In this case there is not heat exchange due to the system isolation. On the other hand the quantum adiabaticity for open quantum systems is also not guaranteed by the slow variation of the Hamiltonian and it has to be reformulated considering the non-unitarity of the evolution. One way to define adiabaticity in this case was put forward by SARANDY, M. S. *et al*[69] for open quantum systems described by convolutionless master equations $\dot{\rho}(t) = \mathcal{L}(t)\rho(t)$. What they did was to first write the the superoperator $\mathcal{L}(t)$ in its Jordan canonical form,[70] and them define as quantum adiabaticity the property of systems with a Hilbert-Schmidt space that can be decomposed into Lindblad-Jordan blocks that evolve independently in time, meaning that if you prepare a system in one of these blocks, it stays there along the evolution. The condition presented for the adiabaticity here is analogous to the closed one, but in this case the demand of slowness is taken upon the supereoperator $\mathcal{L}(t)$,[69] together with the demand on the eigenvalues associated to each one the Lindblad-Jordan

blocks, forcing them to not cross along the time evolution. Despite all the efforts, up to now, no sufficient and necessary condition is known for the general case on both isolated and open systems. Thus, in the case of an open system, the quantum adiabaticity doesn't guarantee that no heat is going to be exchanged, allowing for both cases: with and without heat being exchanged.[71] Therefore the classical and quantum adiabaticity are two different concepts, that in some cases can be both attained.

4.1.2 Quantum Carnot cycle

Analogous to the classical version, it's composed by two adiabatics and two isothermals.[6,72] The complete cycle is depicted in Fig. 12 with λ and p_n representing the working parameter and the probability of occupation of the n_{th} state.

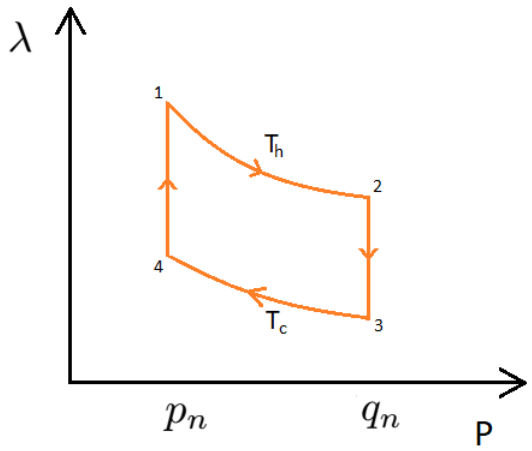

Figure 12 – $\lambda - \text{p}$ diagram of a quantum Carnot cycle. The cycle is composed of two isotherms $1 \to 2$ and $3 \to 4$ and two adiabatics $2 \to 3$ and $4 \to 1$.

Source: By the author.

This engine is built by use of a quantum WS, described by a Hamiltonian $\text{H}(\lambda(t))$ that can be varied by means of an external parameter $\lambda(t)$, known as working parameter. The first stroke is implemented by putting the WS in contact with a thermal bath of temperature T_h and slowly varying its working parameter from λ_1 to λ_2 in a quasi-static and isothermal fashion. Notice that the WS is initiated in a thermal state of temperature T_h before starting the stroke. The work W_1 extracted (or applied) on the WS and the heat Q_1 extracted from the bath are given by

$$\begin{aligned} \text{W}_1 &= \text{F}(\lambda_2, \text{T}_h) - \text{F}(\lambda_1, \text{T}_h), \\ \text{Q}_1 &= \text{T}_h \left[\text{S}(\lambda_2, \text{T}_h) - \text{S}(\lambda_1, \text{T}_h)\right], \end{aligned} \tag{4.1}$$

with $\text{F}(\lambda_i, \text{T}_j)$ and $\text{S}(\lambda_i, \text{T}_j)$ being the WS equilibrium free energy and Von Neumann entropy with $\lambda(t) = \lambda_i$ and bath temperature equal T_j. The second stroke is given by a quasi-static reversible adiabatic change of $\lambda(t)$, so there is no heat and the work is given

by

$$\mathrm{W}_2 = \mathrm{U}(\lambda_3, \mathrm{T}_c) - \mathrm{U}(\lambda_2, \mathrm{T}_h). \tag{4.2}$$

with $\mathrm{U}(\lambda_i, \mathrm{T}_j)$ being the internal energy with $\lambda(t_i) = \lambda_i$ and bath temperature equal T_j. Here are some details that comes in handy to understand what happened in this last stroke. The system started in a Gibbs distribution $\rho_2 \propto e^{-\beta_h \mathrm{H}(\lambda_2)}$ and underwent a quasi-static and reversible process, which means that it was kept in equilibrium all the way through finishing in another thermal state $\rho_3 \propto e^{-\alpha \mathrm{H}(\lambda_3)}$. But in addition to that we know that this process is also adiabatic, so there is no heat being exchanged with the bath, preserving the populations and consequently the entropy of the WS. As a result of that, together with the quasi-static condition, we end up with the probabilities being equal, $p_m(\lambda_2) = p_m(\lambda_3)$, and consequently $\alpha \neq \beta_h$, a thermal state with a different temperature. Observe that for a two-level system, such a process can always be conceived. As for a multi-level system, such a process requires that all gaps in the system spectrum must change by the same multiplicative factor, which specifies the ratio of the initial and final temperatures. In other words, during the adiabatic quantum analogue stroke, the system energy gaps must all be renormalised by the same factor. We will return to that point quantitatively soon. The third stroke is again an isothermal process but this time with a cold bath at temperature T_c. Notice that the temperature of this bath needs to be equal to the temperature of the WS at the end of the previous stroke, $\beta_c = \alpha$, other than that we would observe a relaxation process which is an out-of-equilibrium process. The work and heat generated here is given by

$$\begin{aligned} \mathrm{W}_3 &= \mathrm{F}(\lambda_4, \mathrm{T}_c) - \mathrm{F}(\lambda_3, \mathrm{T}_c), \\ \mathrm{Q}_3 &= \mathrm{T}_c \left[\mathrm{S}(\lambda_4, \mathrm{T}_c) - \mathrm{S}(\lambda_3, \mathrm{T}_c)\right]. \end{aligned} \tag{4.3}$$

And to finish this cycle off we have the final adiabatic process producing the work

$$\mathrm{W}_4 = \mathrm{U}(\lambda_1, \mathrm{T}_h) - \mathrm{U}(\lambda_4, \mathrm{T}_c) \tag{4.4}$$

and making the WS end up with the same initial thermal state of temperature T_h and working parameter λ_1. The efficiency of this engine will be given by

$$\eta = -\frac{\sum_i \mathrm{W}_i}{\mathrm{Q}_1} = 1 - \frac{\mathrm{T}_c}{\mathrm{T}_h}. \tag{4.5}$$

4.1.3 Otto cycle

Now that we've seen an equilibrium cycle it's time to step it up a bit and see how an irreversible quantum cycle can be implemented through the quantum version of the Otto cycle. It's noteworthy that the Otto cycle can actually be transformed in a reversible one by means of an infinite number of small Carnot cycles, and we will show this in the next section. But before proceeding we will need a more general definition of heat and work, considering that we are not going to be using any of those equilibrium

functions, like Helmholtz free energy and thermodynamic entropy. Imagine again a system being described by a Hamiltonian $\mathrm{H}(\lambda)$, with an eigenenergies and eigenstates given by $\{\mathrm{E}_n(\lambda), |n(\lambda)\rangle\}$. With the internal energy defined by

$$\mathrm{U} = \langle \mathrm{H}(\lambda) \rangle = \sum_n p_n(\lambda) E_n(\lambda), \tag{4.6}$$

with probability of occupation of the n_{th} state represented by $p_n(\lambda)$. The variation of U can be divided in two terms

$$d\mathrm{U} = \sum_n dp_n E_n(\lambda) + \sum_n p_n(\lambda) dE_n = đQ + đW, \tag{4.7}$$

with $đQ = \sum_n dp_n E_n(\lambda)$ being the exchanged heat with the bath and $đW = \sum_n p_n(\lambda) dE_n$ the work applied (extracted) on (from) the system. Notice that these two quantities are general and can be calculated even in non-equilibrium processes, but it's worth mentioning that there is more than one definition of work, like the one involving two point measurements. Now that we have defined those quantities let's discuss the cycle in itself.[68]

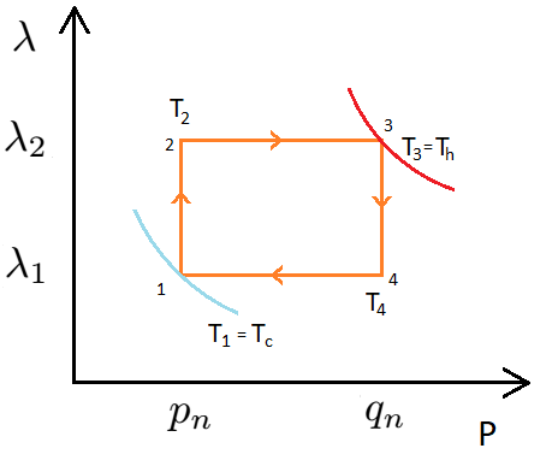

Figure 13 – $\lambda - \mathrm{p}$ diagram of a quantum Otto cycle. The cycle is composed of two adiabatics $1 \to 2$ and $3 \to 4$ and two isochorics $2 \to 3$ and $4 \to 1$.

Source: By the author.

Suppose that we initially prepare the system in a Gibbs state $p_n(\lambda_1) \propto e^{-\beta_c E_n(\lambda_1)}$, with the same temperature $\mathrm{T}_c = \beta_c^{-1}$ than the cold bath used in the cycle. The WS goes through a quantum adiabatic expansion in the **first stroke**, varying the work parameter from λ_1 to λ_2, so there is no heat being exchanged with the bath in this stroke, only work, which is given by

$$\mathrm{W}_{1\to 2} = \sum_n \int_1^2 p_n(\lambda) dE_n = \sum_n p_n [E_n(\lambda_2) - E_n(\lambda_1)]. \tag{4.8}$$

Considering that this is a quantum adiabatic, analogous to the Carnot cycle, the populations don't change along the stroke (that is why the previous integral was easily calculated), so

$p_n(\lambda_1) = p_n(\lambda_2) = p_n$ which makes the system acquire a new temperature T_2 that can be obtained as follows

$$\begin{aligned} p_n(\lambda_1) &= p_n(\lambda_2), \\ \frac{e^{-\beta_c E_n(\lambda_1)}}{\sum_m e^{-\beta_c E_m(\lambda_1)}} &= \frac{e^{-\beta_2 E_n(\lambda_2)}}{\sum_m e^{-\beta_2 E_m(\lambda_2)}}, \\ \frac{1}{\sum_m e^{-\beta_c [E_m(\lambda_1) - E_n(\lambda_1)]}} &= \frac{1}{\sum_m e^{-\beta_2 [E_m(\lambda_2) - E_n(\lambda_2)]}}, \end{aligned} \tag{4.9}$$

and for this equality to hold, $\beta_c[E_m(\lambda_1) - E_n(\lambda_1)] = \beta_2[E_m(\lambda_2) - E_n(\lambda_2)] \ \forall \ m$, which means that all the energy gaps change by the same ratio $\mathrm{T}_2/\mathrm{T}_c$, generating the a final temperature

$$\mathrm{T}_2 = \frac{[E_m(\lambda_2) - E_n(\lambda_2)]}{[E_m(\lambda_1) - E_n(\lambda_1)]}\mathrm{T}_c, \quad \forall \, n \neq m. \tag{4.10}$$

The **second stroke** is an isochoric heating by keeping the WS in contact with a bath of temperature T_h. In this case there is no work being applied, and the heat exchanged is given by

$$\mathrm{Q}_{2\to 3} = \sum_n \int_2^3 E_n(\lambda_2) dp_n = \sum_n E_n(\lambda_2)[q_n(\lambda_2) - p_n(\lambda_2)], \tag{4.11}$$

with $p_n(\lambda_2) = p_n$ and $q_n(\lambda_2) = q_n$ being the populations of the WS before and after the thermalization. Notice here that this stroke is irreversible, because the WS had to equilibrate with the hot bath of temperature $\mathrm{T}_h = \beta_h^{-1}$, relaxing to the Gibbs $q_n(\lambda_2) \propto e^{-\beta_h E_n(\lambda_2)}$ by the cost of entropy production. In the **third stroke** the WS goes through another adiabatic process but this time being compressed.

$$\mathrm{W}_{3\to 4} = \sum_n \int_3^4 q_n dE_n = \sum_n q_n[E_n(\lambda_1) - E_n(\lambda_2)], \tag{4.12}$$

and similar to the previous adiabatic process, ending up with a Gibbs state of temperature T_4 given by

$$\mathrm{T}_4 = \frac{[E_m(\lambda_1) - E_n(\lambda_1)]}{[E_m(\lambda_2) - E_n(\lambda_2)]}\mathrm{T}_h, \quad \forall \, n \neq m. \tag{4.13}$$

The **fourth and final stroke**, an isochoric cooling exchanging the last amount of heat

$$\mathrm{Q}_{4\to 1} = \sum_n \int_4^1 E_n(\lambda_1) dp_n = \sum_n E_n(\lambda_1)[p_n(\lambda_1) - q_n(\lambda_1)], \tag{4.14}$$

and finishing the cycle by irreversibly relaxing to the initial thermal population $p_n(\lambda_1) \propto e^{-\beta_c E_n(\lambda_1)}$. The efficiency of this engine is given by

$$\begin{aligned} \eta_{\mathrm{Otto}} &= -\frac{\mathrm{W}_{1\to 2} + \mathrm{W}_{3\to 4}}{\mathrm{Q}_{2\to 3}} \\ &= \frac{\sum_n (p_n - q_n)[E_n(\lambda_2) - E_n(\lambda_1)]}{\sum_m E_m(\lambda_2)[q_m(\lambda_2) - p_m(\lambda_2)]} \\ &= 1 - \frac{\sum_n (p_n - q_n) E_n(\lambda_1)}{\sum_m (p_m - q_m) E_m(\lambda_2)}. \end{aligned} \tag{4.15}$$

If we make a shift of Δ in all energy levels with $\lambda = \lambda_1$, $E_n(\lambda_1) \to \tilde{E}_n(\lambda_1) = E_n(\lambda_1) + \Delta$, the efficiency η_{Otto} doesn't change, and we are going to use this property to simplify the expression for the efficiency. Setting the shift $\Delta = E_0(\lambda_1)$ and using $m = 0$ on the expressions 4.10 and 4.13 we have

$$\tilde{E}_n(\lambda_1) = \frac{\mathrm{T}_c}{\mathrm{T}_2}\left[E_n(\lambda_2) - E_0(\lambda_2)\right] = \frac{\mathrm{T}_4}{\mathrm{T}_h}\left[E_n(\lambda_2) - E_0(\lambda_2)\right]. \tag{4.16}$$

With this shift and using 4.16 the expression for the efficiency becomes

$$\begin{aligned}
\eta_{\text{Otto}} &= 1 - \frac{\sum_n (p_n - q_n)\tilde{E}_n(\lambda_1)}{\sum_m (p_m - q_m)E_m(\lambda_2)} \\
&= 1 - \frac{\mathrm{T}_c}{\mathrm{T}_2}\frac{\sum_n (p_n - q_n)}{\sum_m (p_m - q_m)E_m(\lambda_2)}\left[E_n(\lambda_2) - E_0(\lambda_2)\right] \\
&= 1 - \frac{\mathrm{T}_c}{\mathrm{T}_2}\frac{\sum_n (p_n - q_n)E_n(\lambda_2)}{\sum_m (p_m - q_m)E_m(\lambda_2)} \\
&= 1 - \frac{\mathrm{T}_c}{\mathrm{T}_2} = 1 - \frac{\mathrm{T}_4}{\mathrm{T}_h}.
\end{aligned} \tag{4.17}$$

An interesting thing is that we can build an Otto[72–74] through the the use of an infinite number of infinitesimal Carnot cycles. In this process the isochoric relaxations from T_2 to $\mathrm{T}_3 = \mathrm{T}_h$ and from T_4 to $\mathrm{T}_1 = \mathrm{T}_c$ in the strokes $2 \to 3$ and $4 \to 1$ respectively can be decomposed in an infinite number of infinitely small isothermals $\mathrm{T}_i \in [\mathrm{T}_1, \cdots, \mathrm{T}_h]$ and $\mathrm{T}_j \in [\mathrm{T}_4, \cdots, \mathrm{T}_c]$ with $\mathrm{T}_{i+1} = \mathrm{T}_i + \delta$ and $\mathrm{T}_{j+1} = \mathrm{T}_j - \delta$. In this limit, the Otto engine, which were initially irreversible due to the isochoric relaxations, can be turned into a reversible cycle. A similar thing can be done to build a Carnot cycle but using infinitesimal Otto cycles.

4.2 Non-thermal heat engines

As we have mentioned before there are certain types of thermodynamic cycles that have non-thermal states along their strokes, engines built using these cycles are called non-thermal heat engines.[75–85] In this chapter we are going to devise a particular type of non-thermal heat engine, which results were already published in Cherubim, C. *et al.*[86] However, first let's give it a look at the conditions for non-thermalization.

4.2.1 Conditions for non-thermalization

In order to build a non-thermal heat engine we use thermal baths and remove them from equilibrium by means of unitary transformations. The question that immediately comes to mind is if the system that we put in contact with those baths is going to either thermalize or end up in a non-equilibrium steady-state.[81] Suppose that the initial state of the WS is given by $\rho_{\text{WS}}(0)$ and the state of the bath is represented by the Gibbs state $\rho_{\text{B}}^{\text{th}}$. The WS evolves over time in contact with the bath and by tracing out the bath we obtain

its final state

$$\rho_{\mathrm{WS}}(t) = \mathrm{tr}_{\mathrm{B}}\left\{\mathrm{U}\left[\rho_{\mathrm{WS}}(0)\otimes\rho_{\mathrm{B}}^{\mathrm{th}}\right]\mathrm{U}^{\dagger}\right\}, \tag{4.18}$$

with U being a unitary operator given by

$$\mathrm{U} = \mathrm{T}_{\leftarrow}\exp\left\{-\frac{i}{\hbar}\int_0^t \mathrm{H}_{\mathrm{int}}d\tau\right\}, \tag{4.19}$$

with $\mathrm{T}_{\leftarrow}$ being the time-ordering operator and $\mathrm{H}_{\mathrm{int}}$ the WS-bath interaction Hamiltonian in the interaction picture. In this case if we wait long enough the WS will thermalize too, but imagine if instead of keeping the bath in a thermal state we drive it away from equilibrium by applying a unitary transformation U_{B}:

$$\rho_{\mathrm{B}}^{\mathrm{non-th}} = \mathrm{U}_{\mathrm{B}}\rho_{\mathrm{B}}^{\mathrm{th}}\mathrm{U}_{\mathrm{B}}^{\dagger}. \tag{4.20}$$

In this case what will be the stationary state for the WS? In order to answer this question we repeat exactly what we've done before, tracing out the bath, which in this case will have a non-thermal initial state for the bath.

$$\begin{aligned}\rho_{\mathrm{WS}}(t) &= \mathrm{tr}_{\mathrm{B}}\left\{\mathrm{U}\left[\rho_{\mathrm{WS}}(0)\otimes\rho_{\mathrm{B}}^{\mathrm{non-th}}\right]\mathrm{U}^{\dagger}\right\},\\ &= \mathrm{tr}_{\mathrm{B}}\left\{\mathrm{U}\left(\mathbb{1}\otimes\mathrm{U}_{\mathrm{B}}\right)\left[\rho_{\mathrm{WS}}(0)\otimes\rho_{\mathrm{B}}^{\mathrm{th}}\right]\left(\mathbb{1}\otimes\mathrm{U}_{\mathrm{B}}^{\dagger}\right)\mathrm{U}^{\dagger}\right\}.\end{aligned} \tag{4.21}$$

Including $\mathbb{1}\otimes\mathbb{1} = \mathbb{1}\otimes\mathrm{U}_{\mathrm{B}}\mathrm{U}_{\mathrm{B}}^{\dagger} = \left(\mathbb{1}\otimes\mathrm{U}_{\mathrm{B}}\right)\left(\mathbb{1}\otimes\mathrm{U}_{\mathrm{B}}^{\dagger}\right)$,

$$\rho_{\mathrm{WS}}(t) = \mathrm{tr}_{\mathrm{B}}\left\{\left(\mathbb{1}\otimes\mathrm{U}_{\mathrm{B}}\right)\left(\mathbb{1}\otimes\mathrm{U}_{\mathrm{B}}^{\dagger}\right)\mathrm{U}\left(\mathbb{1}\otimes\mathrm{U}_{\mathrm{B}}\right)\left[\rho_{\mathrm{WS}}(0)\otimes\rho_{\mathrm{B}}^{\mathrm{th}}\right]\left(\mathbb{1}\otimes\mathrm{U}_{\mathrm{B}}^{\dagger}\right)\mathrm{U}^{\dagger}\right\}. \tag{4.22}$$

Now we are going to use the cyclic property of the trace, but we have to apply it very carefully because it is not a general property to the partial trace, so it can only be applied to specific operators. Imagine a quantum system with Hilbert space $\mathcal{H}_1\otimes\mathcal{H}_2$ and two operators $\mathrm{C}_1 = \mathrm{A}_1\otimes\mathrm{B}_1$ and $\mathrm{C}_2 = \mathrm{A}_2\otimes\mathrm{B}_2$ belonging to it. The partial trace is cyclic $\mathrm{tr}_2\{\mathrm{C}_1\mathrm{C}_2\} = \mathrm{tr}_2\{\mathrm{C}_2\mathrm{C}_1\}$, if $[\mathrm{A}_1,\mathrm{A}_2] = 0$. In our case $\mathrm{C}_1 = \left(\mathbb{1}\otimes\mathrm{U}_{\mathrm{B}}\right)$ and $\mathrm{C}_2 = \left(\mathbb{1}\otimes\mathrm{U}_{\mathrm{B}}^{\dagger}\right)\mathrm{U}\left(\mathbb{1}\otimes\mathrm{U}_{\mathrm{B}}\right)\left[\rho_{\mathrm{WS}}(0)\otimes\rho_{\mathrm{B}}^{\mathrm{th}}\right]\left(\mathbb{1}\otimes\mathrm{U}_{\mathrm{B}}^{\dagger}\right)\mathrm{U}^{\dagger}$, with $\mathrm{A}_1 = \mathbb{1}$ which commutes with any operator.

$$\rho_{\mathrm{WS}}(t) = \mathrm{tr}_{\mathrm{B}}\left\{\left(\mathbb{1}\otimes\mathrm{U}_{\mathrm{B}}^{\dagger}\right)\mathrm{U}\left(\mathbb{1}\otimes\mathrm{U}_{\mathrm{B}}\right)\left[\rho_{\mathrm{WS}}(0)\otimes\rho_{\mathrm{B}}^{\mathrm{th}}\right]\left(\mathbb{1}\otimes\mathrm{U}_{\mathrm{B}}^{\dagger}\right)\mathrm{U}^{\dagger}\left(\mathbb{1}\otimes\mathrm{U}_{\mathrm{B}}\right)\right\}. \tag{4.23}$$

Notice that the Eq. (4.23) is similar to Eq. (4.18), with the same bath's initial thermal state, the only difference being the change in operator $\mathrm{U}\rightarrow\left(\mathbb{1}\otimes\mathrm{U}_{\mathrm{B}}^{\dagger}\right)\mathrm{U}\left(\mathbb{1}\otimes\mathrm{U}_{\mathrm{B}}\right)$. Actually we can go even further and write

$$\left(\mathbb{1}\otimes\mathrm{U}_{\mathrm{B}}^{\dagger}\right)\mathrm{U}\left(\mathbb{1}\otimes\mathrm{U}_{\mathrm{B}}\right) = \mathrm{U}_{\mathrm{B}}^{\dagger}\mathrm{T}_{\leftarrow}\exp\left\{-\frac{i}{\hbar}\int_0^t\mathrm{H}_{\mathrm{int}}d\tau\right\}\mathrm{U}_{\mathrm{B}} = \mathrm{T}_{\leftarrow}\exp\left\{-\frac{i}{\hbar}\int_0^t\mathrm{U}_{\mathrm{B}}^{\dagger}\mathrm{H}_{\mathrm{int}}\mathrm{U}_{\mathrm{B}}d\tau\right\}. \tag{4.24}$$

By looking in the last expression we see that the difference between U and $\left(\mathbb{1}\otimes\mathrm{U}_{\mathrm{B}}^{\dagger}\right)\mathrm{U}\left(\mathbb{1}\otimes\mathrm{U}_{\mathrm{B}}\right)$ appears at the replacement of $\mathrm{H}_{\mathrm{int}}\rightarrow\mathrm{U}_{\mathrm{B}}^{\dagger}\mathrm{H}_{\mathrm{int}}\mathrm{U}_{\mathrm{B}}$. If the Hamiltonian $\mathrm{H}_{\mathrm{int}}$ keeps its original form except for possible renormalizations of its coupling strengths, the stationary state

generated by this bath is going to be the same Gibbs state but with a different temperature.[87] On the other hand if the form of the Hamiltonian H_{int} changes,[79,80] it can either end up in a non-thermal state or not. In principle if energy is exchanged with the bath the WS will relax to a thermal state, but if we add a source of undepleted pump to it, which is our case, the stationary state will not be thermal.

4.2.2 Describing the system

The system to be used in this work for building a non-thermal heat engine is composed of multiple parts, being the Working Substance (WS) a transmon-based qubit of tunable frequency ω_T, which is the subsystem to be kept in a non-equilibrium fashion. The qubit interacts with a superconducting cavity of fixed natural frequency ω_{CPW} with coupling strength g, this cavity is pumped by an external field of tunable amplitude E_d and fixed frequency ω and is the key ingredient to prevent the WS of relaxing to a thermal state. All these subsystems are immersed in a cryogenic classical bath of temperature T (See Fig. 14). In this system the classical bath and the pumped cavity play the game as a

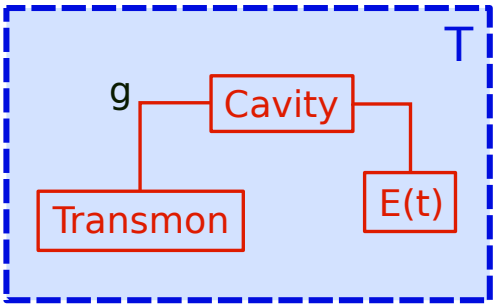

Figure 14 – Sketch of the quantum engine with a transmon qubit as working substance interacting with an externally pumped ($E(t)$) transmission line (cavity). Both systems are embedded in the same cryogenic environment, which plays the role of a standard thermal bath of temperature T. Such a setup gives a dynamics of a working substance in the presence of a controllable *non-thermal* environment.

Source: By the author.

non-thermal heat bath which makes the WS acquire a non-thermal stationary state defined by the two tunable variables (ω_T, E_d). Notice here that the transmon's frequency ω_T stands for the "volume" of the WS and instead of using two baths of different temperatures we replace them by the field's amplitude E_d, which is a variable associated to the non-thermal bath (pumped cavity + classical bath).

The Hamiltonian describing this system is given by the following expression

$$\begin{aligned} H(t) = &\frac{\hbar\omega_T}{2}\sigma_z + \hbar\omega_{CPW}a^\dagger a + g\ \sigma_x(a + a^\dagger) \\ &+ E_d\left(ae^{i\omega t} + a^\dagger e^{-i\omega t}\right), \end{aligned} \tag{4.25}$$

where σ_x and σ_z are the Pauli matrices, $a^\dagger$ and a are the canonical bosonic creation and annihilation operators associated with the cavity excitations, g is the qubit-cavity coupling strength. The last term represents a monochromatic pumping of amplitude E_d and frequency ω applied to the cavity. The experimental characterization of the qubit-cavity dissipative dynamics emerging from their interaction with the common thermal bath shows that the system steady state is determined from the master equation[88]

$$\begin{aligned}\dot{\rho}(t) = &-\frac{i}{\hbar}[H(t),\rho] + K^-_{\mathrm{CPW}}\mathcal{D}[a]\rho \\ &+ K^+_{\mathrm{CPW}}\mathcal{D}[a^\dagger]\rho + \Gamma^-\mathcal{D}[\sigma^-]\rho + \Gamma^+\mathcal{D}[\sigma^+]\rho,\end{aligned} \tag{4.26}$$

with $K^-_{\mathrm{CPW}}(K^+_{\mathrm{CPW}})$ being the cavity decay (excitation) rate, $\Gamma^-(\Gamma^+)$ the qubit relaxation (excitation) rate, which are constant in the asymptotic regime, and $\mathcal{D}[A]\rho = A\rho A^\dagger - 1/2(A^\dagger A\rho + \rho A^\dagger A)$. Those rates satisfy detailed balance for the same bath of temperature T, $K^+_{\mathrm{CPW}}/K^-_{\mathrm{CPW}} = \exp\left(-\hbar\omega_{\mathrm{CPW}}/k_{\mathrm{B}}T\right)$ and $\Gamma^+/\Gamma^- = \exp\left(-\hbar\omega_{\mathrm{T}}/k_{\mathrm{B}}T\right)$. Note that we still have the time-dependence in $H(t)$, so in order to remove it the first step is to rewrite the master equation in the driving-field frame using the following unitary transformation

$$U(t) = e^{i\hbar\omega t(\frac{\sigma_z}{2}+a^\dagger a)}. \tag{4.27}$$

After applying the transformation the ME acquires the following form:

$$\begin{aligned}\dot{\tilde{\rho}}(t) = &-\frac{i}{\hbar}[\tilde{H},\tilde{\rho}] + K^-_{\mathrm{CPW}}\mathcal{D}[\tilde{a}]\tilde{\rho} \\ &+ K^+_{\mathrm{CPW}}\mathcal{D}[\tilde{a}^\dagger]\tilde{\rho} + \Gamma^-\mathcal{D}[\tilde{\sigma}^-]\tilde{\rho} + \Gamma^+\mathcal{D}[\tilde{\sigma}^+]\tilde{\rho},\end{aligned} \tag{4.28}$$

with

$$\begin{aligned}\tilde{H} &= UHU^\dagger + i\hbar\frac{dU}{dt}U^\dagger, \\ \tilde{\rho} &= U\rho U^\dagger, \\ \mathcal{D}[\tilde{A}] &= \mathcal{D}[UAU^\dagger].\end{aligned} \tag{4.29}$$

Applying the Rotating Wave Approximation (RWA) on the Hamiltonian $\tilde{H}$ and using the fact that $\mathcal{D}[\tilde{A}] = \mathcal{D}[A]$ for $A = \{a, a^\dagger, \sigma^-, \sigma^+\}$ we obtain the final ME

$$\begin{aligned}\dot{\tilde{\rho}}(t) = &-\frac{i}{\hbar}[\mathrm{H}_{\mathrm{RWA}},\tilde{\rho}] + K^-_{\mathrm{CPW}}\mathcal{D}[a]\tilde{\rho} \\ &+ K^+_{\mathrm{CPW}}\mathcal{D}[a^\dagger]\tilde{\rho} + \Gamma^-\mathcal{D}[\sigma^-]\tilde{\rho} + \Gamma^+\mathcal{D}[\sigma^+]\tilde{\rho},\end{aligned} \tag{4.30}$$

with

$$\begin{aligned}\mathrm{H}_{\mathrm{RWA}} = &\frac{\hbar}{2}\left(\omega_{\mathrm{T}} - \omega\right)\sigma_z + \hbar\left(\omega_{\mathrm{CPW}} - \omega\right)a^\dagger a \\ &+ g(\sigma_+ a + \sigma_- a^\dagger) + E_d(a + a^\dagger).\end{aligned} \tag{4.31}$$

Since we are interested in the observed dynamics of the WS, it is necessary to find the qubit's reduced density matrix $\rho_{\mathrm{T}}(t) \equiv \mathrm{tr_a}\left\{\rho(t)\right\}$, where $\mathrm{tr_a}\left\{\cdot\right\}$ represents the partial

trace on the cavity's degrees of freedom. In the statioanary regime, which is the one to be used here, the system is in a qubit-cavity product state, i.e., $\rho(t \to \infty) \approx \rho_{\mathrm{T}} \otimes \rho_{\mathrm{C}}$, that emerges in the effective qubit-cavity weak coupling regime due to decoherence into the global environment. In addition, the cavity's stationary state $\rho_{\mathrm{C}}(t)$ is assumed to be mainly determined by the external pumping, which can be easily found for situations of strong pumping and/or weak coupling strength g. This closely resembles a situation, in which the cavity acts as a work source of effectively infinite inertia[89] for the qubit. Thus, changing the state of the qubit does not affect the state of the cavity, but it is still susceptible to the applied field and the cryogenic bath which makes the cavity have a stationary coherent state with $\langle a \rangle$ and $\langle a^\dagger \rangle^*$ given by

$$\langle a \rangle = \langle a^\dagger \rangle^* = \frac{E_d}{\hbar \left[i\kappa_{\mathrm{CPW}}/2 - (\omega_{\mathrm{CPW}} - \omega) \right]}, \tag{4.32}$$

where we defined $K^-_{\mathrm{CPW}} = \kappa_{\mathrm{CPW}}$. Hence, the reduced master equation (4.30) can be written as

$$\dot{\rho}_{\mathrm{T}}(t) = -\frac{i}{\hbar}[\tilde{H}_{\mathrm{T,RWA}}, \rho_{\mathrm{T}}] + \Gamma^- \mathcal{D}[\sigma^-]\rho_{\mathrm{T}} + \Gamma^+ \mathcal{D}[\sigma^+]\rho_{\mathrm{T}}, \tag{4.33}$$

with

$$\tilde{H}_{\mathrm{T,RWA}} = \frac{\hbar}{2}(\omega_{\mathrm{T}} - \omega)\sigma_z + g\left[\langle a \rangle \sigma_+ + \langle a^\dagger \rangle \sigma_-\right]. \tag{4.34}$$

Please note that the effective qubit Hamiltonian carries information about the interaction with the cavity through $\langle a \rangle$ and $\langle a^\dagger \rangle$, which are dependent on the cavity state. It is also worth emphasizing here that the transmon qubit is out of resonance with the applied field, which makes the dynamics work in the weak-coupling regime, which was tested through simulations and experimentally.[88]

4.2.3 Stationary solution

Once we have the master equation describing the evolution of the WS, the first step to build a thermodynamic cycle is to find the stationary solution ρ^{ss}_{T}, which makes $\dot{\rho}^{ss}_{\mathrm{T}} = 0$. The ME (4.33) produces the following set of equations:

$$\begin{aligned}
\frac{d\rho^{ee}_{\mathrm{T}}}{dt} &= \frac{i}{\hbar} g\langle a^\dagger \rangle \rho^{eg}_{\mathrm{T}} - \frac{i}{\hbar} g\langle a \rangle \rho^{ge}_{\mathrm{T}} - \Gamma^- \rho^{ee}_{\mathrm{T}} + \Gamma^+ \rho^{gg}_{\mathrm{T}} = 0, \\
\frac{d\rho^{gg}_{\mathrm{T}}}{dt} &= -\frac{i}{\hbar} g\langle a^\dagger \rangle \rho^{eg}_{\mathrm{T}} + \frac{i}{\hbar} g\langle a \rangle \rho^{ge}_{\mathrm{T}} + \Gamma^- \rho^{ee}_{\mathrm{T}} - \Gamma^+ \rho^{gg}_{\mathrm{T}} = 0, \\
\frac{d\rho^{ge}_{\mathrm{T}}}{dt} &= i(\omega_{\mathrm{T}} - \omega)\rho^{ge}_{\mathrm{T}} - \frac{i}{\hbar} g\langle a^\dagger \rangle \left(\rho^{ee}_{\mathrm{T}} - \rho^{gg}_{\mathrm{T}}\right) - \frac{1}{2}\left(\Gamma^- + \Gamma^+\right)\rho^{ge}_{\mathrm{T}} = 0, \\
\frac{d\rho^{eg}_{\mathrm{T}}}{dt} &= -i(\omega_{\mathrm{T}} - \omega)\rho^{eg}_{\mathrm{T}} + \frac{i}{\hbar} g\langle a \rangle \left(\rho^{ee}_{\mathrm{T}} - \rho^{gg}_{\mathrm{T}}\right) - \frac{1}{2}\left(\Gamma^- + \Gamma^+\right)\rho^{eg}_{\mathrm{T}} = 0,
\end{aligned} \tag{4.35}$$

with

$$\rho^{ss}_{\mathrm{T}} = \begin{pmatrix} \rho^{ee}_{\mathrm{T}} & \rho^{eg}_{\mathrm{T}} \\ \rho^{ge}_{\mathrm{T}} & \rho^{gg}_{\mathrm{T}} \end{pmatrix}, \tag{4.36}$$

in the σ_z basis. Solving for $\{\rho_{\mathrm{T}}^{ee}, \rho_{\mathrm{T}}^{eg}, \rho_{\mathrm{T}}^{ge}, \rho_{\mathrm{T}}^{gg}\}$ we obtain the stationary WS stationary state:

$$
\begin{aligned}
\rho_{\mathrm{T}}^{ee} &= \frac{\frac{g^2E_d^2}{\hbar^4\left[\frac{1}{4}\kappa_{\mathrm{CPW}}^2+(\omega_{\mathrm{CPW}}-\omega)^2\right]} + \frac{1}{1+e^{\beta\hbar\omega_{\mathrm{T}}}}\left[\frac{1}{4}\frac{\Gamma^2}{\tanh^2(\beta\hbar\omega_{\mathrm{T}}/2)} + (\omega_{\mathrm{T}}-\omega)^2\right]}{\frac{2g^2E_d^2}{\hbar^4\left[\frac{1}{4}\kappa_{\mathrm{CPW}}^2+(\omega_{\mathrm{CPW}}-\omega)^2\right]} + \left[\frac{1}{4}\frac{\Gamma^2}{\tanh^2(\beta\hbar\omega_{\mathrm{T}}/2)} + (\omega_{\mathrm{T}}-\omega)^2\right]}, \\
\rho_{\mathrm{T}}^{gg} &= \frac{\frac{g^2E_d^2}{\hbar^4\left[\frac{1}{4}\kappa_{\mathrm{CPW}}^2+(\omega_{\mathrm{CPW}}-\omega)^2\right]} + \frac{1}{1+e^{-\beta\hbar\omega_{\mathrm{T}}}}\left[\frac{1}{4}\frac{\Gamma^2}{\tanh^2(\beta\hbar\omega_{\mathrm{T}}/2)} + (\omega_{\mathrm{T}}-\omega)^2\right]}{\frac{2g^2E_d^2}{\hbar^4\left[\frac{1}{4}\kappa_{\mathrm{CPW}}^2+(\omega_{\mathrm{CPW}}-\omega)^2\right]} + \left[\frac{1}{4}\frac{\Gamma^2}{\tanh^2(\beta\hbar\omega_{\mathrm{T}}/2)} + (\omega_{\mathrm{T}}-\omega)^2\right]}, \\
\rho_{\mathrm{T}}^{eg} = \rho_{\mathrm{T}}^{ge*} &= \frac{\frac{1}{2\hbar}\left[\frac{\Gamma}{\tanh(\beta\hbar\omega_{\mathrm{T}}/2)}i + 2(\omega_{\mathrm{T}}-\omega)\right]\frac{gE_d}{\hbar\left[i\frac{\kappa_{\mathrm{CPW}}}{2}-(\omega_{\mathrm{CPW}}-\omega)\right]}}{\frac{2g^2E_d^2}{\hbar^4\left[\frac{1}{4}\kappa_{\mathrm{CPW}}^2+(\omega_{\mathrm{CPW}}-\omega)^2\right]} + \left[\frac{1}{4}\frac{\Gamma^2}{\tanh^2(\beta\hbar\omega_{\mathrm{T}}/2)} + (\omega_{\mathrm{T}}-\omega)^2\right]}\tanh(\beta\hbar\omega_{\mathrm{T}}/2).
\end{aligned}
\tag{4.37}
$$

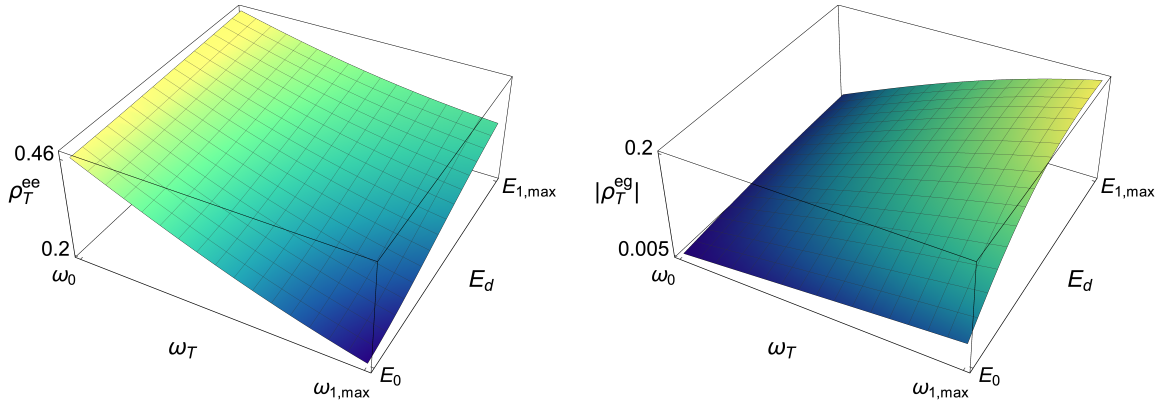

Figure 15 – Stationary state's elements ρ_{T}^{ee} and $|\rho_{\mathrm{T}}^{eg}|$ for different values of $(\omega_{\mathrm{T}}, E_d)$. Important amounts of population and quantum coherence changes can be reached during the engine operation.

Source: By the author.

4.2.4 The Cycle

In equilibrium thermodynamics cycles are constructed by following a closed path on a surface obtained by the equation of state,[1] which characterizes possible equilibrium states for a given set of macroscopic variables. This procedure can be generalized in the context of steady state thermodynamics, where an equation of state is also constructed. For the present purposes, we use the steady state (4.36) to devise a cycle for our heat engine. The equation of state is represented by the stationary state's von Neumann entropy $S(\omega_{\mathrm{T}}, E_d) = -\mathrm{tr}\{\rho_{\mathrm{T}}^{ss} \ln \rho_{\mathrm{T}}^{ss}\}$, which is fully determined by the pair of controllable variables

ω_{T}, the transmon's frequency, and E_d, amplitude field of the pumping applied to the cavity. In order to implement the cycle, the stationary state is slowly varied by changing the "knobs" (ω_{T},E_d). The timescale for which the changes made can be considered slow is such that the conditions imposed to the system state are satisfied, namely the state is a product state and the cavity steady state is a coherent state. The cycle is composed of four strokes, where in each one of them we keep one of the two controllable variables constant and vary the other one, for example, at the first stroke we keep $E_d = E_0$ and vary ω_{T} from ω_0 to ω_1. The complete cycle is sketched in Figure 16.

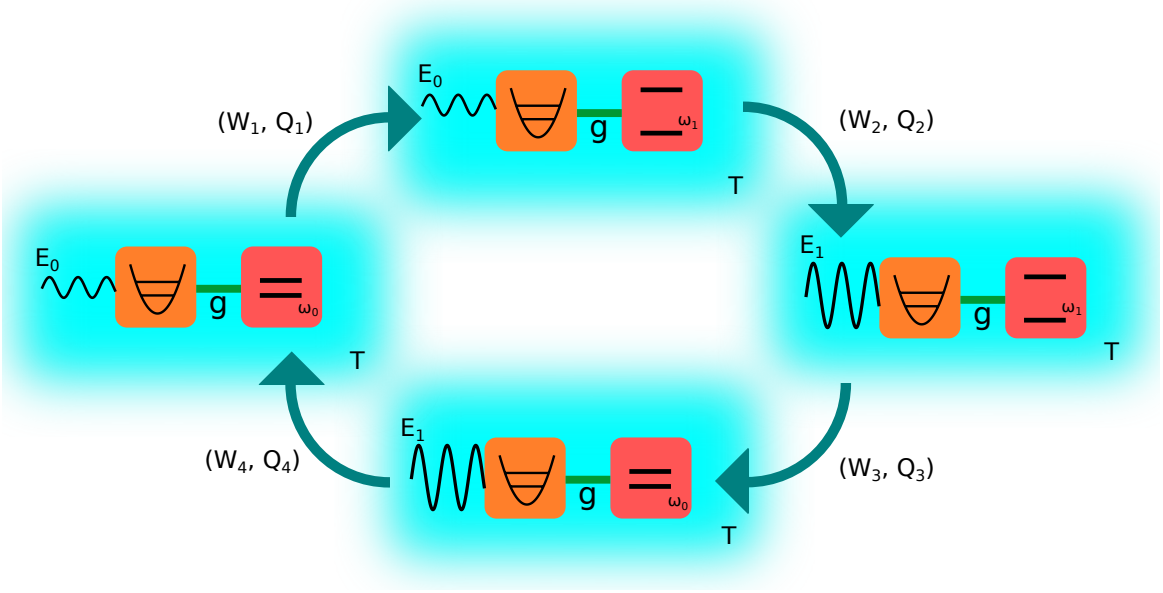

Figure 16 – Sketch of the thermodynamic cycle obtained by varying the tunable parameters ω_{T} and E_d. Each one of the strokes are obtained by keeping one of the variables constant while quasi-statically varying the other one. Along each stroke we have work W_i being applied or extracted and heat Q_i exchanged.

Source: By the author.

Since we are interested in analyzing the engine as a function of its parameters of operation, we simulated several cycles with different boundary values (ω_1, E_1), which will range from the minimum value (ω_0, E_0) to the maximum one $(\omega_{1,\max}, E_{1,\max})$. The corresponding cycles lie on the von Neumann entropy, one of them is depicted in Figure 17 through a red square.

Finally, it is worth emphasizing that in the present analysis all parameters were chosen from an *experimentally accessible* regime,[88,90–92] under the validity of the approximation of weak-coupling interaction between transmon and cavity. The parameters are collected in Table 1. Recall that the cavity is assumed to be a subpart of the bath seen by the WS, and that its state is modified by E_d. Since the WS is always in contact with the environment, one has that both heat and work are exchanged in each stroke. Here, such a calculation is done by using Equation (2.27), considering the stationary state Equation (4.36) and the effective WS Hamiltonian Equation (4.34). Then, for the ith

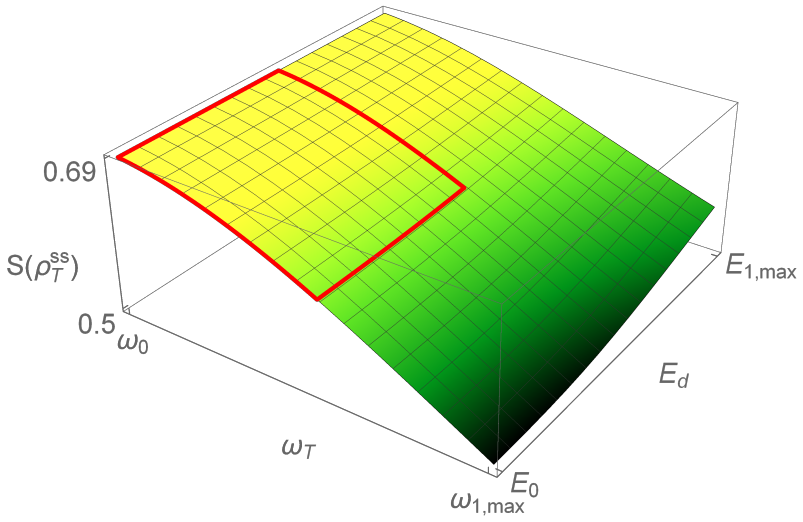

Figure 17 – Stationary state's von Neumann entropy in the regime of operation of the engine. Any thermodynamic cycle must be contained on this surface and in our case it is represented by the red square. Different cycles are created by different upper values (ω_1, E_1), varying the edge of the square.

Source: By the author.

Table 1 – Engine parameters used in the present analysis.

Parameter	**Value**
$\omega_{\mathrm{CPW}}/2\pi$	4.94 GHz
$\omega/2\pi$	4.94 GHz
$g/2\pi\hbar$	120 MHz
T	30 mK
$\Gamma/2\pi$	2 MHz
$\kappa_{CPW}/2\pi$	1 MHz
$\omega_0/2\pi$	100 MHz
$\omega_{1,\mathrm{max}}/2\pi$	1000 MHz
$E_0/2\pi\hbar$	0.2 MHz
$E_{1,\mathrm{max}}/2\pi\hbar$	2 MHz

Source: By the author.

stroke, the corresponding W_i and Q_i integrals, representing the work and heat delivered (extracted) to (from) the WS, can be parametrized in terms of the respective knob variation. These quantities are obtained using the WS effective Hamiltonian $\tilde{H}_{\mathrm{T,RWA}}$, which already takes into account the interaction with the external bath and pumped cavity. It is worth noticing that those physical parameters indicate the system will typically reach the steady state in a time scale of $\sim 1/\Gamma \sim 1\mu$s, determining how slow the pace must be when taking the system throughout the cycle. Furthermore, the experimental realization of the cycle

using 10^3 steps suffices to furnish a high accuracy protocol implementation,[88] meaning that our cycle should take around 1ms to be executed.

Once these quantities are determined, we can calculate the efficiency η of this engine, defined by

$$\eta = -\frac{\sum_{i=1}^{4} W_i}{Q_+}, \tag{4.38}$$

with the delivered heat to the WS in a complete cycle being given by $Q_+ = \sum_{i=1}^{4} Q_+^i$, with Q_+^i the given heat (only positive contributions inside the stroke) during the i_{th} stroke. Therefore, this efficiency represents the amount of work extracted from the engine through the use of the delivered heat to the WS. Here are the explicit expressions of the thermodynamic quantities W_i and Q_i for $i = 1, 2, 3, 4$ and the heat Q_+ given to the WS. These quantities are obtained by changing quasi-statically the parameters ω_{T} and E_d producing a succession of steady states $\hat{\rho}_{\text{T}}^{ss}(\omega_{\text{T}}, E_d)$:

$$\begin{aligned}
W_1 &= \int_{\omega_0}^{\omega_1} \text{tr}\left\{\hat{\rho}_{\text{T}}^{ss}(\omega_{\text{T}}, E_0)\left(\frac{\partial \tilde{H}_{\text{T,RWA}}}{\partial \omega_{\text{T}}}\right)_{E_0}\right\} d\omega_{\text{T}}, \\
W_2 &= \int_{E_0}^{E_1} \text{tr}\left\{\hat{\rho}_{\text{T}}^{ss}(\omega_1, E_d)\left(\frac{\partial \tilde{H}_{\text{T,RWA}}}{\partial E_d}\right)_{\omega_1}\right\} dE_d, \\
W_3 &= \int_{\omega_1}^{\omega_0} \text{tr}\left\{\hat{\rho}_{\text{T}}^{ss}(\omega_{\text{T}}, E_1)\left(\frac{\partial \tilde{H}_{\text{T,RWA}}}{\partial \omega_{\text{T}}}\right)_{E_1}\right\} d\omega_{\text{T}}, \\
W_4 &= \int_{E_1}^{E_0} \text{tr}\left\{\hat{\rho}_{\text{T}}^{ss}(\omega_0, E_d)\left(\frac{\partial \tilde{H}_{\text{T,RWA}}}{\partial E_d}\right)_{\omega_0}\right\} dE_d.
\end{aligned} \tag{4.39}$$

$$\begin{aligned}
Q_1 &= \int_{\omega_0}^{\omega_1} \text{tr}\left\{\left(\frac{\partial \hat{\rho}_{\text{T}}^{ss}}{\partial \omega_{\text{T}}}\right)_{E_0} \tilde{H}_{\text{T,RWA}}(\omega_{\text{T}}, E_0)\right\} d\omega_{\text{T}}, \\
Q_2 &= \int_{E_0}^{E_1} \text{tr}\left\{\left(\frac{\partial \hat{\rho}_{\text{T}}^{ss}}{\partial E_d}\right)_{\omega_1} \tilde{H}_{\text{T,RWA}}(\omega_1, E_d)\right\} dE_d, \\
Q_3 &= \int_{\omega_1}^{\omega_0} \text{tr}\left\{\left(\frac{\partial \hat{\rho}_{\text{T}}^{ss}}{\partial \omega_{\text{T}}}\right)_{E_1} \tilde{H}_{\text{T,RWA}}(\omega_{\text{T}}, E_1)\right\} d\omega_{\text{T}}, \\
Q_4 &= \int_{E_1}^{E_0} \text{tr}\left\{\left(\frac{\partial \hat{\rho}_{\text{T}}^{ss}}{\partial E_d}\right)_{\omega_0} \tilde{H}_{\text{T,RWA}}(\omega_0, E_d)\right\} dE_d.
\end{aligned} \tag{4.40}$$

$$Q_+ = \sum_{i=1}^{4} Q_+^i \tag{4.41}$$

with Q_+^i for $i = 1, 2, 3, 4$ given by

$$\begin{aligned}
Q_+^1 &= \int_{\omega_0}^{\omega_1} \text{tr}\left\{\left(\frac{\partial \hat{\rho}_{\text{T}}^{ss}}{\partial \omega_{\text{T}}}\right)_{E_0} \tilde{H}_{\text{T,RWA}}(\omega_{\text{T}}, E_0)\right\} \Theta\left[\text{tr}\left\{\left(\frac{\partial \hat{\rho}_{\text{T}}^{ss}}{\partial \omega_{\text{T}}}\right)_{E_0} \tilde{H}_{\text{T,RWA}}(\omega_{\text{T}}, E_0)\right\} d\omega_{\text{T}}\right], \\
Q_+^2 &= \int_{E_0}^{E_1} \text{tr}\left\{\left(\frac{\partial \hat{\rho}_{\text{T}}^{ss}}{\partial E_d}\right)_{\omega_1} \tilde{H}_{\text{T,RWA}}(\omega_1, E_d)\right\} \Theta\left[\text{tr}\left\{\left(\frac{\partial \hat{\rho}_{\text{T}}^{ss}}{\partial E_d}\right)_{\omega_1} \tilde{H}_{\text{T,RWA}}(\omega_1, E_d)\right\} dE_d\right], \\
Q_+^3 &= \int_{\omega_1}^{\omega_0} \text{tr}\left\{\left(\frac{\partial \hat{\rho}_{\text{T}}^{ss}}{\partial \omega_{\text{T}}}\right)_{E_1} \tilde{H}_{\text{T,RWA}}(\omega_{\text{T}}, E_1)\right\} \Theta\left[\text{tr}\left\{\left(\frac{\partial \hat{\rho}_{\text{T}}^{ss}}{\partial \omega_{\text{T}}}\right)_{E_1} \tilde{H}_{\text{T,RWA}}(\omega_{\text{T}}, E_1)\right\} d\omega_{\text{T}}\right], \\
Q_+^4 &= \int_{E_1}^{E_0} \text{tr}\left\{\left(\frac{\partial \hat{\rho}_{\text{T}}^{ss}}{\partial E_d}\right)_{\omega_0} \tilde{H}_{\text{T,RWA}}(\omega_0, E_d)\right\} \Theta\left[\text{tr}\left\{\left(\frac{\partial \hat{\rho}_{\text{T}}^{ss}}{\partial E_d}\right)_{\omega_0} \tilde{H}_{\text{T,RWA}}(\omega_0, E_d)\right\} dE_d\right].
\end{aligned} \tag{4.42}$$

where the Heaviside function $\Theta[\cdot]$ is inside the integral, selecting only the positive contributions (heat given to the WS) along the stroke.

Figure 18 shows the engine efficiency η attained in the execution of the strokes as a function of the boundary values (ω_1, E_1), as depicted in Figure 16. Please note that (ω_1, E_1) sweeps the entire spectrum of the tunable parameters (ω_T, E_d), going from (ω_0, E_0) to $(\omega_{1,\max}, E_{1,\max})$ where we find the maximal efficiency. It is worth mentioning here that the highest value of the efficiency is dependent on the chosen regime of parameters, which in our case is based on experimentally attainable values.[88,90–92] As usual, in order to extract the predicted work, one has to couple our engine to another system. We envision using the experimental setup of Ref.,[88] where a mechanical nanoresonator is present and weakly driven by the transmon. Thus, under such a configuration, by following the nanoresonator's state (recall that we have assumed infinite inertia, i.e., the transmon is not capable of changing the cavity's state. In situations where such an assumption does not hold, one has to take into account the possibility of having the transmon doing work on the cavity), one can determine the amount of energy transferred in the form of work. In addition, by observing the transmon's state, one can obtain the amount of heat given by the non-standard bath, providing a full characterization of our engine.

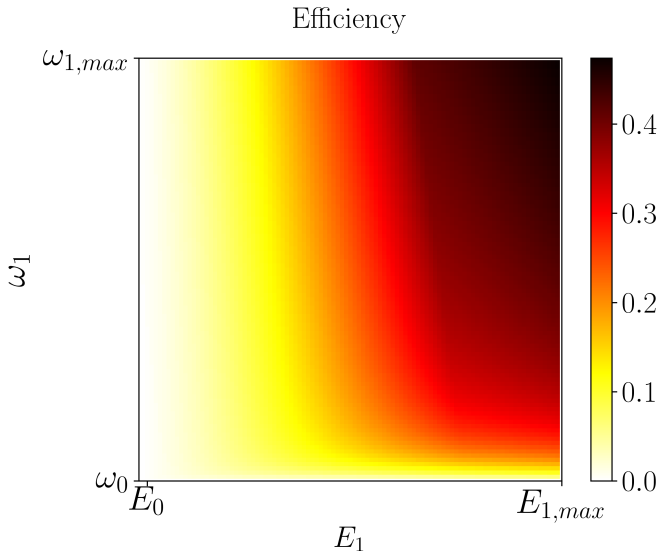

Figure 18 – Efficiency η as a function of the upper values (ω_1, E_1) for the cycle depicted in Figure 16. The observed highest efficiency of about 47% was attained when $(\omega_1, E_1) = (\omega_{1,\max}, E_{1,\max})$, with $\omega_{1,\max}/2\pi = 1000$ MHz and $E_{1,\max}/2\pi\hbar = 2$ MHz.

Source: By the author.

Theoretical research of small heat engines in the quantum domain is common place in quantum thermodynamics.[47,72,93–100] In this chapter, we have devised a transmon-based heat engine using an experimentally realistic regime of parameters reaching a maximal efficiency of 47%, which turns out to be a reasonable value when compared with the state

of the art in quantum heat engines. One of the most recent experiments in quantum heat engine was implemented by Peterson *et al.*[101] using a spin $-1/2$ system and nuclear resonance techniques, performing an Otto cycle with efficiency in excess of 42% at maximum power. It is important to stress that implementing small heat engines constitutes a hard task, even when dealing with classical systems. Indeed, a representative example is the single ion confined in a linear Paul trap with a tapered geometry, which was used to implement a Stirling engine[102] with efficiency of only 0.28%. It is worth emphasizing here that the engine presented in this chapter has an out-of-equilibrium regime of operation and we have to pay an energetic cost to prepare the bath used in it, therefore if we rigorously take that into account the efficiency of the engine would drop. But on the other hand if we look at the side of the "person that is buying" the engine, or more precisely the application that's being using the work delivered by it, it won't necessarily matter if the preparation is more or less expensive, as far as they can use the totality of the engine's output. Therefore the approach used to look at these systems can perfectly change depending on the circumstances. By devising this theoretical protocol for the implementation of a quantum engine, we hope to help the community, and in particular experimentalists, in the formidable task to design and implement quantum thermodynamic systems and to consolidate the concepts of this new exciting field of research.

5 ORDER OF COHERENCE AND ITS RELATION WITH THE EFFICIENCY

5.1 Using coherence to change heat engine's efficiency

Quantum coherence has an important role in quantum mechanics and makes it acquire a behavior quite odd when compared with their classical version, so a natural step would be to look for what this new ingredient has to offer in thermodynamic terms.[103] And as expected coherences turned out to be very important in a lot of different ways, e.g. having an energy cost when creating it by means of unitary operations acting on thermal states[104] , how coherence can or cannot be used to extract work,[105–107] and even costing work to keep system out of equilibrium with coherences.[108] Also playing a part on quantum heat engines and refrigerators.[79,81,82,87,96,97,109–111] Therefore we see that the role played by quantum coherences in quantum thermodynamics can hardly be overstated. With that being said, a variety of ways of quantifying the coherence content present in an arbitrary state has been published recently and these quantifiers can be obtained for two different classes of information,[112] the *speakable* and *unspeakable* information, according to the relevance of their encoding. If the way the information is stored in a quantum state doesn't matter, this information is going to be called speakable. Sending information is an example of it, the states of the basis used to codify the information works only as a label and play no rule on the sending process. The other type of information, the unspeakable one, we have the opposite, therefore the way that information is encoded in the basis is relevant for the task, e.g. when we are dealing with rotations. The quantifiers of coherence for speakable information are are given by[113–116] and for unspeakable.[112,117–120] In this chapter we will quantify the coherence present in the heat engine's WS using the unspeakable approach and see how its different orders take their toll on the engine's behavior.

5.1.1 Modes of asymmetry and coherence

In this section we will see that unspeakable coherences can be interpreted as asymmetry with respect to some group of translations.[112,119] For that, take an observable $\hat{\mathrm{L}}$ acting on a Hilbert space $\mathcal{H}$ with eigenvalues $\{\lambda_i\}_i$ and eigenvectors $\{|\lambda_i,\alpha\rangle\}_{i,\alpha}$ with α being the multiplicity associated to i. This operator generates a group of translations $\hat{\mathcal{U}}_{L,x}$ given by

$$\hat{\mathcal{U}}_{\mathrm{L},x}(\cdot) = e^{-ix\hat{\mathrm{L}}}(\cdot)e^{ix\hat{\mathrm{L}}}, \quad x \in \mathbb{R}. \tag{5.1}$$

Using the eigenvalues of $\hat{\mathrm{L}}$ we define the set Ω, called set of modes, which contains all the gaps $\{\lambda_i - \lambda_j\}_{i,j}$ generated by the eigenvalues of $\hat{\mathrm{L}}$. A particular mode of order $\omega \in \Omega$ is a subset of it containing only the gaps $\lambda_i - \lambda_j$ equal to ω connecting the states $|\lambda_i,\alpha\rangle$ and

$|\lambda_j, \beta\rangle = |\lambda_i + \omega, \beta\rangle$. Each mode ω defines a projector $\hat{\mathcal{P}}^{(\omega)}$ given by

$$\hat{\mathcal{P}}^{(\omega)}(\cdot) = \lim_{x_0 \to \infty} \frac{1}{2x_0} \int_{-x_0}^{x_0} \mathrm{d}x e^{-i\omega x} \hat{\mathcal{U}}_{\mathrm{L},x}(\cdot), \quad x \in \mathbb{R}, \tag{5.2}$$

that when acting on a given operator, erases all its matrix elements except those $|\lambda_i, \alpha\rangle\langle\lambda_i + \omega, \beta|$ associated to the order ω. The set $\{\hat{\mathcal{P}}^{(\omega)}, \omega \in \Omega\}$ form a complete set of projectors to different sub-spaces $\mathcal{B}^{(\omega)}$ of the operator space $\mathcal{B}(\mathcal{H})$ associated to the Hilbert space $\mathcal{H}$. Those sub-spaces are orthogonal by a Hilbert-Schmidt inner product, $\langle \mathrm{A}^{(\omega_i)}, \mathrm{A}^{(\omega_j)} \rangle = \mathrm{tr}\left\{ \mathrm{A}^{(\omega_i)\dagger} \mathrm{A}^{(\omega_j)} \right\}$ for any $\hat{\mathrm{A}}^{(\omega_i)} \in \mathcal{B}^{(\omega_i)}$ and $\hat{\mathrm{A}}^{(\omega_j)} \in \mathcal{B}^{(\omega_j)}$. Therefore the operator space can be decomposed in a direct sum of its constituent modes, $\mathcal{B} = \bigoplus_{\omega \in \Omega} \mathcal{B}^{(\omega)}$. If an operator has a mode ω, i.e. $\hat{\mathrm{A}}^{(\omega)} \in \mathcal{B}^{(\omega)}$, the application of a translation associated to the operator $\hat{\mathrm{L}}$ produces the following expression:

$$\hat{\mathcal{U}}_{\mathrm{L},x}(\hat{\mathrm{A}}^{(\omega)}) = e^{i\omega x} \hat{\mathrm{A}}^{(\omega)}, \quad x \in \mathbb{R}. \tag{5.3}$$

Each one of these operators sub-spaces $\mathcal{B}^{(\omega)}$ are called modes of asymmetry.[119] An operator $\hat{\mathrm{A}} \in \mathcal{B}$ can be decomposed in modes of asymmetry $\mathcal{B}^{(\omega)}$, $\hat{\mathrm{A}} = \sum_{\omega \in \Omega} \hat{\mathrm{A}}^{(\omega)}$. There is a set o transformations $\{\mathcal{E}\}$ that are symmetric with respect to the group of translations generated by $\hat{\mathrm{L}}$ (also called translational covariant), i.e. the following property holds:

$$\mathcal{E}\left[e^{-ix\hat{\mathrm{L}}} (\cdot) e^{ix\hat{\mathrm{L}}} \right] = e^{-ix\hat{\mathrm{L}}} \mathcal{E}(\cdot) e^{ix\hat{\mathrm{L}}}, \quad x \in \mathbb{R}. \tag{5.4}$$

If this property is valid for a certain transformation $\mathcal{E}$, the mode of asymmetry of an operator $\hat{\mathrm{A}}^{(\omega)}$ will not be changed by $\mathcal{E}$:

$$\mathcal{E}(\hat{\mathrm{A}}^{(\omega)}) = \hat{\mathrm{B}}^{(\omega)}, \quad \hat{\mathrm{A}}^{(\omega)}, \hat{\mathrm{B}}^{(\omega)} \in \mathcal{B}^{(\omega)}, \tag{5.5}$$

which means that translational covariant maps with respect to a certain group of symmetry can't transform a mode of asymmetry into another one. The operator $\hat{\mathrm{L}}$ used to generate the group of symmetry could be a variety of obeservables, like the Hamiltonian $\hat{\mathrm{H}}$ with $x = t$ and being responsible for time-translations $e^{-i\hat{\mathrm{H}}t}(\cdot)e^{i\hat{\mathrm{H}}t}$, could also be the z-projection of the angular momentum $\hat{\mathrm{J}}_z$ with $x = \theta$ generating rotations along the z-axis $e^{-i\hat{\mathrm{J}}_z\theta}(\cdot)e^{i\hat{\mathrm{J}}_z\theta}$. Suppose right now that the operators on which we are applying these symmetry transformations were density matrices $\hat{\mathrm{A}} = \hat{\rho} = \sum_{i,j} \rho_{ij} |\lambda_i\rangle\langle\lambda_j|$ describing the quantum system represented by the Hilbert space $\mathcal{H}$, with the matrix elements ρ_{ij} being the coherences of the quantum system in the basis $\{|\lambda_i\rangle\}_i$ of the observable $\hat{\mathrm{L}}$ generating the symmetry transformation. The coherences can be associated to different modes of asymmetry ω, composed by the operators $\hat{\rho}^{(\omega)}$, which in this context they can be called *modes of coherence*[119,121] or coherence orders in the context of NMR.[122] Therefore the density matrix can be written as

$$\hat{\rho} = \sum_{\omega} \hat{\rho}^{(\omega)}, \qquad \text{with} \qquad \hat{\rho}^{(\omega)} = \sum_{\substack{i,j \\ \lambda_i - \lambda_j = \omega}} \rho_{ij} |\lambda_i\rangle\langle\lambda_j|. \tag{5.6}$$

The set $\{\rho_{ij}, \lambda_i - \lambda_j = \omega\}_{i,j}$ will represent the set of coherences associated to the mode of coherence $\hat{\rho}^{(\omega)}$ and they will be very important in the rest of this thesis.

5.1.2 Modes of coherence in a qubit

For the next step we want to use this formalism in the trivial case of a qubit,[122–124] the one used as the WS in the non-thermal heat engine presented in this thesis. The first step is to choose the operators generating the symmetry, which in our case is going to be the rotation along the z-direction generated by $\hat{\sigma_z}$. Once we have defined that we need to write the density matrix of the WS in terms of operators that have a unique mode of coherence. A general density matrix $\hat{\rho}$ of a qubit can be written using the bi-dimensional unity $\hat{\mathbb{1}}$ and the Pauli matrices $\vec{\sigma} = \{\hat{\sigma}_x, \hat{\sigma}_y, \hat{\sigma}_z\}$,

$$\hat{\rho} = \frac{1}{2}\left(\hat{\mathbb{1}} + \vec{r}\cdot\vec{\sigma}\right), \tag{5.7}$$

therefore the density matrix $\hat{\rho}$ is uniquely determined by a tri-dimensional vector $\vec{r} = \{x, y, z\}$ in the Bloch sphere. But if we apply the rotation on the operators $\hat{\sigma}_x$ and $\hat{\sigma}_y$ they are going to have more than one mode of coherence, therefore we will rewrite it in the basis $\{\hat{\mathrm{I}}_0, \hat{\mathrm{I}}_+, \hat{\mathrm{I}}_-, \hat{\mathrm{I}}_z\}$, with $\hat{\mathrm{I}}_\pm = (\hat{\sigma}_x \pm i\hat{\sigma}_y)/2$ representing the ladder operators, $\hat{\mathrm{I}}_z = \hat{\sigma}_z/2$ the re-normalized angular momentum component along the z-direction and $\hat{\mathrm{I}}_0 = \hat{\mathbb{1}}/2$ the re-normalized bi-dimensional unity operator. This change of basis can easily be achieved trough Eq. 5.7:

$$\begin{aligned}
\hat{\rho} &= \frac{1}{2}\left(\hat{\mathbb{1}} + \vec{r}\cdot\vec{\sigma}\right), \\
&= \frac{\hat{\mathbb{1}}}{2} + \frac{x}{2}\hat{\sigma}_x + \frac{y}{2}\hat{\sigma}_y + \frac{z}{2}\hat{\sigma}_z, \\
&= \hat{\mathrm{I}}_0 + \frac{x}{2}(\hat{\mathrm{I}}_+ + \hat{\mathrm{I}}_-) + \frac{y}{2i}(\hat{\mathrm{I}}_+ - \hat{\mathrm{I}}_-) + z\hat{\mathrm{I}}_z, \\
&= \hat{\mathrm{I}}_0 + \frac{1}{2}(x - iy)\hat{\mathrm{I}}_+ + \frac{1}{2}(x + iy)\hat{\mathrm{I}}_- + z\hat{\mathrm{I}}_z, \\
&= a_0\hat{\mathrm{I}}_0 + a_+\hat{\mathrm{I}}_+ + a_-\hat{\mathrm{I}}_- + a_z\hat{\mathrm{I}}_z, \\
&= \sum_j a_j\hat{\mathrm{I}}_j,
\end{aligned} \tag{5.8}$$

with $a_0 = 1$, $a_+ = (x - iy)/2$, $a_- = (x + iy)/2$ and $a_z = z$. The operator representing the rotations along the z-direction is given by $\hat{\mathrm{I}}_z$ and the action of it on the basis $\{\hat{\mathrm{I}}_0, \hat{\mathrm{I}}_+, \hat{\mathrm{I}}_-, \hat{\mathrm{I}}_z\}$ reveal the modes of it one:

- coherence order $m = 0$ (rotationally invariant):

$$e^{-i\theta\hat{\mathrm{I}}_z}\left\{\hat{\mathrm{I}}_0, \hat{\mathrm{I}}_z\right\}e^{i\theta\hat{\mathrm{I}}_z} = \left\{\hat{\mathrm{I}}_0, \hat{\mathrm{I}}_z\right\}; \tag{5.9}$$

- coherence order $m = 1$:

$$e^{-i\theta\hat{\mathrm{I}}_z}\left\{\hat{\mathrm{I}}_+\right\}e^{i\theta\hat{\mathrm{I}}_z} = e^{-i\theta}\left\{\hat{\mathrm{I}}_+\right\}; \tag{5.10}$$

- coherence order $m = -1$:

$$e^{-i\theta\hat{\mathrm{I}}_z}\left\{\hat{\mathrm{I}}_-\right\}e^{i\theta\hat{\mathrm{I}}_z} = e^{i\theta}\left\{\hat{\mathrm{I}}_-\right\}. \tag{5.11}$$

If we had two qubits rather than one, we'd proceed in a similar way but with a Hilbert space $\mathcal{H}_1 \otimes \mathcal{H}_2$ described by the basis $\{\hat{\mathrm{I}}_{j_1} \otimes \hat{\mathrm{I}}_{j_2}\}$ with $j_1, j_2 = (0, +, -, z)$. The density matrix $\hat{\rho}$ would be written as follows:

$$\hat{\rho} = \sum_{j_1, j_2} a_{j_1, j_2} \hat{\mathrm{I}}_{j_1} \otimes \hat{\mathrm{I}}_{j_2}. \tag{5.12}$$

Analogous reasoning can be applied to a system made of N qubits resulting in the density matrix

$$\hat{\rho} = \sum_{j_1, \ldots, j_N} a_{j_1 \ldots j_N} \bigotimes_{j_l}^{N} \hat{\mathrm{I}}_{j_l}. \tag{5.13}$$

Let's take a look at the position of the operator element at the matrix when dealing with systems with more than one constituent, for example, take a two qubit system and look at matrix element a_{++} corresponding to the basis element $\hat{\mathrm{I}}_+ \otimes \hat{\mathrm{I}}_+$ of mode $m = 2$, using the basis ordering $\{|ee\rangle, |eg\rangle, |ge\rangle, |gg\rangle\}$ we have the following:

$$a_{++} \hat{\mathrm{I}}_+ \otimes \hat{\mathrm{I}}_+ = a_{++} \begin{pmatrix} 0 & 1 \\ 0 & 0 \end{pmatrix} \otimes \begin{pmatrix} 0 & 1 \\ 0 & 0 \end{pmatrix} = \begin{pmatrix} 0 & 0 & 0 & a_{++} \\ 0 & 0 & 0 & 0 \\ 0 & 0 & 0 & 0 \\ 0 & 0 & 0 & 0 \end{pmatrix}. \tag{5.14}$$

The mode $m = 2$ corresponds to the states differing by two excitations and in this case it is located at the third secondary diagonal. The next matrix have the modes that every matrix element represent[123] on the two qubit case:

$$\begin{pmatrix} 0 & +1 & +1 & +2 \\ -1 & 0 & 0 & +1 \\ -1 & 0 & 0 & +1 \\ -2 & -1 & -1 & 0 \end{pmatrix}. \tag{5.15}$$

We will see later that this ordering of the modes is different from the case where we have only one system with 4 levels.

5.1.3 Writing the WS in terms of the basis $\{\hat{\mathrm{I}}_0, \hat{\mathrm{I}}_z, \hat{\mathrm{I}}_+, \hat{\mathrm{I}}_-\}$

As we've noticed in the last chapter, along the cycle of the non-thermal heat engine there is some significant amount of coherence in certain segments of the cycle present in the state of the WS, therefore we will write the the stationary density matrix $\hat{\rho}^{ss}(\omega_{\mathrm{T}}, E_d)$ in terms of the basis $\{\hat{\mathrm{I}}_0, \hat{\mathrm{I}}_z, \hat{\mathrm{I}}_+, \hat{\mathrm{I}}_-\}$ to see the explicit expression of the modes of coherence

represented by each one of them, which in this case will be very trivial:

$$\begin{aligned}\hat{\rho}^{ss}(\omega_{\mathrm{T}}, E_d) &= \begin{pmatrix}\rho_{ee} & \rho_{eg}\\ \rho_{ge} & \rho_{gg}\end{pmatrix},\\ &= \begin{pmatrix}\rho_{ee} & 0\\ 0 & 0\end{pmatrix} + \begin{pmatrix}0 & 0\\ 0 & \rho_{gg}\end{pmatrix} + \begin{pmatrix}0 & \rho_{eg}\\ 0 & 0\end{pmatrix} + \begin{pmatrix}0 & 0\\ \rho_{ge} & 0\end{pmatrix},\\ &= \rho_{ee}\left(\hat{\mathrm{I}}_0 + \hat{\mathrm{I}}_z\right) + \rho_{gg}\left(\hat{\mathrm{I}}_0 - \hat{\mathrm{I}}_z\right) + \rho_{eg}\hat{\mathrm{I}}_+ + \rho_{ge}\hat{\mathrm{I}}_-,\\ &= \left(\rho_{ee} + \rho_{gg}\right)\hat{\mathrm{I}}_0 + \left(\rho_{ee} - \rho_{gg}\right)\hat{\mathrm{I}}_z + \rho_{eg}\hat{\mathrm{I}}_+ + \rho_{ge}\hat{\mathrm{I}}_-.\end{aligned} \tag{5.16}$$

with the basis having the following explicit matrix form

$$\hat{\mathrm{I}}_0 = \frac{1}{2}\begin{pmatrix}1 & 0\\ 0 & 1\end{pmatrix}, \qquad \hat{\mathrm{I}}_z = \frac{1}{2}\begin{pmatrix}1 & 0\\ 0 & -1\end{pmatrix}, \qquad \hat{\mathrm{I}}_+ = \begin{pmatrix}0 & 1\\ 0 & 0\end{pmatrix}, \qquad \hat{\mathrm{I}}_- = \begin{pmatrix}0 & 0\\ 1 & 0\end{pmatrix}. \tag{5.17}$$

The above expression is the trivial case containing only the coherences of mode 1 and -1 associated basis vectors $\hat{\mathrm{I}}_+$ and $\hat{\mathrm{I}}_-$ respectively. In order to see how these coherences change the efficiency of the heat engine, and in order to do that we separate the integrand of the relevant quantities o the problem in two different parts, starting with the work.

$$\begin{aligned}\mathrm{tr}\left\{\hat{\rho}^{ss}_{\mathrm{T}}\frac{\partial \tilde{H}_{\mathrm{T,RWA}}}{\partial x}\right\} &= \sum_{m,n}\rho_{mn}\frac{\partial h_{nm}}{\partial x}\\ &= \left(\rho_{ee}\frac{\partial h_{ee}}{\partial x} + \rho_{gg}\frac{\partial h_{gg}}{\partial x}\right) + \left(\rho_{eg}\frac{\partial h_{ge}}{\partial x} + \rho_{ge}\frac{\partial h_{eg}}{\partial x}\right).\end{aligned} \tag{5.18}$$

Each term has only components of one specific coherence mode, the first one is associated to the zeroth mode, containing only the diagonal components $\{\rho_{ee}, \rho_{gg}\}$ and the second one contains the mode 1 and -1, with $\{\rho_{eg}, \rho_{ge}\}$. The variable x being used on the derivative will be ω_{T} or E_d depending on the stroke being executed. Using this division we calculate the different contributions to work at each stroke of the cycle:

$$\begin{aligned}W_1 &= \int_{\omega_0}^{\omega_1}\left(\rho_{ee}\frac{\partial h_{ee}}{\partial \omega_{\mathrm{T}}} + \rho_{gg}\frac{\partial h_{gg}}{\partial \omega_{\mathrm{T}}}\right)_{E_0} d\omega_{\mathrm{T}} + \int_{\omega_0}^{\omega_1}\left(\rho_{eg}\frac{\partial h_{ge}}{\partial \omega_{\mathrm{T}}} + \rho_{ge}\frac{\partial h_{eg}}{\partial \omega_{\mathrm{T}}}\right)_{E_0} d\omega_{\mathrm{T}} = W_1^{\mathrm{D}} + W_1^{\mathrm{C1}},\\ W_2 &= \int_{E_0}^{E_1}\left(\rho_{ee}\frac{\partial h_{ee}}{\partial E_d} + \rho_{gg}\frac{\partial h_{gg}}{\partial E_d}\right)_{\omega_1} dE_d + \int_{E_0}^{E_1}\left(\rho_{eg}\frac{\partial h_{ge}}{\partial E_d} + \rho_{eg}\frac{\partial h_{ge}}{\partial E_d}\right)_{\omega_1} dE_d = W_2^{\mathrm{D}} + W_2^{\mathrm{C1}},\\ W_3 &= \int_{\omega_1}^{\omega_0}\left(\rho_{ee}\frac{\partial h_{ee}}{\partial \omega_{\mathrm{T}}} + \rho_{gg}\frac{\partial h_{gg}}{\partial \omega_{\mathrm{T}}}\right)_{E_1} d\omega_{\mathrm{T}} + \int_{\omega_1}^{\omega_0}\left(\rho_{eg}\frac{\partial h_{ge}}{\partial \omega_{\mathrm{T}}} + \rho_{ge}\frac{\partial h_{eg}}{\partial \omega_{\mathrm{T}}}\right)_{E_1} d\omega_{\mathrm{T}} = W_3^{\mathrm{D}} + W_3^{\mathrm{C1}},\\ W_4 &= \int_{E_1}^{E_0}\left(\rho_{ee}\frac{\partial h_{ee}}{\partial E_d} + \rho_{gg}\frac{\partial h_{gg}}{\partial E_d}\right)_{\omega_0} dE_d + \int_{E_1}^{E_0}\left(\rho_{eg}\frac{\partial h_{ge}}{\partial E_d} + \rho_{ge}\frac{\partial h_{eg}}{\partial E_d}\right)_{\omega_0} dE_d = W_4^{\mathrm{D}} + W_4^{\mathrm{C1}},\end{aligned} \tag{5.19}$$

with W_i^{D} and W_i^{C1} representing the contributions for the work associated to the populations and to the coherences of mode 1 and -1, respectively, on the stroke $i = 1, 2, 3, 4$. The same

separation is done for the heat:

$$\begin{aligned}\mathrm{tr}\left\{\frac{\partial\hat{\rho}_{\mathrm{T}}^{ss}}{\partial x}\tilde{H}_{\mathrm{T,RWA}}\right\} &= \sum_{m,n}\frac{\partial\rho_{mn}}{\partial x}h_{nm} \\ &= \left(\frac{\partial\rho_{ee}}{\partial x}h_{ee}+\frac{\partial\rho_{gg}}{\partial x}h_{gg}\right)+\left(\frac{\partial\rho_{eg}}{\partial x}h_{ge}+\frac{\partial\rho_{ge}}{\partial x}h_{eg}\right).\end{aligned} \tag{5.20}$$

Which allows us to write the expressions Q_i^{D} and Q_i^{C1} representing the contributions for the exchanged heat associated to the populations and to the coherences of mode 1 and -1, respectively, on the stroke $i = 1, 2, 3, 4$:

$$\begin{aligned}
Q_1 &= \int_{\omega_0}^{\omega_1}\left(\frac{\partial\rho_{ee}}{\partial\omega_{\mathrm{T}}}h_{ee}+\frac{\partial\rho_{gg}}{\partial\omega_{\mathrm{T}}}h_{gg}\right)_{E_0}d\omega_{\mathrm{T}}+\int_{\omega_0}^{\omega_1}\left(\frac{\partial\rho_{eg}}{\partial\omega_{\mathrm{T}}}h_{ge}+\frac{\partial\rho_{ge}}{\partial\omega_{\mathrm{T}}}h_{eg}\right)_{E_0}d\omega_{\mathrm{T}} = Q_1^{\mathrm{D}}+Q_1^{\mathrm{C1}},\\
Q_2 &= \int_{E_0}^{E_1}\left(\frac{\partial\rho_{ee}}{\partial E_d}h_{ee}+\frac{\partial\rho_{gg}}{\partial E_d}h_{gg}\right)_{\omega_1}dE_d+\int_{E_0}^{E_1}\left(\frac{\partial\rho_{eg}}{\partial E_d}h_{ge}+\frac{\partial\rho_{ge}}{\partial E_d}h_{eg}\right)_{\omega_1}dE_d = Q_2^{\mathrm{D}}+Q_2^{\mathrm{C1}},\\
Q_3 &= \int_{\omega_1}^{\omega_0}\left(\frac{\partial\rho_{ee}}{\partial\omega_{\mathrm{T}}}h_{ee}+\frac{\partial\rho_{gg}}{\partial\omega_{\mathrm{T}}}h_{gg}\right)_{E_1}d\omega_{\mathrm{T}}+\int_{\omega_1}^{\omega_0}\left(\frac{\partial\rho_{eg}}{\partial\omega_{\mathrm{T}}}h_{ge}+\frac{\partial\rho_{ge}}{\partial\omega_{\mathrm{T}}}h_{eg}\right)_{E_1}d\omega_{\mathrm{T}} = Q_3^{\mathrm{D}}+Q_3^{\mathrm{C1}},\\
Q_4 &= \int_{E_1}^{E_0}\left(\frac{\partial\rho_{ee}}{\partial E_d}h_{ee}+\frac{\partial\rho_{gg}}{\partial E_d}h_{gg}\right)_{\omega_0}dE_d+\int_{E_1}^{E_0}\left(\frac{\partial\rho_{eg}}{\partial E_d}h_{ge}+\frac{\partial\rho_{ge}}{\partial E_d}h_{eg}\right)_{\omega_0}dE_d = Q_4^{\mathrm{D}}+Q_4^{\mathrm{C1}}.
\end{aligned} \tag{5.21}$$

Once we've separated the different terms the next step is to decrease the coherence by a factor $\mathrm{b}\in[0,1]$, taking $\rho_{eg}\to \mathrm{b}\rho_{eg}$ and $\rho_{ge}\to \mathrm{b}\rho_{ge}$, which makes $W_i^{\mathrm{D}}+W_i^{\mathrm{C1}}\to W_i^{\mathrm{D}}+\mathrm{b}W_i^{\mathrm{C1}}$ and $Q_i^{\mathrm{D}}+Q_i^{\mathrm{C1}}\to Q_i^{\mathrm{D}}+\mathrm{b}Q_i^{\mathrm{C1}}$. It is worth mentioning that while changing b from 1 to 0 we are assured that the new density matrix does represent a physical state. As we can see in the next figure, the reduction of coherence by the the factor b along every step of the cycle reduces the efficiency of the engine for a fixed pair of upper values (ω_1, E_1).

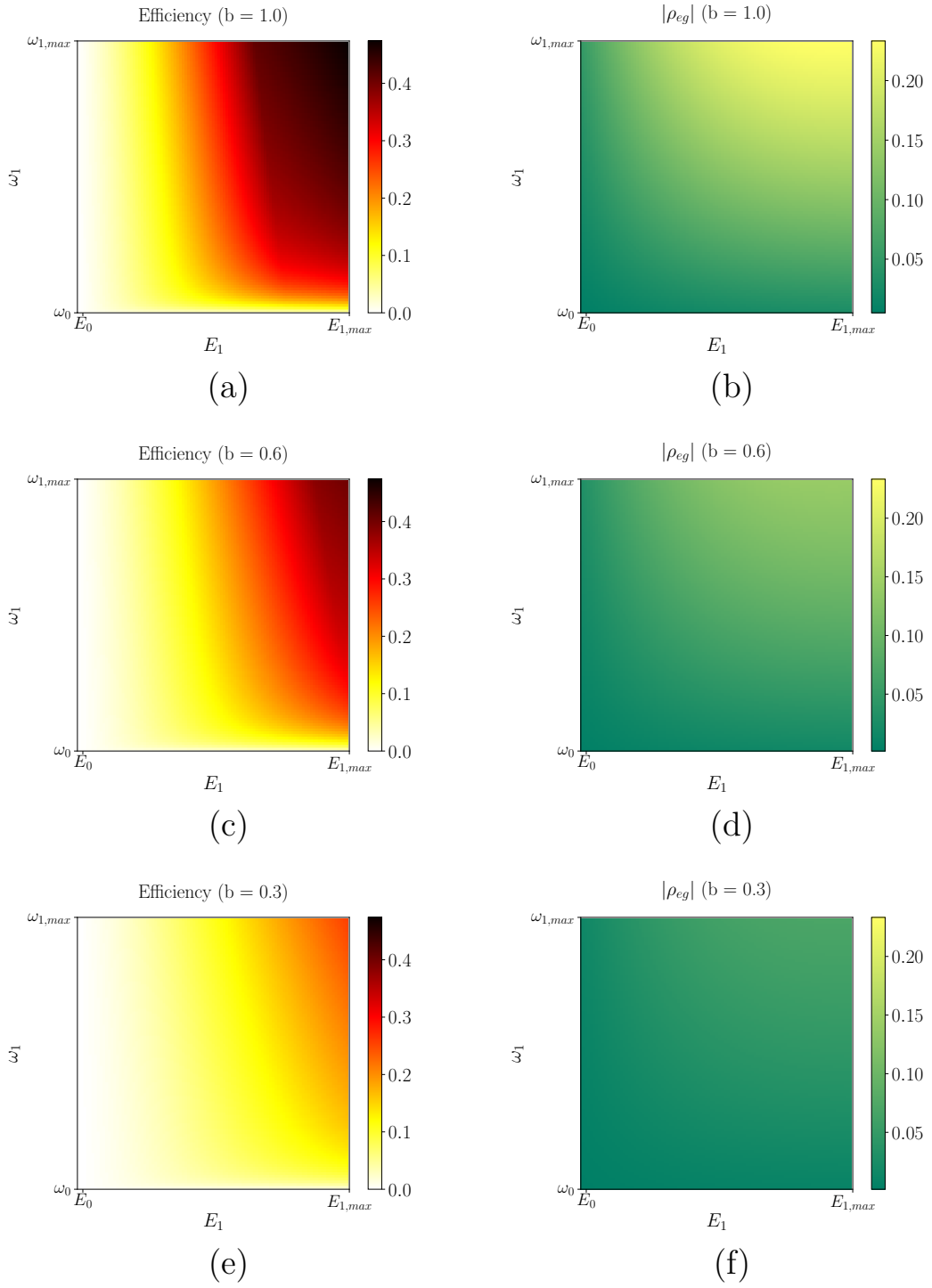

Figure 19 – The plots 19a, 19c and 19e represent the efficiency η as a function of the upper values (ω_1, E_1) for the cycle depicted in Figure 16 with $\omega_{1,\max}/2\pi = 1000$ MHz and $E_{1,\max}/2\pi\hbar = 2$ MHz for different values of b, the factor multiplying the coherences ρ_{eg} and ρ_{ge} to adjust the percentage of dephasing on the stationary state. The plots 19b, 19d and 19f represent the absolute value of coherence $|\rho_{eg}|$ of the WS stationary state as a function of ω_{T} and E_d multiplied by the factor b. For example, 19c represents the efficiency of the cycle as a function of (ω_1, E_1) with 60 % of the original coherences ρ_{eg} and ρ_{ge}. For the dephased case (b = 0), with $\rho_{eg} = \rho_{ge} = 0$, the maximum efficiency attained by the engine, when $(\omega_1, E_1) = (\omega_{1,\max}, E_{1,\max})$, is less than 6 %.

Source: By the author.

The other interesting point that we can see from the previous plots is the monotonic relation of the efficiency and the coherence with the upper values (ω_1, E_1) used in the engine, which makes those cycles involving higher upper values acquire higher amounts of coherence on the WS stationary state.

5.1.4 Systems with higher dimensions

Rather than 2^N dimensional systems composed of N qubits we will be dealing with an N-level atom obtained with the transmon and you are going to see that the ordering of the modes gets a little bit different. Imagine a WS described by the Hamiltonian $\hat{\mathrm{Z}} = \sum_{m=0}^{N-1} f(m)|m\rangle\langle m|$. The rotation generated by this Hamiltonian is given by $e^{-i\theta\hat{\mathrm{Z}}}$ and it can be used to obtain the modes associated to each coherence present in the WS density matrix. Using the computational basis $\{|m\rangle\}_m$ the action of a rotation on the basis element $|p\rangle\langle q|$ is given by

$$e^{-i\theta\hat{\mathrm{Z}}}|p\rangle\langle q|e^{i\theta\hat{\mathrm{Z}}} = e^{-i[f(p)-f(q)]\theta}|p\rangle\langle q|. \tag{5.22}$$

For an equally spaced system, $f(m) = m$, the rotation becomes $e^{-i\theta\hat{\mathrm{Z}}}|p\rangle\langle q|e^{i\theta\hat{\mathrm{Z}}} = e^{-i(p-q)\theta}|p\rangle\langle q|$ with $p-q$ determining the mode associated with the basis operator $|p\rangle\langle q|$. The first difference here when compared with the previous is related with the position of the coherence of order $p-q$ at the matrix associated to the density operator, the coherence of mode 0 is located at the main diagonal, the coherence of mode +1 at the first secondary diagonal and son on as can be seen at the next matrix of a 4-level atom using the matrix ordering $\{|3\rangle, |2\rangle, |1\rangle, |0\rangle\}$.

$$\begin{pmatrix} 0 & +1 & +2 & +3 \\ -1 & 0 & +1 & +2 \\ -2 & -1 & 0 & +1 \\ -3 & -2 & -1 & 0 \end{pmatrix}. \tag{5.23}$$

5.1.5 Spin-1 working substance

Here we will focus on a system of dimension 3 and see how the coherences of 1, -1, 2 and -2 take their toll on the engine's efficiency. The physical system to be used here is the same one used before with a transmon qubit and the master equation associated to it is given by the following result

$$\begin{aligned}\dot{\rho}_{\mathrm{T}}(t) = &-\frac{i}{\hbar}[\tilde{H}_{\mathrm{T,RWA}}, \rho_{\mathrm{T}}] + \sum_{i=0}^{1}\Gamma^{-}_{i,i+1}\mathcal{D}\left[|i\rangle\langle i+1|\right]\rho_{\mathrm{T}} + \sum_{i=0}^{1}\Gamma^{+}_{i+1,i}\mathcal{D}\left[|i+1\rangle\langle i|\right]\rho_{\mathrm{T}} \\ &+ \Gamma^{+}_{2,0}\mathcal{D}\left[|2\rangle\langle 0|\right]\rho_{\mathrm{T}} + \Gamma^{-}_{0,2}\mathcal{D}\left[|0\rangle\langle 2|\right]\rho_{\mathrm{T}},\end{aligned} \tag{5.24}$$

with

$$\tilde{H}_{\mathrm{T,RWA}} = \hbar \sum_{m=0}^{2} (\omega_{0m} - m\omega)|m\rangle\langle m| + \langle a\rangle \sum_{i=0}^{1} g_{i+1,i}|i+1\rangle\langle i| + \langle a^\dagger\rangle \sum_{i=0}^{1} g_{i,i+1}|i\rangle\langle i+1| + \langle a\rangle g_{2,0}|2\rangle\langle 0| + \langle a^\dagger\rangle g_{0,2}|0\rangle\langle 2|. \tag{5.25}$$

Notice that in this case the master equation has two additional terms, $\Gamma^{+}_{2,0}\mathcal{D}\left[|2\rangle\langle 0|\right]\rho_{\mathrm{T}}$ and $\Gamma^{-}_{0,2}\mathcal{D}\left[|0\rangle\langle 2|\right]\rho_{\mathrm{T}}$ that takes into account the excitation and relaxation between the states $|0\rangle$ and $|2\rangle$. The Hamiltonian 5.25 also two more terms responsible for the connection of states differing by one excitation, $\langle a\rangle \sum_{i=0}^{1} g_{i+1,i}|i+1\rangle\langle i| + \langle a^\dagger\rangle \sum_{i=0}^{1} g_{i,i+1}|i\rangle\langle i+1|$, and the Hamiltonian have to have them in order to make the coherences of mode 1 and -1, $\{\rho_{01}, \rho_{12}, \rho_{10}, \rho_{21}\}$, appear at the work and heat expressions. The same thing happens with the terms connecting states differing by two excitations, $\langle a\rangle g_{2,0}|2\rangle\langle 0| + \langle a^\dagger\rangle g_{0,2}|0\rangle\langle 2|$, responsible for making the coherence modes 2 and -2, $\{\rho_{02}, \rho_{20}\}$, play their game at the heat engine. For the stationary case we end up with the following set of equations:

$$\begin{aligned}
&- i\left[(\omega_{0p} - \omega_{0q}) - (p-q)\omega)\right]\rho_{p,q} - i\frac{\langle a^\dagger\rangle}{\hbar}\left[g_{p,p+1}\rho_{p+1,q} - g_{q-1,q}\rho_{p,q-1}\right] \\
&- i\frac{\langle a\rangle}{\hbar}\left[g_{p,p-1}\rho_{p-1,q} - g_{q+1,q}\rho_{p,q+1}\right] - i\frac{\langle a^\dagger\rangle}{\hbar}g_{0,2}\left[\delta_{p,0}\rho_{2,q} - \rho_{p,0}\delta_{2,q}\right] \\
&- i\frac{\langle a\rangle}{\hbar}g_{2,0}\left[\delta_{p,2}\rho_{0,q} - \rho_{p,2}\delta_{0,q}\right] + \delta_{p,q}\Gamma^{-}_{q,q+1}\rho_{q+1,q+1} \\
&- \frac{1}{2}\left[\Gamma^{-}_{p-1,p} + \Gamma^{-}_{q-1,q}\right]\rho_{p,q} + \delta_{p,q}\Gamma^{+}_{q,q-1}\rho_{q-1,q-1} - \frac{1}{2}\left[\Gamma^{+}_{p+1,p} + \Gamma^{+}_{q+1,q}\right]\rho_{p,q} \\
&+ \Gamma^{+}_{2,0}\left[\delta_{p,2}\delta_{2,q}\rho_{0,0} - \frac{1}{2}\left(\delta_{p,0} + \delta_{0,q}\right)\rho_{p,q}\right] + \Gamma^{-}_{0,2}\left[\delta_{p,0}\delta_{0,q}\rho_{2,2} - \frac{1}{2}\left(\delta_{p,2} + \delta_{2,q}\right)\rho_{p,q}\right] = 0,
\end{aligned} \tag{5.26}$$

with $p, q = 0, 1, 2$. The transmon frequencies ω_{0m} will be considered equally spaced in this case, given by

$$\begin{aligned}
\omega_{00} &= 0, \\
\omega_{01} &= \omega_{\mathrm{T}}, \\
\omega_{02} &= 2\omega_{\mathrm{T}}.
\end{aligned} \tag{5.27}$$

The rates of thermal excitation are given by

$$\begin{aligned}
\Gamma^{+}_{i,i-1} &= \Gamma\left[\frac{1}{e^{\beta\Delta E_{i,i-1}} - 1}\right], \\
\Gamma^{-}_{i-1,i} &= \Gamma\left[\frac{1}{e^{\beta\Delta E_{i,i-1}} - 1} + 1\right], \\
\Gamma^{+}_{2,0} &= 10\Gamma\left[\frac{1}{e^{\beta\Delta E_{2,0}} - 1}\right], \\
\Gamma^{-}_{0,2} &= 10\Gamma\left[\frac{1}{e^{\beta\Delta E_{2,0}} - 1} + 1\right],
\end{aligned} \tag{5.28}$$

satisfying the detailed balance relation, $\Gamma^{+}_{i,i-1}/\Gamma^{-}_{i-1,i} = e^{-\beta\Delta E_{i,i-1}}$ with $i = 1, 2$ and $\Gamma^{+}_{2,0}/\Gamma^{-}_{0,2} = e^{-\beta\Delta E_{2,0}}$ with

$$\begin{aligned} \Delta E_{1,0} &= \hbar\omega_{01}, \\ \Delta E_{2,1} &= \hbar(\omega_{02} - \omega_{01}), \\ \Delta E_{2,0} &= \hbar\omega_{02}. \end{aligned} \tag{5.29}$$

Solving for the stationary state ρ^{ss}_{T}:

$$\hat{\rho}^{ss}_{\mathrm{T}} = \begin{pmatrix} \rho_{2,2} & \rho_{2,1} & \rho_{2,0} \\ \rho_{1,2} & \rho_{1,1} & \rho_{1,0} \\ \rho_{0,2} & \rho_{0,1} & \rho_{0,0} \end{pmatrix}. \tag{5.30}$$

And just like we had before, this stationary state also has coherence and these can be distinguished between their orders:

- coherence mode $m = 0$ (rotationally invariant) with elements $\{\rho_{0,0}, \rho_{1,1}, \rho_{2,2}\}$:

$$e^{-i\theta\hat{\mathrm{Z}}} \{|0\rangle\langle 0|, |1\rangle\langle 1|, |2\rangle\langle 2|\} e^{i\theta\hat{\mathrm{Z}}} = \{|0\rangle\langle 0|, |1\rangle\langle 1|, |2\rangle\langle 2|\}; \tag{5.31}$$

- coherence mode $m = 1$ with elements $\{\rho_{1,0}, \rho_{2,1}\}$:

$$e^{-i\theta\hat{\mathrm{Z}}} \{|1\rangle\langle 0|, |2\rangle\langle 1|\} e^{i\theta\hat{\mathrm{Z}}} = e^{-i\theta} \{|1\rangle\langle 0|, |2\rangle\langle 1|\}; \tag{5.32}$$

- coherence mode $m = -1$ with elements $\{\rho_{0,1}, \rho_{1,2}\}$:

$$e^{-i\theta\hat{\mathrm{Z}}} \{|0\rangle\langle 1|, |1\rangle\langle 2|\} e^{i\theta\hat{\mathrm{Z}}} = e^{i\theta} \{|0\rangle\langle 1|, |1\rangle\langle 2|\}; \tag{5.33}$$

- coherence mode $m = 2$ with element $\rho_{2,0}$:

$$e^{-i\theta\hat{\mathrm{Z}}} \{|2\rangle\langle 0|\} e^{i\theta\hat{\mathrm{Z}}} = e^{-2i\theta} \{|2\rangle\langle 0|\}; \tag{5.34}$$

- coherence mode $m = -2$ with element $\rho_{0,2}$:

$$e^{-i\theta\hat{\mathrm{Z}}} \{|0\rangle\langle 2|\} e^{i\theta\hat{\mathrm{Z}}} = e^{2i\theta} \{|0\rangle\langle 2|\}. \tag{5.35}$$

Once we have the stationary state a heat engine is built following the same procedure presented before for changing the control variables $(\omega_{\mathrm{T}}, E_d)$, keeping one fixed and varying the other one. The parameters used to build this non-thermal heat engine are the same ones used in the 2-level case, except for the cavity-qubit coupling strength involving the states $|0\rangle$ and $|2\rangle$, with $\{g_{02}, g_{20}\}/2\pi\hbar = 60$ MHz. Proceeding in a similar way than the 2-level case, we will look for the contributions of each coherence mode at the efficiency of the engine and in order to do that, we first separate the expressions of work and heat in three different terms regarding their coherence order. Using the computational basis $\{|0\rangle, |1\rangle, |2\rangle\}$

to express the WS stationary and its effective Hamiltonian, $\hat{\rho}_{\mathrm{T}}^{ss}(\omega_{\mathrm{T}}, E_0) = \sum_{m,n} \rho_{mn}|m\rangle\langle n|$ and $\tilde{H}_{\mathrm{T,RWA}} = \sum_{m,n} h_{mn}|m\rangle\langle n|$, we rearrange the integrand of quantities of interest, starting with work:

$$\begin{aligned}
\mathrm{tr}\left\{\hat{\rho}_{\mathrm{T}}^{ss}\frac{\partial \tilde{H}_{\mathrm{T,RWA}}}{\partial x}\right\} &= \sum_{m,n}\rho_{mn}\frac{\partial h_{nm}}{\partial x} \\
&= \left(\rho_{00}\frac{\partial h_{00}}{\partial x} + \rho_{11}\frac{\partial h_{11}}{\partial x} + \rho_{22}\frac{\partial h_{22}}{\partial x}\right) \\
&+ \left(\rho_{01}\frac{\partial h_{10}}{\partial x} + \rho_{10}\frac{\partial h_{01}}{\partial x} + \rho_{12}\frac{\partial h_{21}}{\partial x} + \rho_{21}\frac{\partial h_{12}}{\partial x}\right) \\
&+ \left(\rho_{02}\frac{\partial h_{20}}{\partial x} + \rho_{20}\frac{\partial h_{02}}{\partial x}\right).
\end{aligned} \tag{5.36}$$

Each term has only components of one specific coherence mode, the first one is associated to the zeroth mode, containing only the diagonal components $\{\rho_{00}, \rho_{11}, \rho_{22}\}$, the second one is the firs mode, with $\{\rho_{01}, \rho_{10}, \rho_{12}, \rho_{21}\}$, and the last one being associated to the second mode, $\{\rho_{02}, \rho_{20}\}$. The variable x being used on the derivative will be ω_{T} or E_d depending on the stroke being executed. Using this division we calculate the different contributions to work at each stroke of the cycle:

$$\begin{aligned}
W_1 &= \int_{\omega_0}^{\omega_1}\left(\rho_{00}\frac{\partial h_{00}}{\partial \omega_{\mathrm{T}}} + \rho_{11}\frac{\partial h_{11}}{\partial \omega_{\mathrm{T}}} + \rho_{22}\frac{\partial h_{22}}{\partial \omega_{\mathrm{T}}}\right)_{E_0} d\omega_{\mathrm{T}} \\
&+ \int_{\omega_0}^{\omega_1}\left(\rho_{01}\frac{\partial h_{10}}{\partial \omega_{\mathrm{T}}} + \rho_{10}\frac{\partial h_{01}}{\partial \omega_{\mathrm{T}}} + \rho_{12}\frac{\partial h_{21}}{\partial \omega_{\mathrm{T}}} + \rho_{21}\frac{\partial h_{12}}{\partial \omega_{\mathrm{T}}}\right)_{E_0} d\omega_{\mathrm{T}} \\
&+ \int_{\omega_0}^{\omega_1}\left(\rho_{02}\frac{\partial h_{20}}{\partial \omega_{\mathrm{T}}} + \rho_{20}\frac{\partial h_{02}}{\partial \omega_{\mathrm{T}}}\right)_{E_0} d\omega_{\mathrm{T}} = W_1^{\mathrm{D}} + W_1^{\mathrm{C1}} + W_1^{\mathrm{C2}}, \\
W_2 &= \int_{E_0}^{E_1}\left(\rho_{00}\frac{\partial h_{00}}{\partial E_d} + \rho_{11}\frac{\partial h_{11}}{\partial E_d} + \rho_{22}\frac{\partial h_{22}}{\partial E_d}\right)_{\omega_1} dE_d \\
&+ \int_{E_0}^{E_1}\left(\rho_{01}\frac{\partial h_{10}}{\partial E_d} + \rho_{10}\frac{\partial h_{01}}{\partial E_d} + \rho_{12}\frac{\partial h_{21}}{\partial E_d} + \rho_{21}\frac{\partial h_{12}}{\partial E_d}\right)_{\omega_1} dE_d \\
&+ \int_{E_0}^{E_1}\left(\rho_{02}\frac{\partial h_{20}}{\partial E_d} + \rho_{20}\frac{\partial h_{02}}{\partial E_d}\right)_{\omega_1} dE_d = W_2^{\mathrm{D}} + W_2^{\mathrm{C1}} + W_2^{\mathrm{C2}},
\end{aligned} \tag{5.37}$$

$$
\begin{aligned}
W_3 &= \int_{\omega_1}^{\omega_0} \left(\rho_{00} \frac{\partial h_{00}}{\partial \omega_{\mathrm{T}}} + \rho_{11} \frac{\partial h_{11}}{\partial \omega_{\mathrm{T}}} + \rho_{22} \frac{\partial h_{22}}{\partial \omega_{\mathrm{T}}} \right)_{E_1} d\omega_{\mathrm{T}} \\
&+ \int_{\omega_1}^{\omega_0} \left(\rho_{01} \frac{\partial h_{10}}{\partial \omega_{\mathrm{T}}} + \rho_{10} \frac{\partial h_{01}}{\partial \omega_{\mathrm{T}}} + \rho_{12} \frac{\partial h_{21}}{\partial \omega_{\mathrm{T}}} + \rho_{21} \frac{\partial h_{12}}{\partial \omega_{\mathrm{T}}} \right)_{E_1} d\omega_{\mathrm{T}} \\
&+ \int_{\omega_1}^{\omega_0} \left(\rho_{02} \frac{\partial h_{20}}{\partial \omega_{\mathrm{T}}} + \rho_{20} \frac{\partial h_{02}}{\partial \omega_{\mathrm{T}}} \right)_{E_1} d\omega_{\mathrm{T}} = W_3^{\mathrm{D}} + W_3^{\mathrm{C1}} + W_3^{\mathrm{C2}}, \\
W_4 &= \int_{E_1}^{E_0} \left(\rho_{00} \frac{\partial h_{00}}{\partial E_d} + \rho_{11} \frac{\partial h_{11}}{\partial E_d} + \rho_{22} \frac{\partial h_{22}}{\partial E_d} \right)_{\omega_0} dE_d \\
&+ \int_{E_1}^{E_0} \left(\rho_{01} \frac{\partial h_{10}}{\partial E_d} + \rho_{10} \frac{\partial h_{01}}{\partial E_d} + \rho_{12} \frac{\partial h_{21}}{\partial E_d} + \rho_{21} \frac{\partial h_{12}}{\partial E_d} \right)_{\omega_0} dE_d \\
&+ \int_{E_1}^{E_0} \left(\rho_{02} \frac{\partial h_{20}}{\partial E_d} + \rho_{20} \frac{\partial h_{02}}{\partial E_d} \right)_{\omega_0} dE_d = W_4^{\mathrm{D}} + W_4^{\mathrm{C1}} + W_4^{\mathrm{C2}},
\end{aligned}
\tag{5.38}
$$

with W_i^{D}, W_i^{C1} and W_i^{C2} representing the contributions for the work associated to the populations, coherences of mode 1 and -1 and coherences of mode 2 and -2 , respectively, on the stroke $i = 1, 2, 3, 4$. The same separation is done for the heat:

$$
\begin{aligned}
\mathrm{tr}\left\{ \frac{\partial \hat{\rho}_{\mathrm{T}}^{ss}}{\partial x} \tilde{H}_{\mathrm{T,RWA}} \right\} &= \sum_{m,n} \frac{\partial \rho_{mn}}{\partial x} h_{nm} \\
&= \left(\frac{\partial \rho_{00}}{\partial x} h_{00} + \frac{\partial \rho_{11}}{\partial x} h_{11} + \frac{\partial \rho_{22}}{\partial x} h_{22} \right) \\
&+ \left(\frac{\partial \rho_{01}}{\partial x} h_{10} + \frac{\partial \rho_{10}}{\partial x} h_{01} + \frac{\partial \rho_{12}}{\partial x} h_{21} + \frac{\partial \rho_{21}}{\partial x} h_{12} \right) \\
&+ \left(\frac{\partial \rho_{02}}{\partial x} h_{20} + \frac{\partial \rho_{20}}{\partial x} h_{02} \right).
\end{aligned}
\tag{5.39}
$$

Which allows us to write the expressions Q_i^{D}, Q_i^{C1} and Q_i^{C2} representing the contributions for the exchanged heat associated to the populations, coherences of mode 1 and -1 and

coherences of mode 2 and -2 , respectively, on the stroke $i = 1, 2, 3, 4$:

$$
\begin{aligned}
Q_1 &= \int_{\omega_0}^{\omega_1} \left(\frac{\partial \rho_{00}}{\partial \omega_{\mathrm{T}}} h_{00} + \frac{\partial \rho_{11}}{\partial \omega_{\mathrm{T}}} h_{11} + \frac{\partial \rho_{22}}{\partial \omega_{\mathrm{T}}} h_{22} \right)_{E_0} d\omega_{\mathrm{T}} \\
&+ \int_{\omega_0}^{\omega_1} \left(\frac{\partial \rho_{01}}{\partial \omega_{\mathrm{T}}} h_{10} + \frac{\partial \rho_{10}}{\partial \omega_{\mathrm{T}}} h_{01} + \frac{\partial \rho_{12}}{\partial \omega_{\mathrm{T}}} h_{21} + \frac{\partial \rho_{21}}{\partial \omega_{\mathrm{T}}} h_{12} \right)_{E_0} d\omega_{\mathrm{T}} \\
&+ \int_{\omega_0}^{\omega_1} \left(\frac{\partial \rho_{02}}{\partial \omega_{\mathrm{T}}} h_{20} + \frac{\partial \rho_{20}}{\partial \omega_{\mathrm{T}}} h_{02} \right)_{E_0} d\omega_{\mathrm{T}} = Q_1^{\mathrm{D}} + Q_1^{\mathrm{C1}} + Q_1^{\mathrm{C2}}, \\
Q_2 &= \int_{E_0}^{E_1} \left(\frac{\partial \rho_{00}}{\partial E_d} h_{00} + \frac{\partial \rho_{11}}{\partial E_d} h_{11} + \frac{\partial \rho_{22}}{\partial E_d} h_{22} \right)_{\omega_1} dE_d \\
&+ \int_{E_0}^{E_1} \left(\frac{\partial \rho_{01}}{\partial E_d} h_{10} + \frac{\partial \rho_{10}}{\partial E_d} h_{01} + \frac{\partial \rho_{12}}{\partial E_d} h_{21} + \frac{\partial \rho_{21}}{\partial E_d} h_{12} \right)_{\omega_1} dE_d \\
&+ \int_{E_0}^{E_1} \left(\frac{\partial \rho_{02}}{\partial E_d} h_{20} + \frac{\partial \rho_{20}}{\partial E_d} h_{02} \right)_{\omega_1} dE_d = Q_2^{\mathrm{D}} + Q_2^{\mathrm{C1}} + Q_2^{\mathrm{C2}}, \\
Q_3 &= \int_{\omega_1}^{\omega_0} \left(\frac{\partial \rho_{00}}{\partial \omega_{\mathrm{T}}} h_{00} + \frac{\partial \rho_{11}}{\partial \omega_{\mathrm{T}}} h_{11} + \frac{\partial \rho_{22}}{\partial \omega_{\mathrm{T}}} h_{22} \right)_{E_1} d\omega_{\mathrm{T}} \\
&+ \int_{\omega_1}^{\omega_0} \left(\frac{\partial \rho_{01}}{\partial \omega_{\mathrm{T}}} h_{10} + \frac{\partial \rho_{10}}{\partial \omega_{\mathrm{T}}} h_{01} + \frac{\partial \rho_{12}}{\partial \omega_{\mathrm{T}}} h_{21} + \frac{\partial \rho_{21}}{\partial \omega_{\mathrm{T}}} h_{12} \right)_{E_1} d\omega_{\mathrm{T}} \\
&+ \int_{\omega_1}^{\omega_0} \left(\frac{\partial \rho_{02}}{\partial \omega_{\mathrm{T}}} h_{20} + \frac{\partial \rho_{20}}{\partial \omega_{\mathrm{T}}} h_{02} \right)_{E_1} d\omega_{\mathrm{T}} = Q_3^{\mathrm{D}} + Q_3^{\mathrm{C1}} + Q_3^{\mathrm{C2}}, \\
Q_4 &= \int_{E_1}^{E_0} \left(\frac{\partial \rho_{00}}{\partial E_d} h_{00} + \frac{\partial \rho_{11}}{\partial E_d} h_{11} + \frac{\partial \rho_{22}}{\partial E_d} h_{22} \right)_{\omega_0} dE_d \\
&+ \int_{E_1}^{E_0} \left(\frac{\partial \rho_{01}}{\partial E_d} h_{10} + \frac{\partial \rho_{10}}{\partial E_d} h_{01} + \frac{\partial \rho_{12}}{\partial E_d} h_{21} + \frac{\partial \rho_{21}}{\partial E_d} h_{12} \right)_{\omega_0} dE_d \\
&+ \int_{E_1}^{E_0} \left(\frac{\partial \rho_{02}}{\partial E_d} h_{20} + \frac{\partial \rho_{20}}{\partial E_d} h_{02} \right)_{\omega_0} dE_d = Q_4^{\mathrm{D}} + Q_4^{\mathrm{C1}} + Q_4^{\mathrm{C2}}.
\end{aligned}
\tag{5.40}
$$

In analogy to what we've done before we decrease the different modes of coherence to see how it affects the efficiency of the engine. We introduce two factors, $\mathrm{b}_1, \mathrm{b}_2 \in [0, 1]$, taking $\{\rho_{01} \to \mathrm{b}_1\rho_{01}, \quad \rho_{10} \to \mathrm{b}_1\rho_{10}, \quad \rho_{12} \to \mathrm{b}_1\rho_{12}, \quad \rho_{21} \to \mathrm{b}_1\rho_{21}\}$ and $\{\rho_{02} \to \mathrm{b}_2\rho_{02}, \quad \rho_{20} \to \mathrm{b}_2\rho_{20}\}$, which makes $W_i^{\mathrm{D}} + W_i^{\mathrm{C1}} + W_i^{\mathrm{C2}} \to W_i^{\mathrm{D}} + \mathrm{b}_1 W_i^{\mathrm{C1}} + \mathrm{b}_2 W_i^{\mathrm{C2}}$ and $Q_i^{\mathrm{D}} + Q_i^{\mathrm{C1}} + Q_i^{\mathrm{C2}} \to Q_i^{\mathrm{D}} + \mathrm{b}_1 Q_i^{\mathrm{C1}} + \mathrm{b}_2 Q_i^{\mathrm{C2}}$. Therefore, by varying the coefficients b_1 and b_2 we change the contributions to work and heat associated to the coherence orders 1 and -1, and 2 and -2, respectively. This engine has a behavior pretty similar to the previous one with the two level system, as we can see through the functional dependence of η with the upper values (ω_1, E_1) (see Fig. 20a) for the cycle depicted in Figure 16. We first look at the behavior of this engine due to changes in their coherences of order 2 and -2 by a factor of b_2 while keeping their coherences of order 1 and -1 at their original values, setting $\mathrm{b}_1 = 1$. As we decrease the value of b_2 we observe an increase of the yellowy area, which has higher values of η, indicating that the coherence terms ρ_{02} and ρ_{20} undermines the engine

functioning by reducing its efficiency along a determined cycle given by some pair of upper values (ω_1, E_1). When all the coherence ρ_{02} and ρ_{20} are kept intact ($b_2 = 1$) as shown in Fig. 20a, the maximum attained efficiency in this regime of operation is around 29% with $(\omega_1, E_1) = (\omega_{1,\max}, E_{1,\max})$ and when these same coherences completely vanishes (Fig. 20d) by setting $b_2 = 0$ its maximum efficiency ends up with a value around 34%, again at the same upper values $(\omega_1, E_1) = (\omega_{1,\max}, E_{1,\max})$. In the following plots we can see the modes of coherence 2 and -2 playing their role in the efficiency of this non-thermal engine.

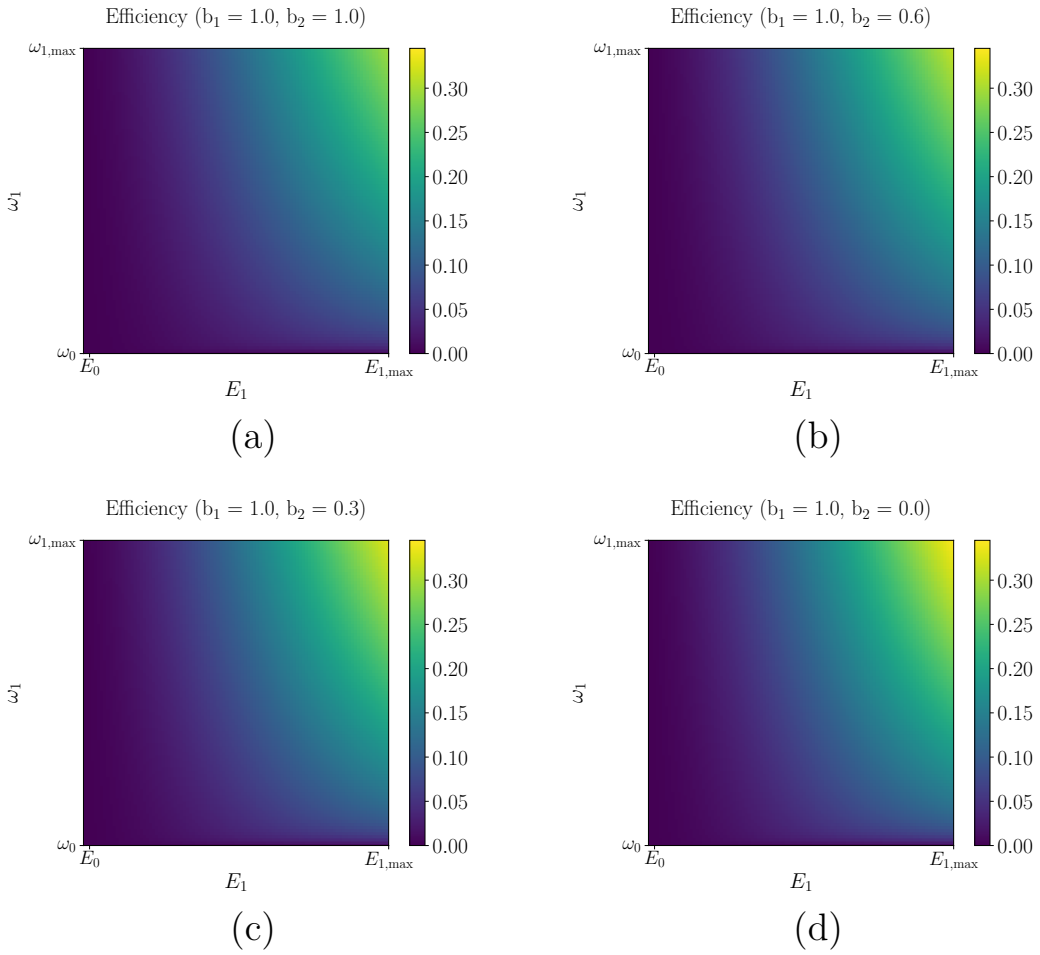

Figure 20 – The plots 20a, 20b, 20c and 20d represent the efficiency η as a function of the upper values (ω_1, E_1) for the cycle depicted in Figure 16 with $\omega_{1,\max}/2\pi = 1000$ MHz and $E_{1,\max}/2\pi\hbar = 2$ MHz for different values of b_2, the factor multiplying the coherences ρ_{02} and ρ_{20} to adjust the percentage of dephasing on these elements of the stationary state of the 3-level system. As we decrease the value of b_2 we observe an increase of the yellowy area, which has higher values of η. When all the coherences ρ_{02} and ρ_{20} are kept intact as shown in Fig. 20a, the maximum attained efficiency in this regime of operation is around 29%, and when these same coherences completely vanishes (Fig. 20d) its maximum efficiency ends up with a value around 34%.

Source: By the author.

A similar procedure is repeated with the coherences of order 1 and -1, reducing

them by a factor b_1 while keeping the coherences 2 and -2 at their original values by setting $b_2 = 1$. In this case we observe how important the coherences $\{\rho_{01}, \rho_{10}, \rho_{12}, \rho_{21}\}$ are for the proper work of this cycle as a heat engine. Looking at the Fig. 21a we see a drastic decrease in the efficiency of the engine as we decrease the value of b_1, going from the 29%, with $b_1 = 1$, in the upper values $(\omega_1, E_1) = (\omega_{1,\max}, E_{1,\max})$ to almost 0% with $b_1 = 0$. In the following plots we can see the modes of coherence 1 and -1 playing their role in the efficiency of this non-thermal engine.

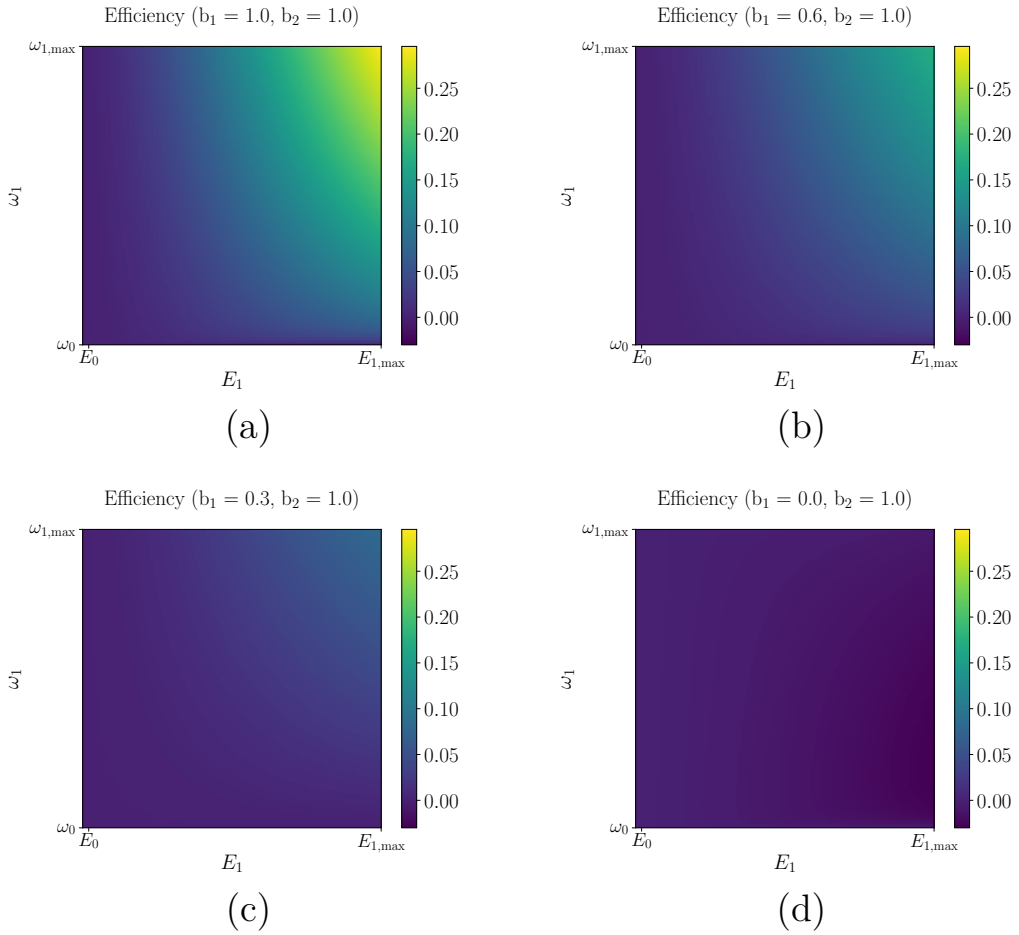

Figure 21 – The plots 21a, 21b, 21c and 21d represent the efficiency η as a function of the upper values (ω_1, E_1) for the cycle depicted in Figure 16 with $\omega_{1,\max}/2\pi = 1000$ MHz and $E_{1,\max}/2\pi\hbar = 2$ MHz for different values of b_1, the factor multiplying the coherences $\{\rho_{01}, \rho_{10}, \rho_{12}, \rho_{21}\}$ to adjust the percentage of dephasing on these elements of the stationary state of the 3-level system. As we decrease the value of b_1 we once more observe a suppression of the area with positive η. An additional feature that we see is the appearance of negative values for η, which is going to become clearer in the Fig. 22b.

Source: By the author.

An additional change that we observe in the efficiency of the engine when reducing the coherences of order 1 and -1 is the appearance of a region with negative values for η indicating that it could be used as a refrigerator. We had plotted the color map of the

η as a function of the upper values (ω_1, E_1) and in order to make it easier to visualize the appearance of negative values of η we are going to plot the diagonal curve that appears on the aforementioned color maps, which is a straight line connecting $\eta(\omega_0, E_0)$ to $\eta(\omega_{1,\max}, E_{1,\max})$.

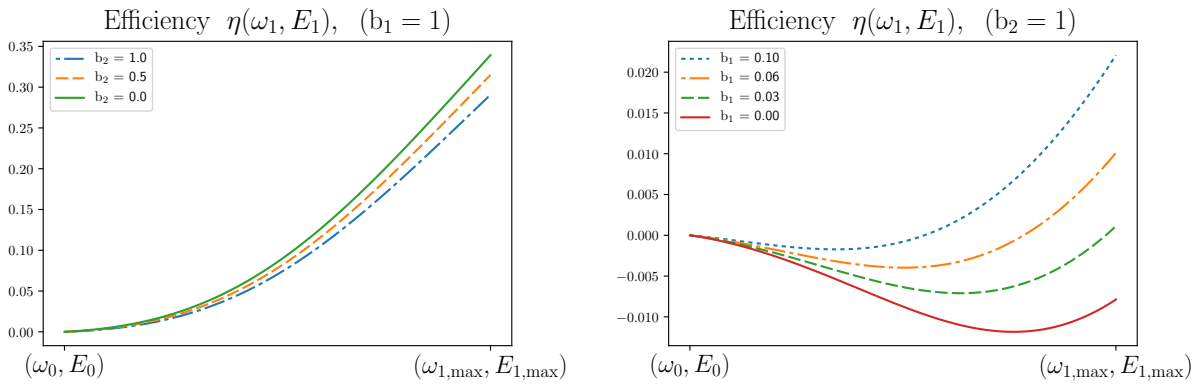

(a) (b)

Figure 22 – Plots of the curve described by efficiency $\eta(\omega_1, E_1)$ along the diagonal of the colormaps 20a and 21a connecting througt a straight line the points $\eta(\omega_0, E_0)$ and $\eta(\omega_{1,\max}, E_{1,\max})$. (a) In this first one, the coherences of order 1 and -1 are kept at their original values $(b_1 = 1)$, while b_2 acquires the values 1.0, 0.5 and 0.0. (b) The second one, follows the same procedure but this time the coherences of order 2 and -2 are the ones being kept at their original values $(b_2 = 1)$ and b_1 acquires the values 0.10, 0.06, 0.03 and 0.0.

Source: By the author.

The Fig. 22a shows how this efficiency $\eta(\omega_1, E_1)$ behaves along this diagonal line for different values of b_2 while keeping the coherences of order 1 and -1 at their original values. Notice that the efficiency has this monotonically increasing behavior and only positive values. As verified before, the coherences of order 2 and -2 actually reduces the engine's efficiency, and this can be seen in this plot when we decrease the values of b_2. In the second plot 22b the procedure is repeated, but this time keeping the coherences of order 2 and -2 at their original values. In this case we not only see a strong reduction of the efficiency due to the reduction of the coherences of mode 1 and -1, as previously shown, but we observe that the monotonicity of the efficiency starts to disappear and a new regime of operation appears, with $\eta(\omega_1, E_1) < 0$, as we decrease the value of b_1.

In conclusion we have seen that the coherences do play an important role to the functioning of the engine, not only to the absolute value of their efficiencies, actually with the possibility of eventually worsening their performance, which means that quantumness not only comes for the good,[125] but to their regimes of operation, with the possibility of their use as refrigerators. These results will be further elaborated and eventually appear in a paper.

6 CONCLUSIONS AND FINAL REMARKS

As we have stated before quantum thermodynamics is an effervescent area of research worth dedicating for, presenting a great deal of knowledge about the interconnection between thermodynamics and quantum mechanics. One of the goals aimed here with this thesis was to give a little bit of an introduction to the area in some specific points, with particular attention to the fluctuation theorems, that lies in the core of the study of out-of-equilibrium systems, and non-equilibrium stationary states, not only due to the fact that we'd be using them along this thesis but also because we wanted to make it easier for the ones planning to join the community at studying this area of research, by giving them an extra material, especially for the new graduate students.

Besides the educational purposes and the explanation of content to be used along this thesis, our first result was carried out in the context of out of equilibrium stationary states, trying to explore quantum systems at these non-thermal regimes to build quantum engines, so in order to accomplish that we devised an experimentally relevant thermodynamic cycle for a transmon qubit WS interacting with a non-thermal environment composed by two subsystems, an externally excited cavity and a classical heat bath with temperature T. The WS undergoes a non-conventional cycle through a succession of non-thermal stationary states obtained by slowly varying its bare frequency and the amplitude of the field applied on the cavity. The efficiency of this engine has attained a maximum value up to 47% in the regime of operation used and it doesn't take into account the energy necessary to prepare the non-thermal heat bath, which is not necessarily a bad thing if we only want to look for the amount of work delivered by the engine regardless of how expensive it is to make it possible. On the other hand, if we want to reconcile with the 2nd law of thermodynamics we need to consider every single thermodynamic trade made on the process. This result was published at Cherubim, C. *et al.*[86] and selected for the Editor's Choice Articles.

Still exploring the capabilities and limitations of these engines the next step that we took, which represents our second result, consisted of looking for the role played by the different types of coherences present at the WS used to build the engine. The classification of those coherences was based on how they respond to rotations generated by the qubit's bare Hamiltonian. We did that for the trivial case of the qubit, that only contained the called modes of coherence 1 and -1, and those turned out to be very important for the efficiency of the machine, being responsible for almost all the efficiency obtained, that fell to around 6%. In order to see what would happen when adding more modes, we used the transmon again as a WS, but this time working as a 3-level system, which added more two modes of coherence, 2 and -2, to the WS. As in the first case, the modes 1 and -1 played their game in the engine's functioning, not only to the absolute value of the engine's

efficiency but to the regime of operation of the machine, that started to present negative values for the efficiency η. The additional orders, 2 and -2, had a negative impact on the efficiency, reducing its absolute value from 34% to 29% when they were present, indicating that not always a quantum "ingredient" improves the performance of thermodynamic systems.

As a future prospect we will try to further understand the dependence of a series of thermodynamic process on the specific orders of coherence and specific evolutions dictated by covariant maps, but not only on heat engines. The first thing is to define covariant maps for time-dependent Hamiltonians and their respective symmetry transformations, and then look for the entropy production for maps that are covariant under these symmetry transformations of time-dependent Hamiltonians, and what role each order of coherence play along those trajectories. Once we build up some intuition on that, we go back to the heat engines, but in this case working with finite time strokes, and see how these features affect the engine's behavior. We will also look to fluctuation theorems for states that start with specific orders of coherence and undergo work protocols covariant with those same symmetry transformations mentioned above. When working on these topics we'll have to choose one quantifier for these orders of coherence and their respective relation with the entropy production, usually achieved through the relative entropy.

In short what we intended to accomplish here with this thesis, was to give our two cents of contribution to the scientific community on the topic of non-thermal heat engines operating in a quantum regime.

REFERENCES

1 CALLEN, H. B. **Thermodynamics and an introduction to thermostatistics**. New York: Wiley, 1985.

2 OLIVEIRA, M. J. de. **Equilibrium thermodynamics**. Berlin: Springer Verlag, 2013.

3 SEARS, F. W.; SALINGER, G. L. **Thermodynamics, kinetic theory, and statistical thermodynamics.** 3rd ed. New York: Addison Wesley, 1975.

4 BOLES, M.; CENGEL, Y. **Thermodynamics:** an engineering approach. New York: McGraw-Hill Education, 2018.

5 SCHROEDER, D. V. **An introduction to thermal physics**. New York: Adisson Wesley, 1999.

6 DEFFNER, S.; CAMPBELL, S. **Quantum thermodynamics**. San Raphael, CA: Morgan & Claypool Publishers, 2019.

7 GROOT, S. R. D.; MAZUR, P. **Non-equilibrium thermodynamics**. New York: Dover Publications, 2011. (Dover Books on Physics).

8 KONDEPUDI, D.; PRIGOGINE, I. **Modern thermodynamics:** from heat engines to dissipative structures. New York: Wiley, 2014.

9 PRIGOGINE, I. **Introduction to thermodynamics of irreversible processes**. New York: Interscience Publishers, 1968.

10 EVANS, D. J.; COHEN, E. G. D.; MORRISS, G. P. Probability of second law violations in shearing steady states. **Physical Review Letters**, American Physical Society, v. 71, p. 2401, Oct. 1993.

11 SEVICK, E.; PRABHAKAR, R.; WILLIAMS, S. R.; SEARLES, D. J. Fluctuation theorems. **Annual Review of Physical Chemistry,** Annual Reviews, v. 59, n. 1, p. 603–633, 2008.

12 EVANS, D. J.; SEARLES, D. J. The fluctuation theorem. **Advances in Physics**, Informa UK Limited, v. 51, n. 7, p. 1529, Nov. 2002.

13 SEIFERT, U. Stochastic thermodynamics, fluctuation theorems and molecular machines. **Reports on Progress in Physics**, IOP Publishing, v. 75, n. 12, p. 126001, Nov. 2012.

14 SEKIMOTO, K. **Stochastic energetics**. Berlin: Springer Verlag, 2010. (Lecture Notes in Physics).

15 JARZYNSKI, C. Nonequilibrium equality for free energy differences. **Physical Review Letters**, American Physical Society, v. 78, p. 2690, Apr. 1997.

16 CROOKS, G. E. Nonequilibrium measurements of free energy differences for microscopically reversible markovian systems. **Journal of Statistical Physics**, Springer Nature, v. 90, n. 5/6, p. 1481, 1998.

17 CROOKS, G. E. Entropy production fluctuation theorem and the non-equilibrium work relation for free energy differences. **Physical Review E**, American Physical Society, v. 60, p. 2721, Sept. 1999.

18 TOMÉ, T.; OLIVEIRA, M. J. de. **Stochastic dynamics and irreversibility**. Berlin: Springer International Publishing, 2015.

19 TALKNER, P.; LUTZ, E.; HÄNGGI, P. Fluctuation theorems: work is not an observable. **Physical Review E**, American Physical Society, v. 75, p. 050102, May 2007.

20 KURCHAN, J. **A quantum fluctuation theorem.** Available from: arXiv:cond-mat/0007360v2. Aug. 2001. Accessible at: May 11, 2020.

21 TASAKI, H. **Jarzynski relations for quantum systems and some applications.** Available from: arXiv:cond-mat/0009244v2. Sept. 2000. Accessible at: May 11, 2020.

22 MUKAMEL, S. Quantum extension of the jarzynski relation: analogy with stochastic dephasing. **Physical Review Letters**, American Physical Society, v. 90, p. 170604, May 2003.

23 MONNAI, T. Unified treatment of the quantum fluctuation theorem and the Jarzynski equality in terms of microscopic reversibility. **Physical Review E**, American Physical Society, v. 72, p. 027102, Aug. 2005.

24 ESPOSITO, M.; HARBOLA, U.; MUKAMEL, S. Nonequilibrium fluctuations, fluctuation theorems, and counting statistics in quantum systems. **Reviews of Modern Physics**, American Physical Society, v. 81, p. 1665, Dec. 2009.

25 CAMPISI, M.; HÄNGGI, P.; TALKNER, P. Colloquium: quantum fluctuation relations: foundations and applications. **Reviews of Modern Physics**, American Physical Society, v. 83, p. 771, July 2011.

26 TALKNER, P.; HäNGGI, P. The Tasaki–Crooks quantum fluctuation theorem. **Journal of Physics A:** mathematical and theoretical, IOP Publishing, v. 40, n. 26, p. F569, June 2007.

27 LANDAUER, R. $dq = t$dS far from equilibrium. **Physical Review A**, American Physical Society, v. 18, p. 255, July 1978.

28 OONO, Y.; PANICONI, M. Steady state thermodynamics. **Progress of Theoretical Physics Supplement**, Oxford Academic, v. 130, p. 29, 1998.

29 RUELLE, D. P. Extending the definition of entropy to nonequilibrium steady states. **Proceedings of the National Academy of Sciences**, National Academy of Sciences, v. 100, n. 6, p. 3054, 2003.

30 KOMATSU, T. S.; NAKAGAWA, N.; SASA, S.-I.; TASAKI, H. Steady-state thermodynamics for heat conduction: microscopic derivation. **Physical Review Letters**, American Physical Society, v. 100, p. 230602, June 2008.

31 KOMATSU, T. S.; NAKAGAWA, N.; SASA, S.-i.; TASAKI, H. Entropy and nonlinear nonequilibrium thermodynamic relation for heat conducting steady states. **Journal of Statistical Physics**, Springer Nature, v. 142, n. 1, p. 127, Jan. 2011.

32 SAITO, K.; TASAKI, H. Extended clausius relation and entropy for nonequilibrium steady states in heat conducting quantum systems. **Journal of Statistical Physics**, Springer Nature, v. 145, n. 5, p. 1275, Dec. 2011.

33 SASA, S.-I.; TASAKI, H. Steady state thermodynamics. **Journal of Statistical Physics**, Springer Nature, v. 125, n. 1, p. 125, Oct. 2006.

34 LEBOWITZ, J. L.; SPOHN, H. A Gallavotti–Cohen-type symmetry in the large deviation functional for stochastic dynamics. **Journal of Statistical Physics**, Springer Nature, v. 95, n. 1, p. 333, Apr. 1999.

35 PRADHAN, P.; RAMSPERGER, R.; SEIFERT, U. Approximate thermodynamic structure for driven lattice gases in contact. **Physical Review E**, American Physical Society, v. 84, p. 041104, Oct. 2011.

36 SPECK, T.; SEIFERT, U. Integral fluctuation theorem for the housekeeping heat. **Journal of Physics A:** mathematical and general, IOP Publishing, v. 38, n. 34, p. L581, Aug. 2005.

37 ESPOSITO, M.; BROECK, C. Van den. Three detailed fluctuation theorems. **Physical Review Letters**, American Physical Society, v. 104, p. 090601, Mar. 2010.

38 ESPOSITO, M.; HARBOLA, U.; MUKAMEL, S. Entropy fluctuation theorems in driven open systems: Application to electron counting statistics. **Physical Review E**, American Physical Society, v. 76, p. 031132, Sept. 2007.

39 HATANO, T.; SASA, S.-I. Steady-state thermodynamics of Langevin systems. **Physical Review Letters**, American Physical Society, v. 86, p. 3463, Apr. 2001.

40 SAGAWA, T.; HAYAKAWA, H. Geometrical expression of excess entropy production. **Physical Review E**, American Physical Society, v. 84, p. 051110, Nov. 2011.

41 YUGE, T.; SAGAWA, T.; SUGITA, A.; HAYAKAWA, H. Geometrical excess entropy production in nonequilibrium quantum systems. **Journal of Statistical Physics**, Springer Nature, v. 153, n. 3, p. 412, Nov. 2013.

42 HOROWITZ, J. M.; SAGAWA, T. Equivalent definitions of the quantum nonadiabatic entropy production. **Journal of Statistical Physics**, Springer Nature, v. 156, n. 1, p. 55, July 2014.

43 GARDAS, B.; DEFFNER, S. Thermodynamic universality of quantum carnot engines. **Physical Review E**, American Physical Society, v. 92, p. 042126, Oct. 2015.

44 ESPOSITO, M.; BROECK, C. V. den. Second law and landauer principle far from equilibrium. **Europhysics Letters**, IOP Publishing, v. 95, n. 4, p. 40004, Aug. 2011.

45 DEFFNER, S.; LUTZ, E. **Information free energy for nonequilibrium states.** Available from: arXiv:cond-mat/1201.3888. Jan. 2012. Accessible at: May 11, 2020.

46 PARRONDO, J. M. R.; HOROWITZ, J. M.; SAGAWA, T. Thermodynamics of information. **Nature Physics**, Springer Science and Business Media LLC, v. 11, n. 2, p. 131, Feb. 2015.

47 ALICKI, R. The quantum open system as a model of the heat engine. **Journal of Physics A:** mathematical and general, IOP Publishing, v. 12, n. 5, p. L103, 1979.

48 NIEDENZU, W.; MUKHERJEE, V.; GHOSH, A.; KOFMAN, A. G.; KURIZKI, G. Quantum engine efficiency bound beyond the second law of thermodynamics. **Nature Communications**, Springer Nature, v. 9, p. 165, Jan. 2018.

49 PUSZ, W.; WORONOWICZ, S. L. Passive states and KMS states for general quantum systems. **Communications in Mathematical Physics**, Springer Nature, v. 58, n. 3, p. 273, Oct. 1978.

50 ALLAHVERDYAN, A. E.; BALIAN, R.; NIEUWENHUIZEN, T. M. Maximal work extraction from finite quantum systems. **Europhysics Letters**, IOP Publishing, v. 67, n. 4, p. 565, Aug. 2004.

51 TINKHAM, M. **Introduction to superconductivity.** 2nd ed. New York: Dover Publications, 2004. (Dover Books on Physics).

52 GIRVIN, S. M. Circuit QED: Superconducting qubits coupled to microwave photons. *In*: DEVORET, R. J. S. M. H.; HUARD, B. (ed.). **Proceedings of the 2011 Les Houches Summer School on Quantum**. Oxford: Oxford University Press, 2014. p. 155.

53 GIRVIN, S. M. Circuit QED: superconducting qubits coupled to microwave photons. *In*: DEVORET, M. *et al.* (ed.). **Quantum machines:** measurement and control of engineered quantum systems. Oxford: Oxford University Press, 2014. p. 113.

54 BOUCHIAT, V.; VION, D.; JOYEZ, P.; ESTEVE, D.; DEVORET, M. H. Quantum coherence with a single cooper pair. **Physica Scripta**, IOP Publishing, T76, n. 1, p. 165, 1998.

55 COTTET, A. **Implementation of a quantum bit in a superconducting circuit**. 2002. 259p. These (Doctorat) – Universite Paris VI, Paris, 2002.

56 CALDEIRA, A. O. **An introduction to macroscopic quantum phenomena and quantum dissipation**. Cambridge: Cambridge University Press, 2014.

57 FEYNMAN, R. P. **Statistical mechanics:** a set of lectures. Oxford: CRC Press, 1998. (Frontiers in Physics).

58 MANGIN, P.; KAHN, R. **Superconductivity**. Berlin: Springer International Publishing, 2017.

59 MAKHLIN, Y.; SCHÖN, G.; SHNIRMAN, A. Quantum-state engineering with Josephson-junction devices. **Reviews of Modern Physics**, American Physical Society, v. 73, p. 357, May 2001.

60 WAELE, A. de; OUBOTER, R. de B. Quantum-interference phenomena in point contacts between two superconductors. **Physica**, Elsevier, v. 41, n. 2, p. 225, 1969.

61 KOCH, J.; YU, T. M.; GAMBETTA, J.; HOUCK, A. A.; SCHUSTER, D. I.; MAJER, J.; BLAIS, A.; DEVORET, M. H.; GIRVIN, S. M.; SCHOELKOPF, R. J. Charge-insensitive qubit design derived from the cooper pair box. **Physical Review A**, American Physical Society, v. 76, p. 042319, Oct. 2007.

62 GRIFFITHS, D. J. **Introduction to quantum mechanics**. Cambridge: Cambridge University Press, 2016.

63 BLAIS, A.; HUANG, R.-S.; WALLRAFF, A.; GIRVIN, S. M.; SCHOELKOPF, R. J. Cavity quantum electrodynamics for superconducting electrical circuits: an architecture for quantum computation. **Physical Review A**, American Physical Society, v. 69, p. 062320, June 2004.

64 WALLRAFF, A.; SCHUSTER, D. I.; BLAIS, A.; FRUNZIO, L.; HUANG, R.-S.; MAJER, J.; KUMAR, S.; GIRVIN, S. M.; SCHOELKOPF, R. J. Strong coupling of a single photon to a superconducting qubit using circuit quantum electrodynamics. **Nature**, Springer Nature, v. 431, n. 7005, p. 162, Sept. 2004.

65 GRIFFITHS, D. J. **Introduction to electrodynamics**. Cambridge: Cambridge University Press, 2017.

66 DEVORET, M. H. Quantum fluctuations in electrical circuits. *In*: REYNAUD, S.; GIACOBINO, E.; ZINN-JUSTIN, J. (ed.). **Fluctuations quantiques/quantum fluctuations.** Amsterdam: Elsevier, 1997. p. 351.

67 KIEU, T. D. Quantum heat engines, the second law and maxwell's daemon. **The European Physical Journal D:** atomic, molecular, optical and plasma physics, Springer Science and Business Media LLC, v. 39, n. 1, p. 115, Apr. 2006.

68 QUAN, H. T.; ZHANG, P.; SUN, C. P. Quantum heat engine with multilevel quantum systems. **Physical Review E**, American Physical Society, v. 72, p. 056110, Nov. 2005.

69 SARANDY, M. S.; LIDAR, D. A. Adiabatic approximation in open quantum systems. **Physical Review A**, American Physical Society, v. 71, n. 1, p. 012331, Jan. 2005.

70 HORN, R. **Matrix analysis**. Cambridge: Cambridge University Press, 2012.

71 HU, C.-K.; SANTOS, A. C.; CUI, J.-M.; HUANG, Y.-F.; SOARES-PINTO, D. O.; SARANDY, M. S.; LI, C.-F.; GUO, G.-C. Quantum thermodynamics in adiabatic open systems and its trapped-ion experimental realization. **npj Quantum Information**, v. 6, n. 1, p. 73, Aug. 2020.

72 QUAN, H. T.; LIU, Y.-X.; SUN, C. P.; NORI, F. Quantum thermodynamic cycles and quantum heat engines. **Physical Review E**, American Physical Society, v. 76, p. 031105, Sept. 2007.

73 ARNAUD, J.; CHUSSEAU, L.; PHILIPPE, F. **A simple quantum heat engine.** Available from: arXiv:quant-ph/0211072v2. June 2003. Accessible at: May 11, 2020.

74 KIEU, T. D. Quantum heat engines, the second law and Maxwell's daemon. **The European Physical Journal D:** atomic, molecular, optical and plasma physics, Springer Nature, v. 39, n. 1, p. 115, Apr. 2006.

75 KLAERS, J.; FAELT, S.; IMAMOGLU, A.; TOGAN, E. Squeezed thermal reservoirs as a resource for a nanomechanical engine beyond the carnot limit. **Physical Review X**, American Physical Society, v. 7, p. 031044, Sept. 2017.

76 DILLENSCHNEIDER, R.; LUTZ, E. Energetics of quantum correlations. **Europhysics Letters**, IOP Publishing, v. 88, n. 5, p. 50003, Dec. 2009.

77 HUANG, X. L.; WANG, T.; YI, X. X. Effects of reservoir squeezing on quantum systems and work extraction. **Physical Review E**, American Physical Society, v. 86, p. 051105, Nov. 2012.

78 ABAH, O.; LUTZ, E. Efficiency of heat engines coupled to nonequilibrium reservoirs. **Europhysics Letters**, IOP Publishing, v. 106, n. 2, p. 20001, May 2014.

79 ROSSNAGEL, J.; ABAH, O.; SCHMIDT-KALER, F.; SINGER, K.; LUTZ, E. Nanoscale heat engine beyond the carnot limit. **Physical Review Letters**, American Physical Society, v. 112, p. 030602, Jan. 2014.

80 HARDAL, A. Ü. C.; MÜSTECAPLIOĞLU, Ö. E. Superradiant quantum heat engine. **Scientific Reports**, Springer Nature, v. 5, p. 12953, Aug. 2015.

81 NIEDENZU, W.; GELBWASER-KLIMOVSKY, D.; KOFMAN, A. G.; KURIZKI, G. On the operation of machines powered by quantum non-thermal baths. **New Journal of Physics**, IOP Publishing, v. 18, n. 8, p. 083012, Aug. 2016.

82 MANZANO, G.; GALVE, F.; ZAMBRINI, R.; PARRONDO, J. M. R. Entropy production and thermodynamic power of the squeezed thermal reservoir. **Physical Review E**, American Physical Society, v. 93, p. 052120, May 2016.

83 AGARWALLA, B. K.; JIANG, J.-H.; SEGAL, D. Quantum efficiency bound for continuous heat engines coupled to noncanonical reservoirs. **Physical Review B**, American Physical Society, v. 96, p. 104304, Sept. 2017.

84 STEFANATOS, D. Optimal efficiency of a noisy quantum heat engine. **Physical Review E**, American Physical Society, v. 90, p. 012119, July 2014.

85 TORRONTEGUI, E.; KOSLOFF, R. Quest for absolute zero in the presence of external noise. **Physical Review E**, American Physical Society, v. 88, p. 032103, Sept. 2013.

86 CHERUBIM, C.; BRITO, F.; DEFFNER, S. Non-thermal quantum engine in transmon qubits. **Entropy**, MDPI, v. 21, n. 6, 2019.

87 SCULLY, M. O.; ZUBAIRY, M. S.; AGARWAL, G. S.; WALTHER, H. Extracting work from a single heat bath via vanishing quantum coherence. **Science**, American Association for the Advancement of Science, v. 299, n. 5608, p. 862, 2003.

88 ROUXINOL, F.; HAO, Y.; BRITO, F.; CALDEIRA, A. O.; IRISH, E. K.; LAHAYE, M. D. Measurements of nanoresonator-qubit interactions in a hybrid quantum electromechanical system. **Nanotechnology**, IOP Publishing, v. 27, n. 36, p. 364003, Aug. 2016.

89 DEFFNER, S.; JARZYNSKI, C. Information processing and the second law of thermodynamics: nn inclusive, hamiltonian approach. **Physical Review X**, American Physical Society, v. 3, p. 041003, Oct. 2013.

90 KOK, P.; MUNRO, W. J.; NEMOTO, K.; RALPH, T. C.; DOWLING, J. P.; MILBURN, G. J. Linear optical quantum computing with photonic qubits. **Reviews of Modern Physics**, American Physical Society, v. 79, n. 1, p. 135, Jan. 2007.

91 HOFHEINZ, M.; WEIG, E. M.; ANSMANN, M.; BIALCZAK, R. C.; LUCERO, E.; NEELEY, M.; O'CONNELL, A. D.; WANG, H.; MARTINIS, J. M.; CLELAND, A. N. Generation of fock states in a superconducting quantum circuit. **Nature**, Springer Nature, v. 454, n. 7202, p. 310, Jan. 2008.

92 MALLET, F.; ONG, F. R.; PALACIOS-LALOY, A.; NGUYEN, F.; BERTET, P.; VION, D.; ESTEVE, D. Single-shot qubit readout in circuit quantum electrodynamics. **Nature Physics**, Springer Nature, v. 5, n. 11, p. 791, Jan. 2009.

93 GEVA, E.; KOSLOFF, R. A quantum-mechanical heat engine operating in finite time. a model consisting of spin-1/2 systems as the working fluid. **The Journal of Chemical Physics**, AIP Publishing LLC, v. 96, p. 3054, Feb. 1992.

94 KIEU, T. D. The second law, maxwell's demon, and work derivable from quantum heat engines. **Physical Review Letters**, American Physical Society, v. 93, p. 140403, Sept. 2004.

95 LINDEN, N.; POPESCU, S.; SKRZYPCZYK, P. How small can thermal machines be? The smallest possible refrigerator. **Physical Review Letters**, American Physical Society, v. 105, p. 130401, Sept. 2010.

96 CORREA, L. A.; PALAO, J. P.; ALONSO, D.; ADESSO, G. Quantum-enhanced absorption refrigerators. **Scientific Reports**, Springer Nature, v. 4, p. 3949, Feb. 2014.

97 UZDIN, R.; LEVY, A.; KOSLOFF, R. Equivalence of quantum heat machines, and quantum-thermodynamic signatures. **Physical Review X**, American Physical Society, v. 5, p. 031044, Sept. 2015.

98 ABAH, O.; ROSSNAGEL, J.; JACOB, G.; DEFFNER, S.; SCHMIDT-KALER, F.; SINGER, K.; LUTZ, E. Single-ion heat engine at maximum power. **Physical Review Letters**, American Physical Society, v. 109, p. 203006, Nov. 2012.

99 ZHANG, K.; BARIANI, F.; MEYSTRE, P. Quantum optomechanical heat engine. **Physical Review Letters**, American Physical Society, v. 112, p. 150602, Apr. 2014.

100 DAWKINS, S. T.; ABAH, O.; SINGER, K.; DEFFNER, S. Single atom heat engine in a tapered ion trap. *In*: BINDER, F.; CORREA, L. A.; GOGOLIN, C.; ANDERS, J.; ADESSO, G. (ed.). **Thermodynamics in the quantum regime:** fundamental aspects and new directions. Berlin: Springer International Publishing, 2018. p. 887.

101 PETERSON, J. P. S.; BATALHÃO, T. B.; HERRERA, M.; SOUZA, A. M.; SARTHOUR, R. S.; OLIVEIRA, I. S.; SERRA, R. M. Experimental characterization of a spin quantum heat engine. **Physical Review Letters**, American Physical Society, v. 123, p. 240601, Dec. 2019.

102 ROSSNAGEL, J.; DAWKINS, S. T.; TOLAZZI, K. N.; ABAH, O.; LUTZ, E.; SCHMIDT-KALER, F.; SINGER, K. A single-atom heat engine. **Science**, American Association for the Advancement of Science, v. 352, n. 6283, p. 325, 2016.

103 STRELTSOV, A.; ADESSO, G.; PLENIO, M. B. Colloquium: quantum coherence as a resource. **Reviews of Modern Physics**, American Physical Society, v. 89, p. 041003, Oct. 2017.

104 MISRA, A.; SINGH, U.; BHATTACHARYA, S.; PATI, A. K. Energy cost of creating quantum coherence. **Physical Review A**, American Physical Society, v. 93, p. 052335, May 2016.

105 KORZEKWA, K.; LOSTAGLIO, M.; OPPENHEIM, J.; JENNINGS, D. The extraction of work from quantum coherence. **New Journal of Physics**, IOP Publishing, v. 18, n. 2, p. 023045, Feb. 2016.

106 ÅBERG, J. Catalytic coherence. **Physical Review Letters**, American Physical Society, v. 113, p. 150402, Oct. 2014.

107 KAMMERLANDER, P.; ANDERS, J. Coherence and measurement in quantum thermodynamics. **Scientific Reports**, Springer Nature, v. 6, n. 1, p. 22174, Feb. 2016.

108 VACANTI, G.; ELOUARD, C.; AUFFEVES, A. **The work cost of keeping states with coherences out of thermal equilibrium.** Available from: arXiv:quant-ph/1503.01974. Mar. 2015. Accessible at: May 11, 2020.

109 SCULLY, M. O.; CHAPIN, K. R.; DORFMAN, K. E.; KIM, M. B.; SVIDZINSKY, A. Quantum heat engine power can be increased by noise-induced coherence. **Proceedings of the National Academy of Sciences**, National Academy of Sciences, v. 108, n. 37, p. 15097, 2011.

110 RAHAV, S.; HARBOLA, U.; MUKAMEL, S. Heat fluctuations and coherences in a quantum heat engine. **Physical Review A**, American Physical Society, v. 86, p. 043843, Oct. 2012.

111 ABAH, O.; LUTZ, E. Efficiency of heat engines coupled to nonequilibrium reservoirs. **Europhysics Letters**, IOP Publishing, v. 106, n. 2, p. 20001, Apr. 2014.

112 MARVIAN, I.; SPEKKENS, R. W. How to quantify coherence: distinguishing speakable and unspeakable notions. **Physical Review A**, American Physical Society, v. 94, p. 052324, Nov. 2016.

113 ÅBERG, J. **Quantifying superposition.** Available from: arXiv:quant-ph/0612146. Dec. 2006. Accessible at: May 11, 2020.

114 BAUMGRATZ, T.; CRAMER, M.; PLENIO, M. B. Quantifying coherence. **Physical Review Letters**, American Physical Society, v. 113, p. 140401, Sept. 2014.

115 LEVI, F.; MINTERT, F. A quantitative theory of coherent delocalization. **New Journal of Physics**, IOP Publishing, v. 16, n. 3, p. 033007, Mar. 2014.

116 VICENTE, J. I. de; STRELTSOV, A. Genuine quantum coherence. **Journal of Physics A:** mathematical and theoretical, IOP Publishing, v. 50, n. 4, p. 045301, Dec. 2016.

117 MARVIAN, I.; SPEKKENS, R. W. The theory of manipulations of pure state asymmetry: I. basic tools, equivalence classes and single copy transformations. **New Journal of Physics**, IOP Publishing, v. 15, n. 3, p. 033001, Mar. 2013.

118 MARVIAN, I.; SPEKKENS, R. W. Extending Noether's theorem by quantifying the asymmetry of quantum states. **Nature Communications**, Springer Nature, v. 5, n. 1, p. 3821, May 2014.

119 MARVIAN, I.; SPEKKENS, R. W. Modes of asymmetry: the application of harmonic analysis to symmetric quantum dynamics and quantum reference frames. **Physical Review A**, American Physical Society, v. 90, p. 062110, Dec. 2014.

120 MARVIAN, I.; SPEKKENS, R. W.; ZANARDI, P. Quantum speed limits, coherence, and asymmetry. **Physical Review A**, American Physical Society, v. 93, p. 052331, May 2016.

121 LOSTAGLIO, M.; KORZEKWA, K.; JENNINGS, D.; RUDOLPH, T. Quantum coherence, time-translation symmetry, and thermodynamics. **Physical Review X**, American Physical Society, v. 5, p. 021001, Apr. 2015.

122 KEELER, J. **Understanding NMR spectroscopy**. New York: Wiley, 2005.

123 PIRES, D. P.; SILVA, I. A.; DEAZEVEDO, E. R.; SOARES-PINTO, D. O.; FILGUEIRAS, J. G. Coherence orders, decoherence, and quantum metrology. **Physical Review A**, American Physical Society, v. 98, p. 032101, Sept. 2018.

124 SØRENSEN, O.; EICH, G.; LEVITT, M.; BODENHAUSEN, G.; ERNST, R. Product operator formalism for the description of nmr pulse experiments. **Progress in Nuclear Magnetic Resonance Spectroscopy**, Elsevier, v. 16, p. 163, Mar. 1984.

125 CAMATI, P. A.; SANTOS, J. F. G.; SERRA, R. M. Coherence effects in the performance of the quantum otto heat engine. **Physical Review A**, American Physical Society, v. 99, p. 062103, June 2019.